APPLICATION OF FINITE ELEMENT METHOD (FEM) AND ARTIFICIAL INTELLIGENCE (AI) FOR RESPONSE-BASED ASSESSMENT OF REINFORCED CONCRETE (RC) BEAM-COLUMN CONNECTIONS

APPLICATION OF FEM AND AI FOR RESPONSE-BASED ASSESSMENT OF RC BEAM-COLUMN CONNECTIONS

Authors

Mehran Sahil 2019234
Muhammad Mansoor Khan 2019344
Abdul Wahid Anwar 2019013
Waqas Khan 2019540

Supervisor

Dr. Hafiz Ahmed Waqas

Co-Supervisor

Engr. Muhammad Ilyas

GHULAM ISHAQ KHAN INSTITUTE OF ENGINEERING SCIENCES AND TECHNOLOGY, TOPI SWABI

DEPARTMENT OF CIVIL ENGINEERING

MAY 31, 2023

ACKNOWLEDGMENTS

We would like to express our sincere gratitude to our supervisor, Dr. Hafiz Ahmed Waqas, for his invaluable guidance, unwavering support, and technical expertise throughout the duration of our final year project. His mentorship has been instrumental in shaping our research direction and creating a conducive environment for our project activities. We are also immensely thankful to our co-supervisor, Engr. Muhammad Illyas, for his valuable contributions and insights that have enhanced the quality of our project. His expertise and assistance have been invaluable in achieving our research goals.

We extend our deepest appreciation to the Department of Civil Engineering at Ghulam Ishaq Khan Institute of Engineering Sciences and Technology for providing us with an effective project title and facilitating our research endeavors. The department's commitment to academic excellence and research opportunities has greatly enriched our learning experience. We would like to acknowledge the Head of the Department, Dr. Ashraf Tannoli, for his unwavering support, encouragement, and hospitality. His guidance and availability to address our challenges have been pivotal in the success of our project.

Our heartfelt thanks go to our parents for their unwavering love, support, and belief in our abilities. Their encouragement and understanding during the demanding and stressful times of our project have been crucial in keeping us motivated and focused. We would also like to extend our appreciation to our friends and family members for their continuous support throughout our academic journey. Their unwavering belief in us and their understanding of the sacrifices we made have been a source of inspiration. Furthermore, we would like to acknowledge the faculty members of the Department of Civil Engineering for their effective knowledge dissemination. Their expertise, dedication, and passion for teaching have significantly contributed to our overall growth and understanding of the subject matter.

Finally, we would like to express our gratitude **to Pakistan Engineering Council (PEC)** for funding this project and making it a reality. Their valuable contributions have played a vital role in shaping our academic journey and preparing us for future endeavors. We are truly grateful for their support and assistance.

ABSTRACT

This study focuses on the critical role of beam-column joints in reinforced concrete structures under seismic loads. Failure of these joints can lead to partial or complete collapses, emphasizing the need for efficient structural design and performance optimization. The Finite Element (FE) method is utilized to assess joint performance through numerical modeling, considering various response parameters. The comparison of damage and different response parameters aids in identifying optimal failure characterization and joint design.

Addressing the challenges posed by excessive reinforcement congestion at joint regions, this research employs Finite Element Modeling (FEM) to enhance joint performance. Twelve models with different reinforcement configurations, replacing conventional shear stirrups, are developed. In-plane diagonal bars prove more effective in minimizing core damage than out-of-plane diagonal bars. The model featuring X-shaped reinforcement is identified as optimal for preventing joint failure, providing high rotational stiffness while minimizing core damage in tension and compression.

Moreover, an empirical model is presented for predicting the capacity of exterior beam-column joints subjected to cyclic loading. Gene expression programming (GEP), a nonlinear regression analysis technique, is used to develop the model. Incorporating material and geometric factors often overlooked in existing models, the proposed model demonstrates good accuracy and reliability, contributing to the cost-effective and safe design of reinforced concrete structures.

In conclusion, this research offers valuable insights for optimizing the design and performance of beam-column joints in reinforced concrete structures under seismic loads. The findings highlight the importance of response parameters, reinforcement configurations, perforated steel haunches, and accurate prediction models in enhancing joint behavior, ductility, and overall structural resilience.

KEYWORDS: Beam-column joints, damage assessment, response parameters, FEM, reinforcement congestion, core damage, diagonal reinforcement, load-carrying capacity, gene expression programming (GEP), reinforced concrete, exterior joint, joint capacity.

[This page is left intentionally blank]

Table of Contents

Chapter 1: Introduction

1. Background:

Reinforced concrete (RC) structures are widely used in construction, and the performance of these structures under seismic loads is of utmost importance. Beam-column joints are critical components of RC structures as they transfer loads and accommodate deformations during seismic events. However, failures in beam-column joints can lead to partial or complete collapse of the structures, emphasizing the need for understanding and optimizing the performance of these joints.

The design standards for beam-column joints are still under development, and further research is necessary to enhance their performance. One of the significant challenges in joint design is the excessive reinforcement congestion at joint regions, which hampers effective concrete pouring and compaction. This congestion can result in weakened joints that may not withstand earthquake deformations. Overcoming this challenge requires innovative approaches to improve joint performance and mitigate damage caused by reinforcement congestion.

Moreover, the limited ductility of beam-column joints, particularly in the exterior regions of RC frame structures, is a concern. These joints often exhibit reduced capacity to absorb and dissipate energy during seismic events, increasing the risk of structure collapse. Therefore, there is a critical need to design joints that are both robust and ductile to improve the overall performance of RC structures.

2. Motivation

The motivation behind this research is to address the aforementioned challenges and contribute to the optimization of beam-column joints in RC structures under seismic loads. By conducting numerical modeling and analysis using advanced techniques such as Finite Element Modeling (FEM), the performance of beam-column joints can be assessed considering various response parameters.

The comparison of damage in beam-column joints and the evaluation of different response parameters will enable the identification of effective indicators for characterizing failure modes and optimizing joint designs. This optimization process is essential for efficient structural design and performance enhancement, ensuring the safety and resilience of RC structures in seismic-prone areas.

Additionally, this study aims to improve joint performance by introducing various reinforcement enhancement details in the joint area to overcome reinforcement congestion and insufficient concrete compaction. By investigating different reinforcement configurations and enhancement strategies, the research seeks to identify effective methods to minimize core damage and improve joint robustness and ductility.

Furthermore, the proposed empirical model for predicting the joint capacity of exterior RC joints subjected to cyclic loading is motivated by the need for reliable prediction models in the design of RC structures. The model incorporates material and geometric factors often overlooked in existing models, providing a more accurate and reliable estimation of joint capacity. This empowers engineers to design cost-effective and safe RC structures by ensuring that joint capacities are accurately predicted and accounted for.

Overall, the background and motivation of this research revolve around enhancing the design methodology, optimizing the performance, and improving the safety and resilience of RC beam-column joints under seismic loads. By addressing the challenges related to reinforcement congestion, limited ductility, and accurate capacity prediction, this study aims to contribute to the advancement of structural engineering practices in seismic design.

3. Objectives of the Research

The objectives of this research are as follows:

1. To assess beam-column joint performance under seismic loads using the Finite Element method and optimize joint design based on identified response parameters.
2. To improve the robustness and ductility of beam-column joints by addressing reinforcement congestion and compaction issues through Finite Element Modeling.
3. To develop an AI-based model using gene expression programming to accurately predict the capacity of exterior beam-column joints under seismic events, considering material and geometric factors to enhance design accuracy and reliability.

4. Organization of Dissertation

This dissertation describes a combination of experimental and numerical research used to investigate and document the response of reinforced concrete beam-column connections under seismic events.

The content of the dissertation as follows:

- The motivation and objectives of the dissertation as well as background information pertaining to seismic loads and methods of analysis are presented in Chapter 1.
- Chapter 2: This chapter emphasizes the importance of beam-column joints in reinforced concrete structures under seismic loads. The Finite Element method is used to assess joint performance and identify response parameters for optimizing joint design.
- Chapter 3: This chapter addresses the challenges of designing robust and ductile beam-column joints. Finite Element Modeling is employed to enhance joint performance by overcoming reinforcement congestion. In-plane diagonal bars and X-shaped reinforcement are found to be effective in minimizing core damage.
- Chapter 4: This chapter proposes an empirical model for predicting the capacity of exterior beam-column joints under cyclic loading. The model considers material and geometric factors often overlooked in existing models, demonstrating good accuracy and reliability for joint capacity predictions.

The chapter 2, 3, and 4 are mapped with objectives 1, 2, and 3.

Chapter 2: Numerical Evaluation of Response Parameters and Damage in The Reinforced Concrete Beam-Column Connection Joint.

Abstract: Beam-column joints are essential components that indicate the performance of reinforced concrete structures in response to seismic loads. Failures of the beam-column joints can lead to partial or complete collapses of the structures. Therefore, a response parameter for characterizing the failure mode of the beam-column joints under seismic load plays a pivotal role in efficient structural design and performance optimization. In this study, the Finite Element (FE) method is applied to assess the performance of the beam-column joint considering various response parameters through numerical modeling. The comparison of damage of beam-column joint and different response parameters is made to identify the ability of selected response parameters to characterize the failure type and help optimize the design of beam-column joints.

Keywords: Beam-column joints, damage assessment, FE modeling, response parameters

1. Introduction

The beam-column joints of reinforced concrete structures experience significant inelastic deformations because of severe earthquakes. The joints' response can substantially impact the overall response of the moment-resisting frames if they are not appropriately designed and detailed. In numerous investigations carried out in the context of prior severe earthquakes, beam-column connections have been identified as one of the leading causes of damage in pre-existing reinforced concrete (RC) structures (Murty, C. V. R., Rupen, Goswami., A. R. Vijayanarayanan., 2012). Joint shear failures have reportedly been observed in many RC structures that have been in service and have experienced severe earthquake loading (Lowes & Mitra, 2004). The beam-column joint is a crucial region in frames that can resist moments induced by various loads (such as gravity loading, wind loading, seismic loading, etc.). These moments are induced by loads on the floors and beams and transmitted through the beam-column joint. If the joint fails, the moment cannot be transferred, and the entire structure will tend to collapse. Also, a significant amount of shear stress may be concentrated on the beam-column joint area during a strong earthquake, which may cause the joint to break before the beam or column (Allam et al., 2018). This brittle shear failure in the joint area could have enormous consequences, including severe damage and complete building collapse (Hassan & Mosalam, 2015). Therefore, the reinforced concrete frames must perform satisfactorily under extreme seismic load situations to sustain huge lateral loads without suffering irreversible damage.

A structure's ability to resist destructive forces depends on its ductility, particularly its seismic ductility. Ductility is the ability of parts or structures to deform without significantly reducing their strength or stiffness (Chitra & Mohan, 2021). Moreover, because of the twisting effect brought on by the uneven moment distribution on the outer side, the external joints of a structure are more likely to fail than the interior joints. A range of experimental methodologies (Attari et al., 2019; Dabiri et al., 2020) and numerical analysis (Najafgholipour & Arabi, 2019) are currently available in the literature to investigate the mechanical behavior of beam-column connections. Experimentation on scaled-down or full-scale structures, or sub-assemblies, is the primary approach for estimating the mechanical behavior of beam-column joints (Masi et al., 2013). This latter is beneficial for creating capacity models that may be used for both the planning of new structures and the evaluation of the state of already-built ones, the aging of which is a significant problem in many areas of the world. The concrete's compressive strength, the joint's size, the type of steel (i.e., smooth, or deformed bars), the area of shear reinforcement, and the axial load on the column, if used, all affect the joint's capacity.

Within the experimentation investigations group, an experimental study on RC joints was conducted based on these fundamental parameters to assess the shear behavior of the joints (Kotsovou & Mouzakis, 2011). Various joint types were tested on multiple scales, including the exterior, interior, knee, and T joints. These experimental studies looked at the effects of various factors on the joint shear strength and load-displacement curves of the RC joints, including the

geometrical characteristics of the joint panel, concrete compressive strength, beam longitudinal reinforcement, transverse joint reinforcement existence of RC slab, axial column load, etc. (Park & Mosalam, 2012).

Within the empirical and analytical investigations, researchers have compiled test findings in the literature and created mathematical and empirical relationships to forecast the RC joint shear capability (Pauletta et al., 2020). For instance, a compilation of experimental findings from quasi-static cyclic tests on various RC beam-column connections conducted by various researchers on the exterior, interior, and corner joints. The study's primary goal was to identify the factors that significantly influenced joint shear load-displacement behavior. Material property, joint panel geometry, confining reinforcement, reinforcement bond state, and column axial force were examined to investigate the influence on structural response. It was discovered that the most crucial effect factors on joint shear behavior varied depending on the kind of connection and the failure mode sequence. However, concrete compressive strength was the most prevalent controlling parameter affecting joint shear behavior (Kim & LaFave, 2007). The empirical relationship for estimating joint strength is also provided in the code standards (EN 1992-1-1: Eurocode 2: Design of Concrete Structures - Part 1-1: General Rules and Rules for Buildings, 2004), which is based on control factors like concrete compressive strength, and effective joint area. The columns' dimensions parallel to the direction of the longitudinal reinforcement of the beams are used to calculate the effective joint depth. The code standards also consider modification factors to get comparable results with the findings of experiments. The causes and challenges of empirical approaches have led to an increase in the adoption of data-driven techniques with pattern recognition capabilities in various domain applications (Hon et al., 2020; Kreuzer et al., 2020; Mahmoodzadeh et al., 2021).

Numerical investigations of RC joints have also been the subject of several studies employing FEM tools. For instance, Niroomandi (2014) conducted a numerical analysis of the factors that affect the shear failure of non-ductile exterior joints. Their numerical findings showed that joint aspect ratio and beam longitudinal reinforcement ratio were two important variables affecting joint shear (Niroomandi et al., 2014). Various response parameters have been put forward in past studies, including the force-displacement relationship, moment-rotation curve, ductility ratio, etc., to explain the modes of failure of beam-column joint (Dabiri et al., 2022; Kristiawan et al., 2022). Even though several beam-column joint response parameters have been suggested, none explicitly identifies the failure behavior through a single response parameter. Therefore, this study compares the response of different RC beam-column joint damage indicators to find a clear relationship between damage to RC beam-column connection and the selected response parameter. This study investigated the effectiveness of different response parameters by comparing various response parameters such as rotation, deflection, stress, and reinforcement strain with the joint's damage. Knowing how damage is related to different parameters is necessary to control the damage by limiting the directly influencing parameter. The overall scheme of the present study is provided in Figure 1.

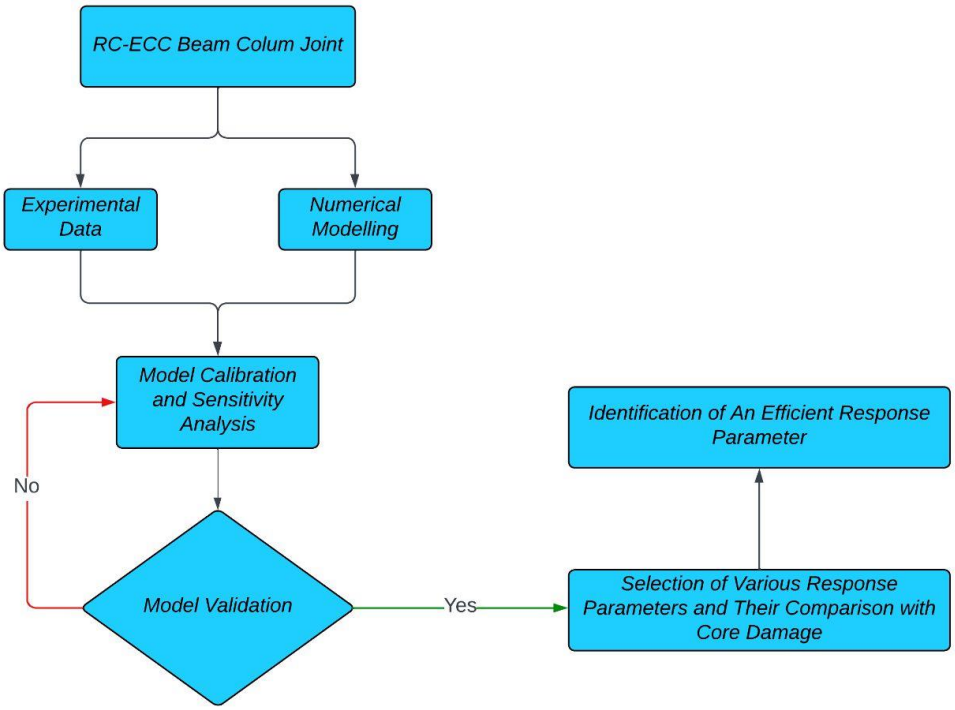

Figure 1: Overall scheme of the present study

2. Materials and Methods

2.1 Model Description

The aim of this investigation was to analyze the performance of a beam-column joint in a reinforced concrete building system, which is a crucial element of constructions designed for moment-resistance. This study utilizes the experimental data from a large-scale BCJ test conducted by Badrashi et al. under reversed-cyclic loading. The specimen was designed to meet the design standards set for Special Moment Resistance Frame SMRF buildings. The numerical model of the specimen was constructed using the Abaqus software. The model includes a beam with cross-sectional dimensions of 304 mm by 457 mm and a length of 2438 mm and joined to columns at mid-height. The beams have a total reinforcement percentage of 1.22%, comprising of three #19 bars at the top and bottom. Shear reinforcement in the beams near the beam-column joint is provided by closed ties measuring 10 mm in diameter and spaced at 76 mm center-to-center, extending 812 mm from the support surface. In addition, after that point, the shear reinforcement is provided with a center-to-center spacing of 152 mm. The stirrup ends meet the SMRF detailing requirements by bending at 135 degrees. The column's dimensions are 2743 mm in height, 304 mm in width, and a depth that is equivalent to that of the beams. The column reinforcement consists of eight uniformly distributed #19 bars along the perimeter, resulting in a total reinforcement percentage of 1.83%. Closed ties are placed at 76 mm center-to-center spacing to reinforce shear in the column along its entire length, including the joint section. To comply with the reinforcement detailing specifications for SMRF buildings, the ties terminate with 135-degree seismic bends. The model's reinforcement detailing is depicted in Figure 2.

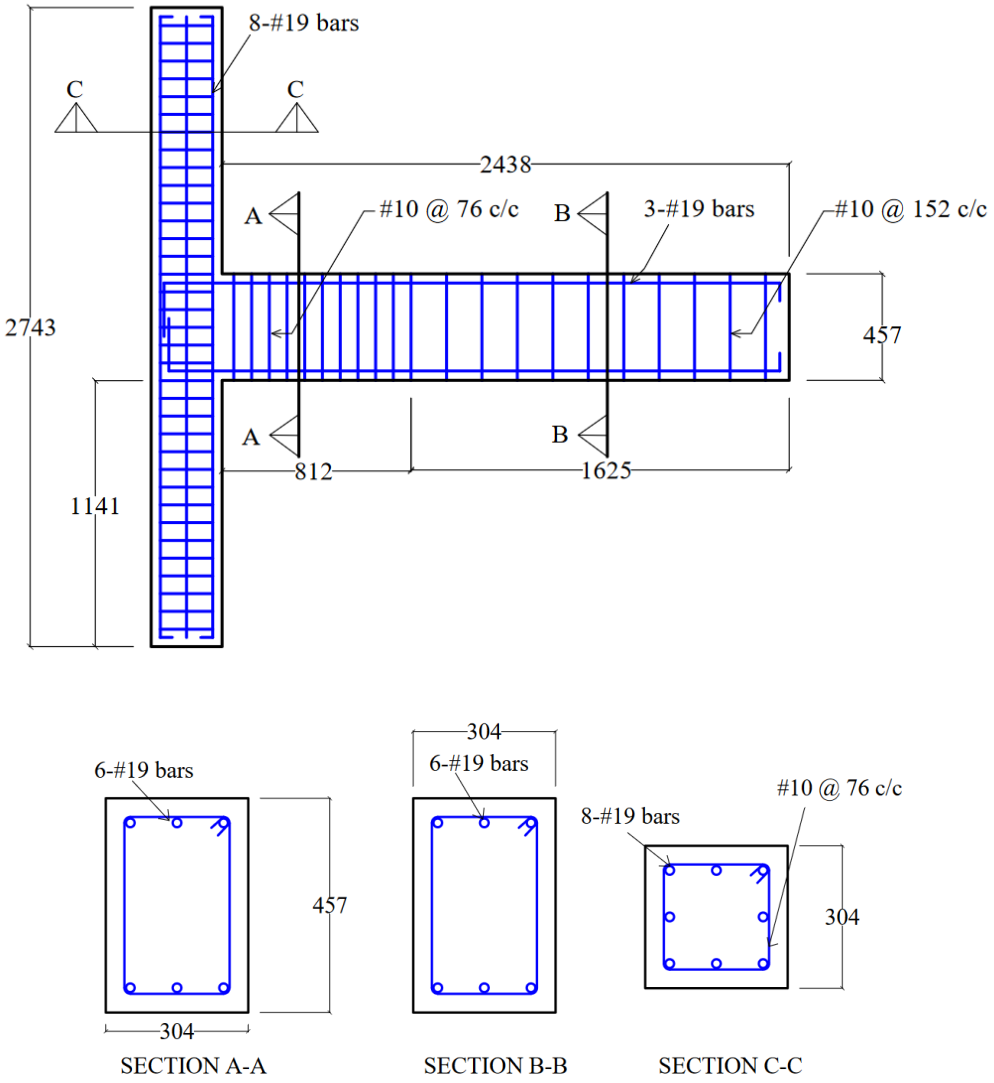

Figure 2: Reinforcement details of specimens (all dimensions in mm)

2.2 Materials

The Concrete Damage Plasticity (CDP) model is utilized as the primary constitutive model for the concrete material. To simulate the behavior of the steel material, an elastic-plastic model is employed. The CDP model is a commonly used numerical method that can replicate the nonlinear behavior of concrete, such as damage initiation and propagation, plastic deformation, and post-peak softening, under complicated loading scenarios. The model is formulated based on a combination of damage and plasticity mechanics principles. It considers the effects of micro-cracking, tensile and compressive strength, and the material's stress-strain relationship. The initiation of damage in the CDP model is determined through a holistic evaluation of both tensile and compressive stresses, while the advancement of damage is depicted by utilizing a degradation function. The plastic response of concrete is modeled using a plasticity law, which considers the material's stress-strain relationship as follows.

$$\boldsymbol{\varepsilon_c^{pl} = \varepsilon_c^{in} - \frac{d_c}{(1 - d_c)} \frac{\sigma_c}{E_0}} \tag{1}$$

The compression damage parameter is denoted by d_c, while the tension damage parameter is represented by d_t, E_0 is modulus of elasticity of the material ε_c^{pl} is compressive plastic strain and ε_c^{in} is compressive inelastic strain. Similarly, it is defined for tension region.

$$\boldsymbol{\varepsilon_t^{pl} = \varepsilon_t^{in} - \frac{d_t}{(1 - d_t)} \frac{\sigma_t}{E_0}} \quad (2)$$

Where ε_t^{pl} is tensile plastic strain and ε_t^{in} is tensile inelastic strain.

The uniaxial stress-strain response of concrete is usually classified into three distinct phases: linear-elastic, hardening, and post-peak softening. The linear-elastic stage corresponds to the initial loading up to the elastic limit (5.52 MPa), as illustrated in **Error! Reference source not found.**a. During the hardening stage, the stress-strain curve exhibits an upward trend from the elastic point (5.52 MPa) to the peak (13.79 MPa). The post-peak softening phase marks the onset and development of compressive damage in the concrete material until it reaches the ultimate compressive strain. This characterization of the concrete behavior is important for understanding the failure mechanisms and predicting the failure loads of concrete structures.

In the CDP model, the initiation of damage in uniaxial compression is defined during the softening procedure, which begins at the peak compressive strength, typically around 13.79 MPa, and corresponds to a strain level of 0.0014 or zero cracking strain. As the cracking strain increases, the damage increases in a non-linear manner, with damage reaching 10% at 0.003 cracking strain and almost 90% at 0.021 cracking strain, as illustrated in **Error! Reference source not found.**b. Having knowledge about the correlation between cracking strain and damage is critical in comprehending the failure mechanisms of concrete, as well as in designing and analyzing concrete structures.

The uniaxial stress-strain behavior of concrete in tension is modeled using a two-phase approach, as depicted in **Error! Reference source not found.**c. The initial phase of the concrete's behavior is characterized by its linear elastic response until it reaches its tensile strength, which is typically at about 1.134 MPa. The second phase involves the development and spread of cracks in the concrete, leading to a nonlinear descending branch in the uniaxial tensile stress-strain curve. Understanding the non-linear behavior of concrete under tensile loading is essential for enhancing the design and analysis of concrete structures, as it enables more precise prediction of their performance.

The initiation of damage in uniaxial tension within the CDP model is defined at the point of tensile strength, which is typically around 1.134 MPa and corresponds to a strain level of 0.0011, or the onset of cracking as shown in **Error! Reference source not found.**d as the cracking strain increases, the damage to the concrete material also increases in a non-linear manner. At a cracking strain of 0.01, the damage to the concrete material is observed to be almost 94%.

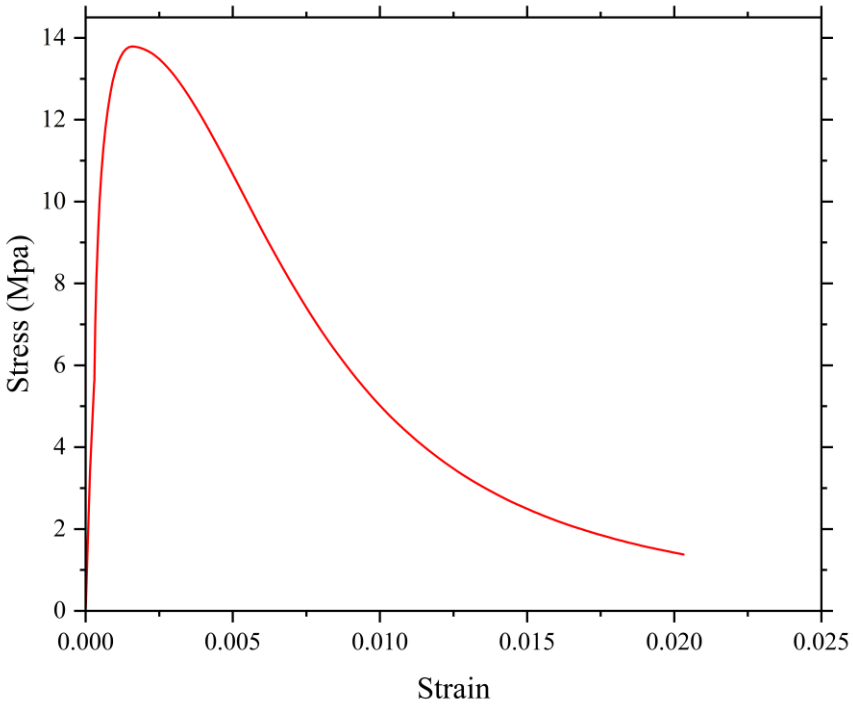
Stress (Mpa)
Strain
0
2
4
6
8
10
12
14
0.000
0.005
0.010
0.015
0.020
0.025

(a)

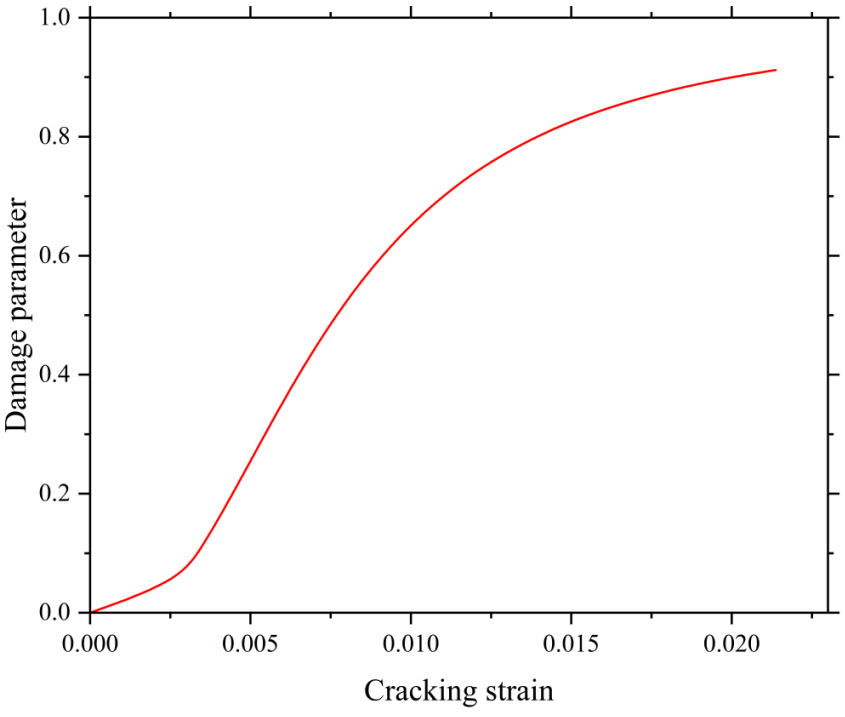
Damage parameter
Cracking strain
0.0
0.2
0.4
0.6
0.8
1.0
0.000
0.005
0.010
0.015
0.020

(b)

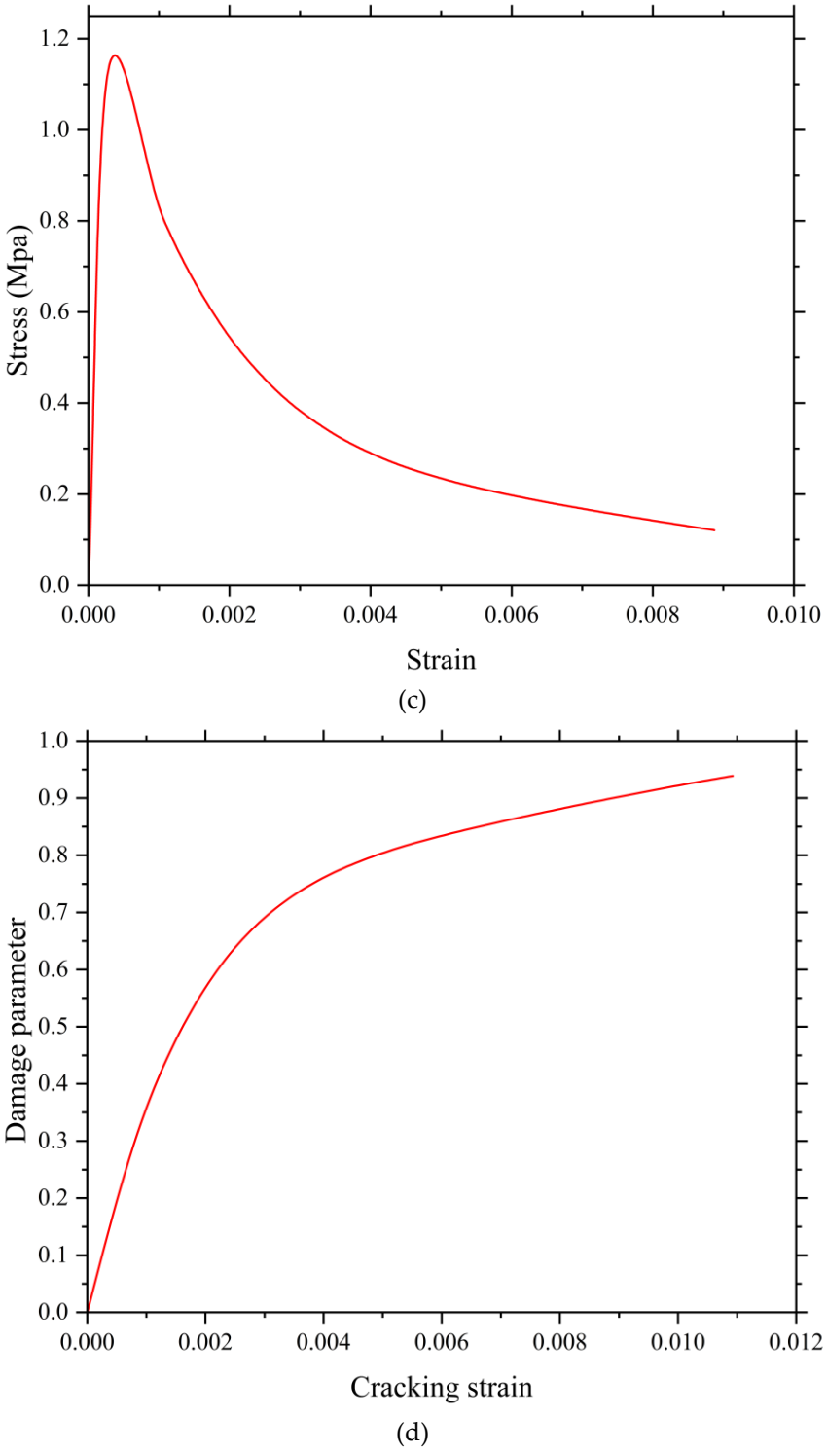

Figure 3. (a) Concrete Uniaxial Compressive Stress-Strain Curve; (b) Concrete compression damage; (c) Concrete Uniaxial Tensile Stress-Strain Curve; (d) Concrete tension damage.

In the Abaqus software, the model requires four parameters, which include dilation angle, eccentricity, ratio of biaxial stress to yield compressive stress, and K parameter to define the yield surface. The dilation angle (ψ) describes the angle at which the plastic behavior of concrete occurs. It determines the extent of plastic dilation in concrete under different loading conditions. The value typically falls between 30-40. The eccentricity (ϵ) represents the speed at which the function approaches the asymptote. It characterizes the discrepancy between the major and minor principal stresses in

concrete, and it impacts the plastic behavior of concrete, specifically with regard to the arrangement and spread of cracks. The ratio of biaxial stress to yield compressive stress $\left(\frac{\sigma_{b0}}{\sigma_{c0}}\right)$ denotes the connection between biaxial stress and yield compressive stress in concrete. This parameter is used to determine the conditions under which plastic deformation begins to occur in concrete. The K parameter represents the ratio of the second stress invariant on the tensile meridian to the compressive meridian at the point of yield, and it characterizes the rate of plastic hardening in concrete. The K parameter has an impact on the behavior of concrete following the point of peak stress, including the rate at which the stress-strain relationship becomes linear. The viscosity parameter describes the rate of plastic deformation in concrete. It is used to model the viscosity of concrete and to simulate its behavior under different loading conditions.

The values of ψ, ϵ, $\frac{\sigma_{b0}}{\sigma_{c0}}$ and K are determined from complete triaxial tests of concrete, while laboratory tests under biaxial loading conditions are necessary to ascertain the value of $\frac{\sigma_{b0}}{\sigma_{c0}}$. In this study, however, the values are accepted from the previous research. Table 1 shows the properties of steel and concrete materials, and Table 6 shows the flow parameters of the CDP model. The model validation and calibration section discuss calibration for various plastic flow parameters.

Table 1: Material information of the study [56]

Details	Concrete	Steel
Mass Density (Kg/m^3)	2400	7850
Compressive Strength (MPa)	13.79	414
Yield Strength (MPa)	-	276
Tensile Strength (MPa)	1.134	414
Poisson's ratio	0.2	0.3
Elastic Modulus (MPa)	19546	200000
Post Yield Modulus of Elasticity (MPa)	-	20000

Table 2: Plasticity flow parameters for CDP model

Plasticity Parameters	Notation	Values
Dilation angle	ψ	30 (Calibrated)
Eccentricity	ϵ	0.1 (Default)
Stress Ratio	$\frac{\sigma_{b0}}{\sigma_{c0}}$	1.16 (Default)
Shape Factor	K	0.66 (Default)
Viscosity	μ	0.0045 (Calibrated)

The material behavior of steel reinforcement is characterized by both elastic and plastic behavior, with the elastic behavior described by Young's modulus and the plastic behavior defined by the post-yielding Young's modulus. The properties of the plastic phase are modeled using bilinear behavior. This approach is crucial for understanding the failure mechanisms and predicting the failure loads of reinforced concrete (RC) structures as it enables the simulation of the complex behavior of reinforcement under tensile loading.

2.3 Boundary conditions and interactions

In the analysis of the exterior BCJ, the boundary conditions were established to replicate the work of Badrashi et al. At the lower end, the column was secured by a pin joint, while at the upper end, it was supported by a roller joint, with the out-of-plane degree of freedom constrained. These boundary conditions are shown in the Figure 12.

The embedded region method was utilized to account for the bond between steel and concrete. This method enables the evaluation of reinforcement elements stiffness independently from concrete elements. By employing this technique, the concrete and steel elements are perfectly joined, and the concrete component in the surrounding can be displaced compatibly with steel bars.

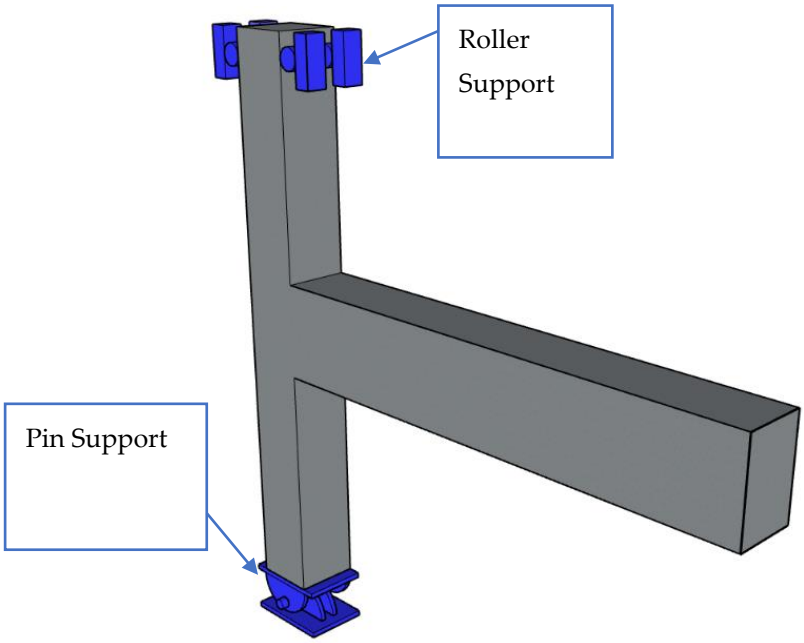

Figure 4: Boundary conditions of test specimen

2.4 Loading

The upper end of the column was subjected to a vertical axial load of 191.229 kN, which was distributed uniformly across the cross-sectional area of the column according to the test setup. The cantilever end of the beam was subjected to a displacement-controlled loading, which imposed a monotonic load of 124 mm as shown in Figure 13. The laboratory experiment applied a two-step loading procedure to the specimen to simulate the actual loading conditions.

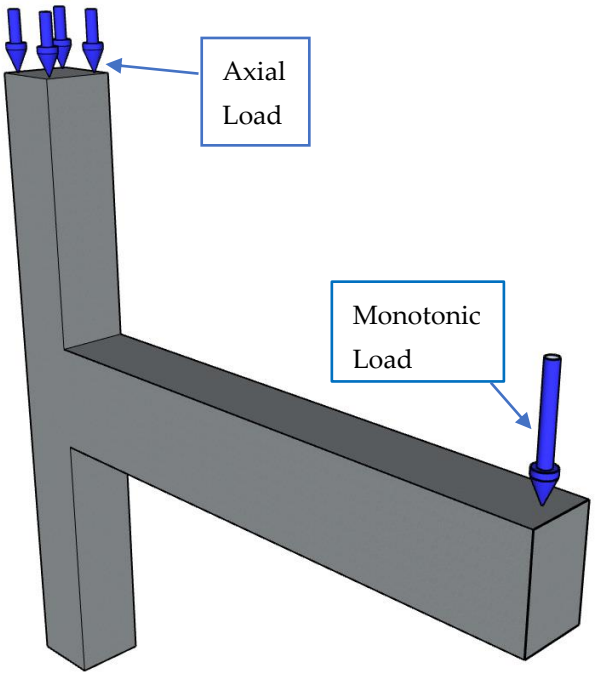

Figure 5: Monotonic load at the beam end and column axial load at top of column

2.5 Meshing

To perform FEM analysis, the steel and concrete elements were discretized into distinct sections. The reinforcing elements were represented by three-dimensional wire elements, while the concrete components were modeled using 3D solid elements. The reinforcement components were represented by 3D Truss, 2 node (T3D2) elements, withstand axial loads and were not intended to consider moments or forces that act perpendicular to the central axis which only withstand axial loads and do not intend to consider moments or forces that act perpendicular to the centerline. The concrete components in the analysis were divided into smaller segments using C3D8R elements, which are 3D, 8 node continuum elements with reduced integration. These elements are commonly used for stress analysis and have a lower number of integration points compared to other types of elements. The mesh convergence analysis was conducted to determine the appropriate mesh size for the simulation. The size of mesh was varied to achieve mesh convergence, with coarser meshes yielding faster solution convergence and finer meshes providing more accurate results at the cost of additional computational expense. The meshed geometry of model is shown in Figure 14 and results of mesh sensitivity analysis are discussed in the next section.

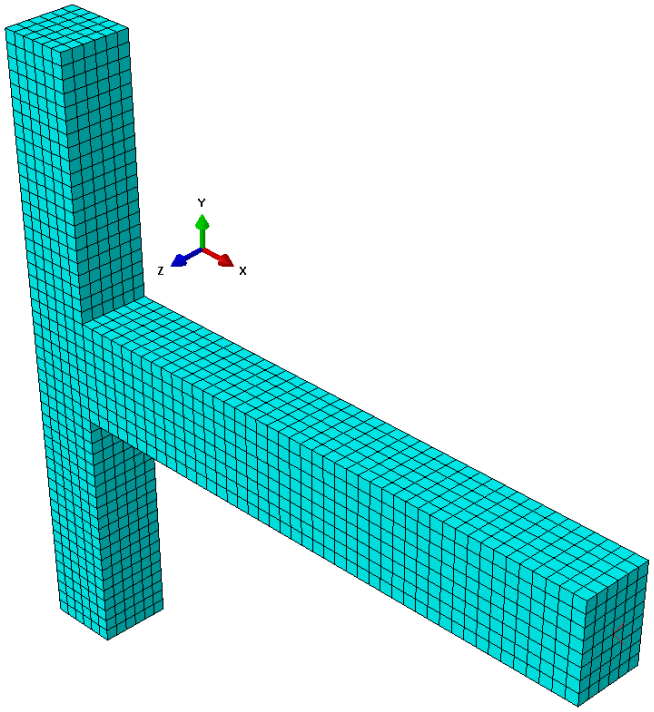

Figure 6: Meshed geometry of structure

3. Model Validation

A thorough analysis was carried out to investigate the impact of parameters on the constitutive equations of the CDP model and to precisely calibrate the model. The investigation includes evaluating the impact of varying the viscosity parameter and dilation angle on the model's behavior. Additionally, a mesh sensitivity analysis has been performed to ensure the reliability of the results. The concept of dilatancy in concrete pertains to the occurrence of inelastic strain due to the expansion of the material's volume when subjected to a triaxial stress state. In the case of connection joint specimens under simulated lateral loads, high shear stress in the joint core creates a compound stress state that is highly sensitive to dilatancy in the analytical model.

A sensitivity analysis was carried out on the dilation angle to examine the impact of dilatancy on the lateral load-displacement response. Figure 15a displays the results, indicating that an increase in the dilation angle leads to a subsequent increase in the ultimate failure load and displacement capacity of the connection.

Previous studies [57]–[59] have suggested that a dilation angle parameter ranging between 30° to 42° is appropriate for modeling concrete materials. The results depicted in Figure 15a indicate that a dilation angle value of 30° is capable of accurately reproducing the load-deformation curve.

The impact of visco-plastic regularization on the CDP constitutive equations was assessed in this study by introducing a viscosity parameter, which was also incorporated in the calibration process of the FEM. The results demonstrated that selecting a relatively small value of 0.0045 for the viscosity parameter, while maintaining a constant element mesh size, led to accurate numerical results that closely matched the experimental data. Figure 15b demonstrates a comparison between the experimental and calculated outcomes, demonstrating the effectiveness of the viscosity parameter in achieving accurate calibration of the FEM model.

To assess the impact of mesh size on the behavior and predicted results of an FEM analysis of an RC exterior beam-column joint, a mesh sensitivity analysis was performed. Four distinct mesh sizes were employed for the concrete, longitudinal rebars, and stirrups, as depicted in the Figure 15c and outlined in the Table 7. The model featured identical geometry, support conditions, loading, mechanical properties, and material models. Through this analysis, it was

determined that further refinement of the mesh size beyond 55 mm for concrete, 55 mm for longitudinal rebars, and 20 mm for stirrups had a minimal impact on the predicted results and did not significantly alter the behavior of the model. This suggests that these mesh sizes provide an appropriate level of resolution for the analysis.

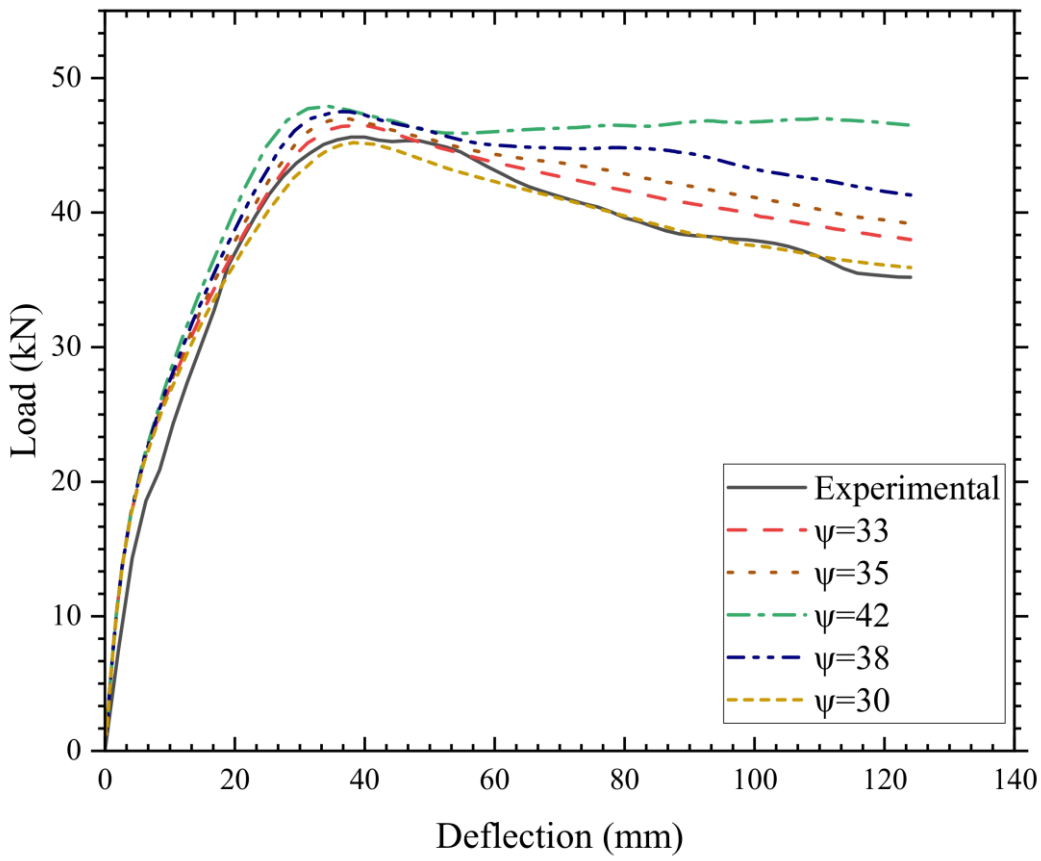

(a)

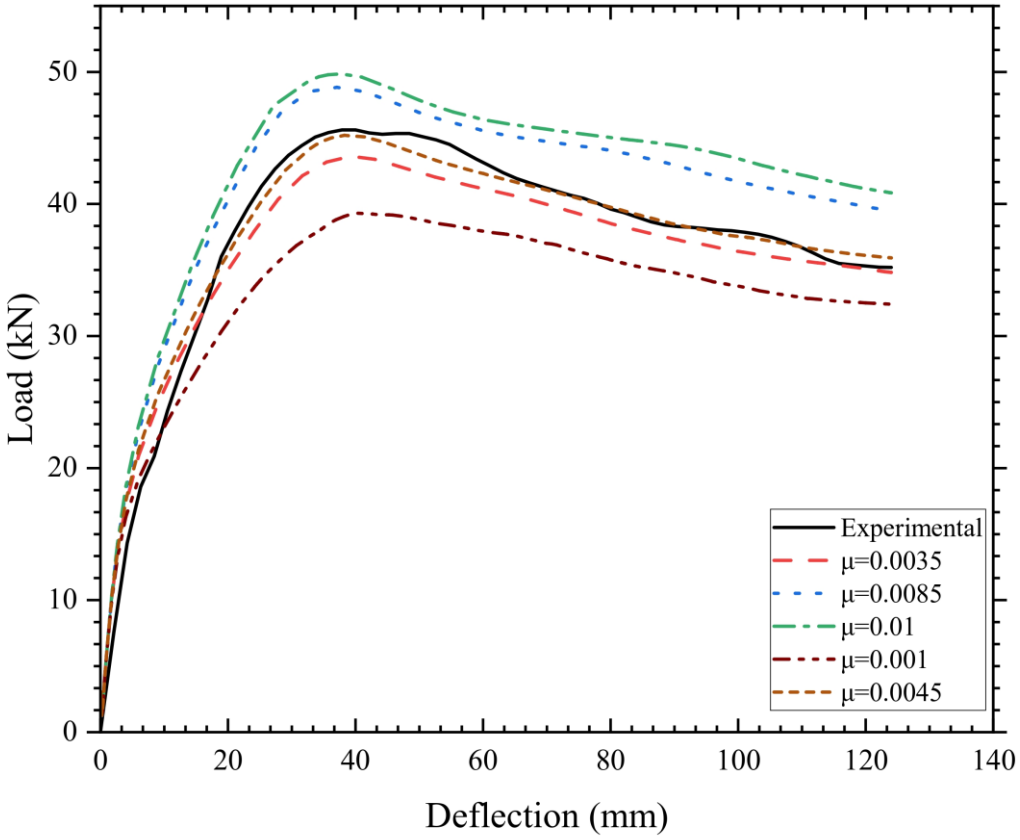
Load (kN)
Deflection (mm)
Experimental
μ=0.0035
μ=0.0085
μ=0.01
μ=0.001
μ=0.0045

(b)

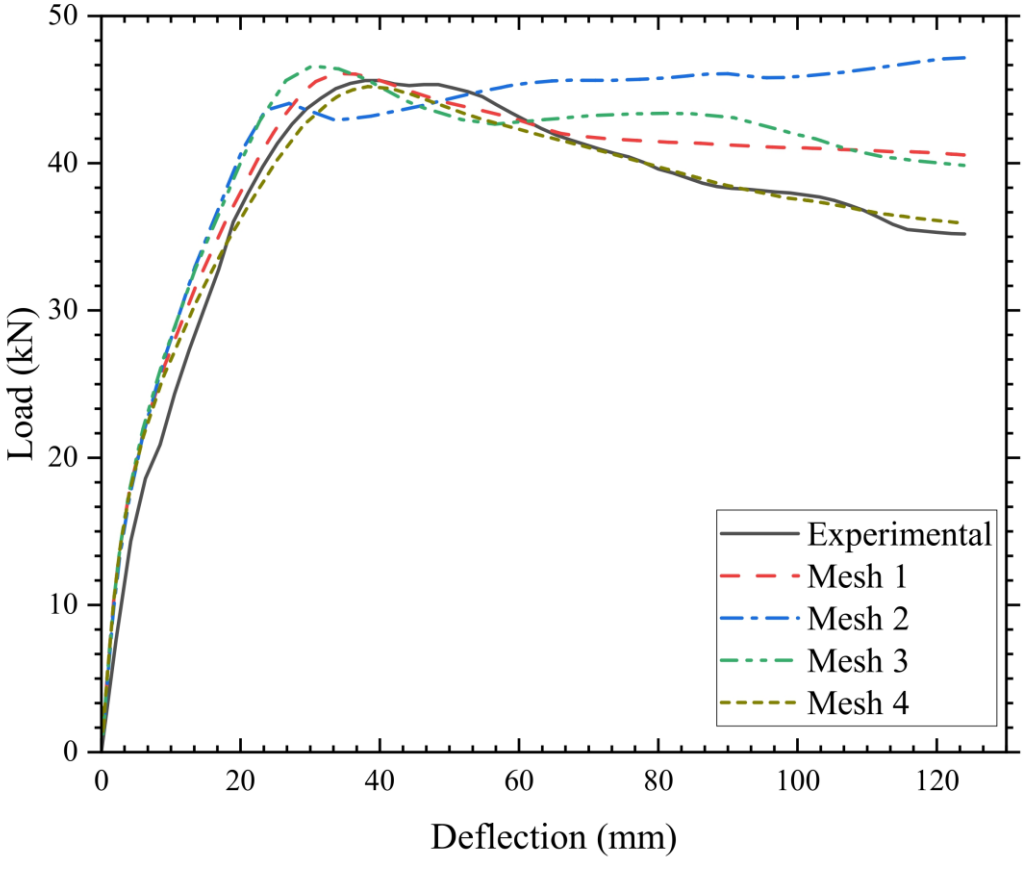
Load (kN)
Deflection (mm)
Experimental
Mesh 1
Mesh 2
Mesh 3
Mesh 4

(c)

Figure 7. (a) Force deflection curve of FEM for different values of dilation angle; (b) Force deflection curve of FEM for different values of viscosity parameter; b) Mesh sensitivity analysis for the numerical model depicting the influence of mesh size on the accuracy of the simulation results.

Table 3: Results of mesh sensitivity analysis

Mesh Name	**Mesh Size(mm)**		
	Concrete	**Longitudinal Rebar**	**Stirrups**
Mesh-1	150	150	50
Mesh-2	100	100	40
Mesh-3	70	70	30
Mesh-4	55	55	20

To evaluate the performance of a reinforced concrete BCJ using FEM, it is essential to validate the numerical model against experimental findings. To validate the numerical model, an exterior beam-column joint specimen was utilized as a reference experiment in this study. The experimental data from a large-scale experimental test by Badrashi et al [54] was utilized for validation. The load-displacement response of the numerical model was compared to experimental findings, which were in close agreement with those reported by Badrashi et al as shown in Figure 16. The agreement between FEM and experimental results is good in terms of ultimate and failure load, and deformation as shown in **Error! Reference source not found.**.

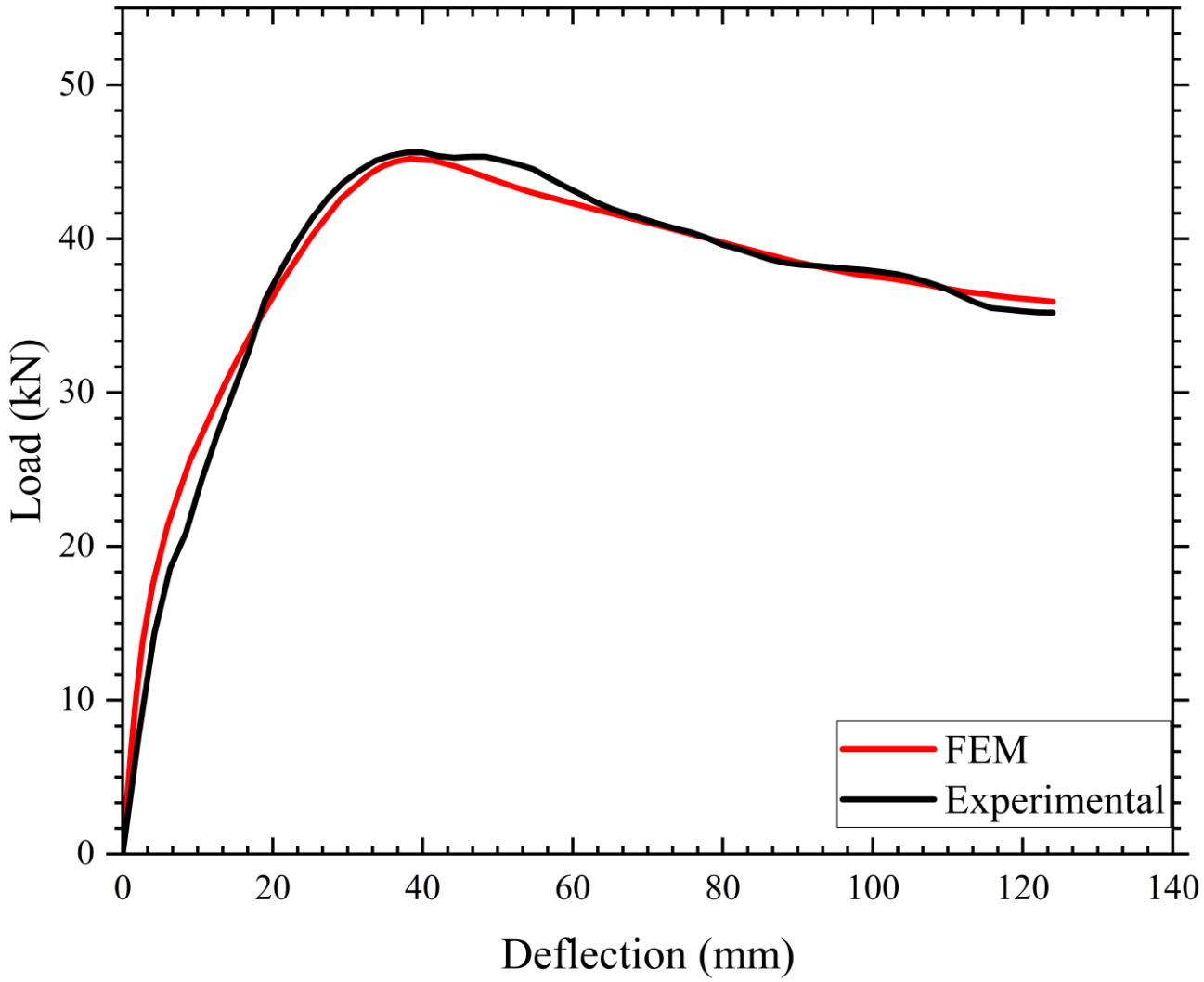

Figure 8: Comparison of experimental and numerical results

Table 4. Comparison of peak and failure loads obtained from FEM and experimental results.

Loads	Experimental	FEM	Percentage Difference
Peak	45.6	45.2	0.88
Failure	35.2	35.9	1.97

4. Results and Discussions

The results of this analysis provided the deflection at free end, deformation, and strain time history of steel reinforcement in the joint. The joint rotation was computed as additional response parameter by the formula given below.

$$\theta = \tan^{-1}\left(\frac{U'_1 - U_1}{h}\right) \times \frac{180^\circ}{\pi\ rad} \quad (3)$$

In this equation, U1′ is displacement of the upper node taken at the upper edge of the beam-column joint and U1 is displacement of the lower node taken at the lower edge of the beam-column joint. For performance enhancement of RC

joint, these response parameters are compared with damage of joint to identify an efficient response parameter, directly related with the failure response of RC joint.

The damage distribution in the specimens was analyzed by quantifying the percentage of damage in joint elements as follows.

$$\text{Damage} = \frac{n_{de}}{nt} \tag{4}$$

Where, nde is total number of elements experienced more than 50 % damage and nt is total elements in the joint. The comparison of damage in joint and response parameters is presented in the Figure 9.

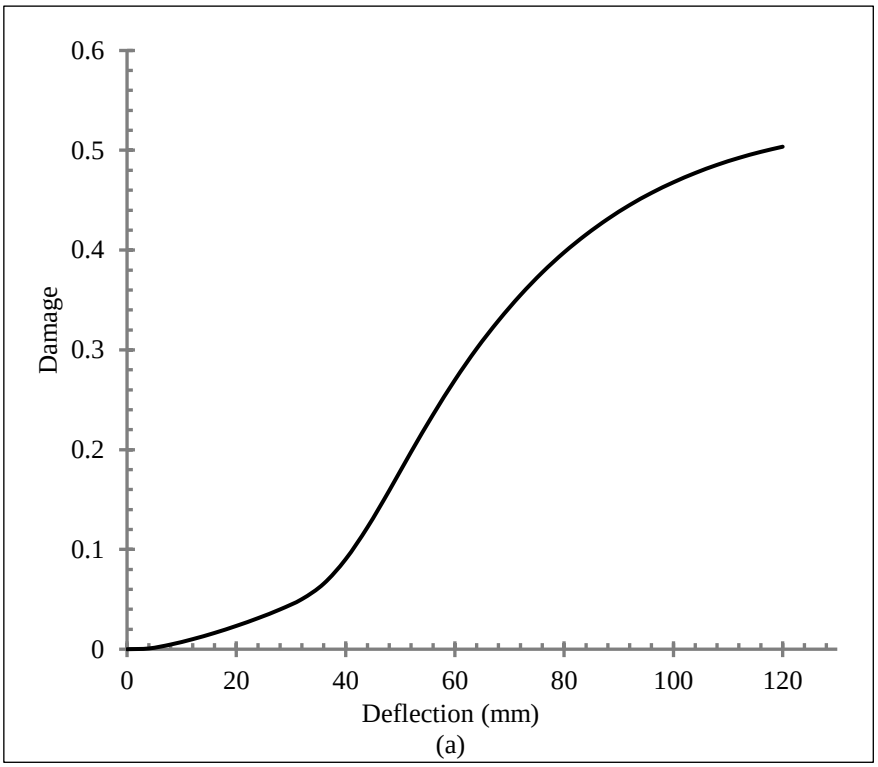

(a)

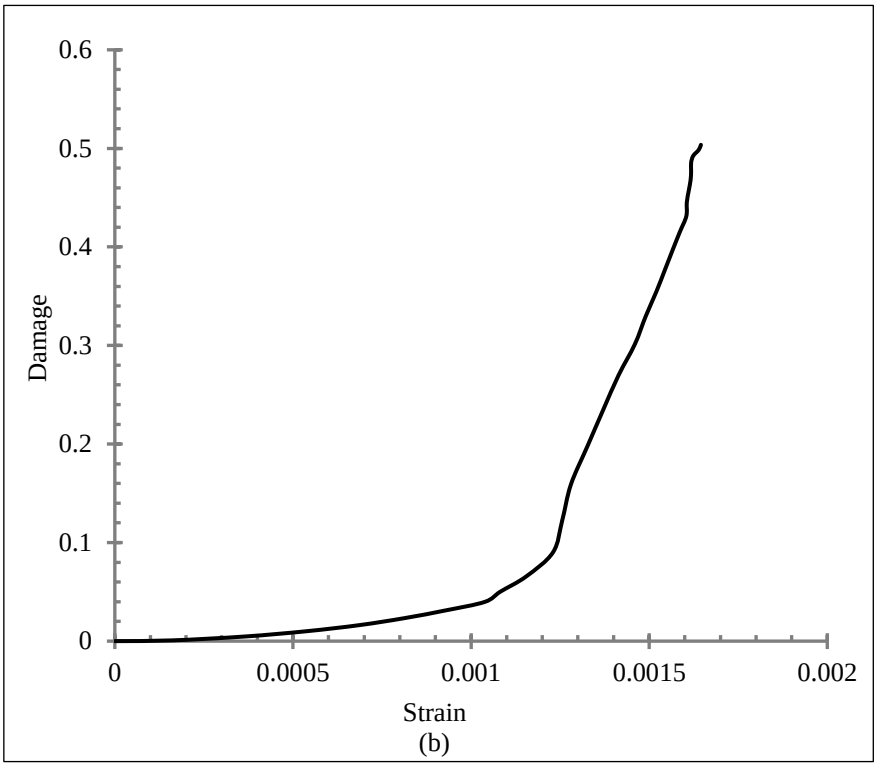

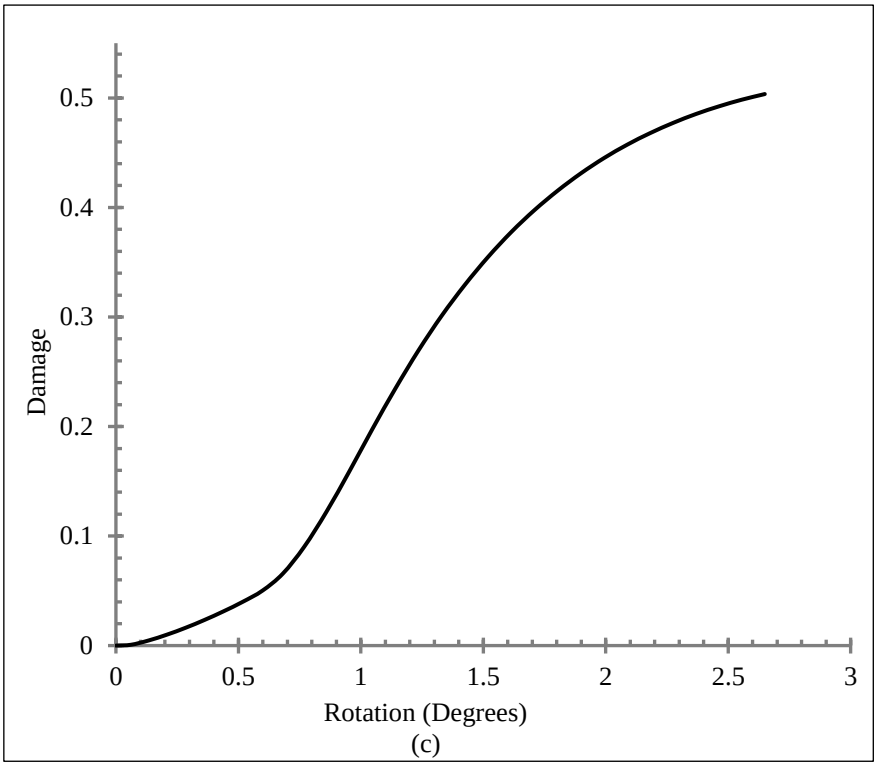

Figure 9: (a) Damage versus deflection (b) Damage versus strain in the steel present in the joint (c)Damage versus rotation of the joint

Figure 9(a) shows the relationship between damage and deflection at the far end of the beam. The figure displays a linear trend until 5% damage, after which the curve becomes parabolic. This indicates that the joint initially exhibits

elastic behavior until a certain level of damage is reached. Beyond this point, the joint enters the plastic range and exhibits more significant deformations. Figure 9(b) depicts the correlation between damage and strain in the bottom steel at the core of the joint. This indicates that the strain level in the steel alone cannot be used to characterize the damage behavior of the joint. Figure 9(c) demonstrates a direct correlation between beam column joint damage and rotation. At 0.5 degrees of rotation, damage is estimated as 5%, increasing to 10% at 0.75 degrees, 20% at 1 degree, and 30% at 1.5 degrees. Subsequent increases in rotation lead to further increases in damage, with an estimated 45% value at 2 degrees of rotation. The beam column joint's maximum rotation value is 2.7 degrees, at which point the damage is estimated to be approximately 50%. These findings have significant implications for understanding the joint's rotational capacity and its potential to correlate with failure mechanisms.

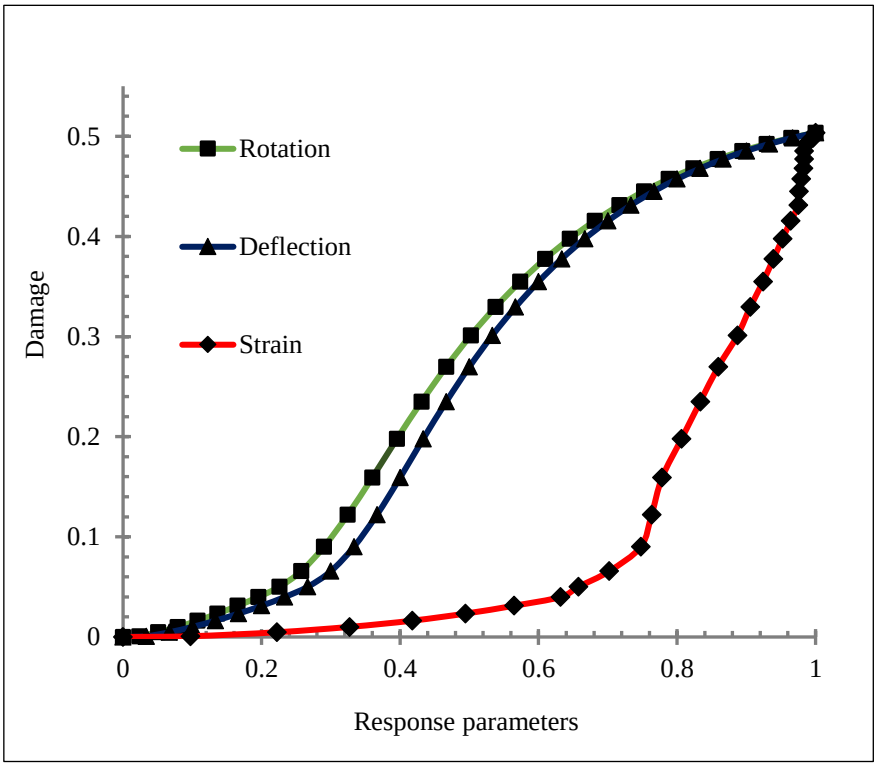

Figure 10: Relationship between damage and response parameters normalized with their maximum values.

Figure 10 is the comparison of all response parameters with damage in the joint. These response parameters were normalized with their corresponding maximum values and were plotted on the same figure. Figure 10 clearly shows that rotation of the joint has the fair relationship with the damage and could be adopted as an efficient response parameter to assess the performance of joint and effectiveness of strengthening method. In the next section, the influence of different reinforcement configurations is discussed, and their effect is evaluated with joint rotation as performance indicator.

4. Conclusions

This study investigated the performance of beam-column joints using FEM and compared the damage of beam-column joints with different response parameters to characterize the failure behaviour and enhance the joint performance. This study identified the effective response parameter that demonstrated a direct relationship to damage in the joint. The main conclusion of this study is given below:

- Through a comparison of response parameters such as rotation, deflection, and strain of reinforcement, it was identified that rotation of the joint has the clearer relationship with joint damage. The most effective response parameter can be valuable in optimizing design in future investigations.

References

Allam, S. M., Elbakry, H. M. F., & Arab, I. S. E. (2018). Exterior reinforced concrete beam column joint subjected to monotonic loading. Alexandria Engineering Journal, 57(4), 4133–4144. https://doi.org/10.1016/j.aej.2018.10.015

Attari, N., Youcef, Y. S., & Amziane, S. (2019). Seismic response of reinforced concrete beam–column joint strengthening by frp sheets. Structures, 20, 353–364. https://doi.org/10.1016/J.ISTRUC.2019.04.007

Chitra, R., & Mohan, S. J. (2021). Materials Today : Proceedings Reinforced concrete beam-column joint ' s ductility behavior. Materials Today: Proceedings, xxxx, 1–5. https://doi.org/10.1016/j.matpr.2021.07.096

Dabiri, H., Kaviani, A., & Kheyroddin, A. (2020). Influence of reinforcement on the response of non-seismically detailed RC beam-column joints. Journal of Building Engineering, 31, 101333. https://doi.org/10.1016/J.JOBE.2020.101333

Dabiri, H., Rahimzadeh, K., & Kheyroddin, A. (2022). A comparison of machine learning- and regression-based models for predicting ductility ratio of RC beam-column joints. Structures, 37, 69–81. https://doi.org/10.1016/J.ISTRUC.2021.12.083

EN 1992-1-1: Eurocode 2: Design of concrete structures - Part 1-1: General rules and rules for buildings. (2004).

Hafezolghorani, M., Hejazi, F., Vaghei, R., Jaafar, M. S. bin, & Karimzade, K. (2017). Simplified damage plasticity model for concrete. Structural Engineering International, 27(1), 68–78. https://doi.org/10.2749/101686616X1081

Hassan, W. M., & Mosalam, K. (2015). SEISMIC RESPONSE OF OLDER-TYPE REINFORCED CONCRETE CORNER JOINTS. July 2009.

Hon, K. K., Ng, C. W., & Chan, P. W. (2020). Machine learning based multi-index prediction of aviation turbulence over the Asia-Pacific. Machine Learning with Applications, 2, 100008. https://doi.org/10.1016/J.MLWA.2020.100008

Kim, J., & LaFave, J. M. (2007). Key influence parameters for the joint shear behaviour of reinforced concrete (RC) beam–column connections. Engineering Structures, 29(10), 2523–2539. https://doi.org/10.1016/J.ENGSTRUCT.2006.12.012

Kotsovou, G., & Mouzakis, H. (2011). Seismic behaviour of RC external joints. Magazine of Concrete Research, 63(4), 247–264. https://doi.org/10.1680/MACR.9.00194

Kreuzer, D., Munz, M., & Schlüter, S. (2020). Short-term temperature forecasts using a convolutional neural network — An application to different weather stations in Germany. Machine Learning with Applications, 2, 100007. https://doi.org/10.1016/j.mlwa.2020.100007

Kristiawan, S. A., Hapsari, I. R., Purwanto, E., & Marwahyudi, M. (2022). Evaluation of damage limit state for rc frame based on fe modeling. Buildings, 12(1). https://doi.org/10.3390/buildings12010021

Lowes, L., & Mitra, N. (2004). A Beam-Column Joint Model for Simulating the Earthquake Response of Reinforced Concrete Frames. Undefined.

Mahmoodzadeh, A., Mohammadi, M., Ibrahim, H. H., Ahmed Rashid, T., Aldalwie, A. H. M., Ali, H. F. H., & Daraei, A. (2021). Tunnel geomechanical parameters prediction using Gaussian process regression. Machine Learning with Applications, 3, 100020. https://doi.org/10.1016/J.MLWA.2021.100020

Masi, A., Santarsiero, G., Lignola, G. P., & Verderame, G. M. (2013). Study of the seismic behavior of external RC beam–column joints through experimental tests and numerical simulations. Engineering Structures, 52, 207–219. https://doi.org/10.1016/J.ENGSTRUCT.2013.02.023

Murty, C. V. R., Rupen, Goswami., A. R. Vijayanarayanan., V. V. Mehta. (2012). E a r t h q u a k e B e h a v i o u r o f B u i l d i n g s. Gujarat State Disaster Management Authority Government of Gujarat, 268.

Najafgholipour, M. A., & Arabi, A. R. (2019). A non-linear model to apply beam-column joint shear failure in analysis of RC moment resisting frames. Structures, 22, 13–27. https://doi.org/10.1016/J.ISTRUC.2019.07.011

Niroomandi, A., Najafgholipour, M. A., & Ronagh, H. R. (2014). Numerical investigation of the affecting parameters on the shear failure of Nonductile RC exterior joints. Engineering Failure Analysis, 46, 62–75. https://doi.org/10.1016/J.ENGFAILANAL.2014.08.003

Park, S., & Mosalam, K. M. (2012). Parameters for shear strength prediction of exterior beam–column joints without transverse reinforcement. Engineering Structures, 36, 198–209. https://doi.org/10.1016/J.ENGSTRUCT.2011.11.017

Pauletta, M., di Marco, C., Frappa, G., Somma, G., Pitacco, I., Miani, M., Das, S., & Russo, G. (2020). Semi-empirical model for shear strength of RC interior beam-column joints subjected to cyclic loads. Engineering Structures, 224, 111223. https://doi.org/10.1016/J.ENGSTRUCT.2020.111223

Chapter 3: Reinforcement Strategies for Improving the Performance of Reinforced Concrete Beam-Column Joints under Seismic Loading

Abstract: This study focuses on the importance of beam-column joints (BCJs) in reinforced concrete (RC) structures and their performance during seismic loads. Failure of these joints can cause partial or complete collapse of the structure, making it crucial to design robust and ductile joints. However, current design standards are still in development, and further research is necessary to enhance joint performance. Excessive reinforcement congestion at joint regions poses a significant challenge for concrete pouring and compaction, resulting in weakened joints that may not withstand earthquake deformations. The study employs Finite Element Modeling (FEM) to improve joint performance by introducing various reinforcement enhancement details in the joint area to overcome reinforcement congestion and insufficient concrete compaction. Twelve different models were developed, each having a beam-column connection with different reinforcement configurations replacing conventional shear stirrups in the joint area. The findings suggest that the utilization of in-plane diagonal bars is more effective in minimizing core damage than out-of-plane diagonal bars. The model with X-shaped reinforcement was identified as the optimal solution for preventing joint failure as it provides high additional rotational stiffness while minimizing core damage in both tension and compression. The study's results are expected to enhance the design methodology of RC joints under seismic loads.

Keywords: Beam-column joints, FEM, reinforcement congestion, core damage, diagonal reinforcement.

1. Introduction

Beam-column joints are an essential constituent of building frames, serving as a link between horizontal and vertical structural elements and thereby facilitating the transfer of seismic forces. These joints play a crucial role in resisting moments generated by different loads, including gravity, wind, and seismic actions. These moments are transmitted through the joints, and failure of a joint can disrupt the load pathway from the beam to the column, which may lead to the progressive collapse of the structure. The primary reason for joint failure in reinforced concrete frames is the high concentration of shear stresses in the joint region, resulting in insufficient joint shear strength [1]. The component materials of the joints have restricted strength and force-carrying capacity, which can lead to severe damage or destruction during an earthquake [2], [3]. Inadequate reinforcement at the junction region contribute to insufficient joint shear strength [4].

During earthquakes, the joints between beams and columns undergo extensive inelastic deformations. If these connections are not properly designed and detailed, they can greatly affect the overall performance of moment-resisting frames. Studies conducted in the aftermath of past catastrophic earthquakes have repeatedly identified beam-column connections as a major cause of damage to existing RC structures [5][6]. Researchers have reported instances of joint shear failures in a number of in-service RC structures subjected to severe seismic loads [7],[8]. This joint shear failure is brittle in nature and can lead to devastating consequences, such as extensive damage and collapse of the entire building [9]. To guarantee the structural soundness of RC frames during earthquakes, it is crucial to properly design the joint and ensure its ductile performance. This is because the ability of a structure to resist destructive forces, specifically seismic loads, is dependent on its ductility. Ductility, in this context, refers to the ability of components or structures to undergo significant deformation without losing strength or rigidity [10]. Furthermore, compared to the interior joints, the exterior joints of a structure are more susceptible to failure because of the torsional effect resulting from the uneven distribution of moments on the exterior joint.

Several studies conducted after significant earthquakes have identified beam-column joints as a leading cause of damage in existing reinforced concrete structures. In many countries that are prone to seismic events, the building codes that were in place prior to seismic activity do not meet current standards for reinforced concrete structures [11]. Although recent earthquakes such as the M7.4 Oaxaca (Mexico), M7.0 Aegean Sea (Turkey-Greece), and M6.4 Croatia have

primarily caused damage to masonry buildings, reinforced concrete buildings have also sustained heavy damage in some cases [12]–[14]. This can be attributed in part to insufficient shear strength and ductility in the beam-column joints of moment-resisting reinforced concrete frame constructions [15]. Since given the difficulty of repairing a fractured joint, it is imperative to minimize the extent of damage during the construction process through the implementation of various techniques. To ensure the earthquake-resistance of a frame, the column must be stronger than the beam. Effective joint panel stirrups are necessary to provide adequate confining pressure and shear strength, which can prevent early brittle collapses [16].

Improving the seismic resistance of structures is a key area of focus for researchers and designers, with special emphasis placed on the BCJs region [17]. These joints are subjected to significant stress during earthquakes and must be designed with sufficient strength and ductility to prevent failure [18]. The susceptibility of beam-column joints to seismic activity is heightened due to the presence of shear stresses that act in several directions [19]. The ACI-ASCE Committee 352R recommends using sufficient lateral hoops in the design of BCJs to reduce diagonal stress failure [20]. However, employing a significant amount of lateral reinforcement may result in congestion in the joint area, making it difficult to pour and compact concrete and potentially weakening the joints' ability to withstand earthquake deformations [21]. Various measures have been suggested to enhance the joint region; however, these have caused construction complications and insufficient compaction of concrete, particularly for exterior BCJs. A 90◦ hook is typically required at the end of beams' longitudinal reinforcements. Researchers have investigated the use of twisting-opposing spiral transverse rebar arrangements to increase joint strength while avoiding congestion [22]. However, strict requirements for joint stirrups resulted in reduced stirrup spacing and did not adequately address joint congestion. Over-congestion of reinforcement bars can lead to improper consolidation, reduced concrete strength, and increased permeability [23].

The existing standards encompass a design guideline aimed at achieving adequate strength in beam-column joints. These guidelines emphasize the provision of sufficient anchorage for beam and column bars within or near the joint region, along with appropriate flexural strength for the beam and column to ensure desired beam-failure mechanisms [24], [25]. Tsonos et al. [26] provided a comprehensive analysis of modern design codes, specifically the Eurocode family of codes, pertaining to the seismic performance of reinforced concrete (RC) beam-column joints, while also comparing them with older standards. Bossio et al. [27] presented a simplified model for strengthening internal RC beam-column joints, which can aid designers in assessing the performance of new structures and facilitating the design of external retrofit measures for existing joints, thereby shifting the initial failure mode to a more desirable one.

In order to improve the structural behavior of precast beam–column connections, Hanif and Kanakubo [28] investigated the use of fiber-reinforced cementitious composite (FRCC) for precast beam-column connections. Steel fibers exhibited increased shear capacity and the largest hysteretic region. PVA fibers performed best in terms of fracture width. Valuable insights were gained for enhancing these connections.

Li et al. [29] examined the cyclic behavior of joints using prefabricated beams and columns made of engineered cementitious composite (ECC). ECC improved load-carrying capacity and ductility of the joints. Longitudinal bars and splicer sleeves increased load-carrying capacity but reduced ductility by shifting the failure mechanism. Connection location had no effect on cyclic behavior when ECC was used.

In a study by Ravichandran [30], fourteen specimens were tested under cyclic loads. One specimen followed seismic code IS 13920 [31], while the others lacked seismic details based on ACI 318 [32]. HyFRC replaced regular concrete at the joint location. Results showed that high-strength concrete with 80% steel and 20% polyolefin improved ductility, energy absorption, and overall strength. Notably, the hybrid fibers specimen with 2% volume fraction (80% steel/20% polyolefin) outperformed the seismic detail specimen in energy absorption capacity and ductility.

Various retrofit techniques are available for non-seismically designed beam-column joints, including jacketing, fiber-reinforced polymer (FRP) wrapping, near-surface mounting, and steel haunch retrofitting. These techniques have demonstrated their efficacy in enhancing joint strength, stiffness, and energy dissipation capacity. However, they are not without limitations. Concrete jacketing, for instance, requires wet construction and reduces usable space [33]–[35]. Steel jacketing and CFRP sheet wrapping face challenges due to the complex geometries of the beam-column-slab joint,

often leading to premature debonding [36]–[39]. The near-surface mounting technique entails a complicated construction process and may lack reliability in terms of near-surface strengthening [40].

Oinam et al. [41] studied the impact of steel fiber volume and reinforced steel detailing in external beam-column joints. Diagonal positioning of longitudinal beam bars led to interfacial shear fractures, while straight bars exhibited flexural plastic hinges away from the joints. Steel fiber-reinforced concrete (SFRC) in the joint region demonstrated remarkable ductility, energy absorption, and consistent hysteresis response, despite increased hoop spacing.

In recent studies, the implementation of diagonal reinforcement has been proposed as a means to strengthen joints and enhance their behavior [42]–[44]. Tsons et al. [45] observed that the use of diagonal bars in reinforced concrete (RC) exterior beam-column joints enables them to sustain higher horizontal shear stress compared to conventional stirrups. Au et al. [46] reported that interior beam-column joints with diagonal bars exhibited increased load-carrying capacity and improved bond conditions, contributing to the overall stiffness of the structure. Chalioris et al. [47] investigated the seismic performance of exterior beam-column joints and found that specimens with X-bars demonstrated higher load-carrying capacity and increased energy dissipation. These findings indicate that the inclusion of crossed inclined bars can enhance joint performance. Various analytical models have also been developed to estimate the shear strength of beam-column joints with diagonal bars, showing that such bars can withstand higher shear stress [48], [49].
Several methods have been employed by researchers to study the performance of RC beam-column connections and develop techniques to enhance their performance. The use of high-cost and practically limited strengthening options, such as fiber-reinforced polymer (FRP) composites and shape memory alloys (SMAs), has been explored in the literature [50], [51]. Alternative reinforcement detailing options have also been investigated by several researchers, with a focus on factors such as bond condition, bar diameter, column steel cage, and vertical bars, to improve BCJs performance [52], [53].

Despite the existing methods to analyze the behavior of BCJs and to propose strengthening strategies, there remains a gap in the understanding of the mechanisms that lead to the observed improvements in the failure behavior and performance of BCJs. Current methods have limitations in providing a direct explanation of these mechanisms, which can hinder the development of effective strengthening strategies. Additionally, the high level of congestion in practical applications poses a significant challenge to the effective implementation of strengthening strategies. Thus, there is a pressing need for new approaches that can address these limitations and provide a deeper understanding of the failure mechanisms of BCJs in the context of congested joints, to enable the development of more effective strengthening strategies that can be practically implemented to effectively improve the safety and resilience of RC structures.

In summary, Beam-column joints are crucial components in building frames that connect horizontal and vertical structural elements, facilitating the transfer of seismic forces. Failure of these joints can lead to the collapse of the structure. The main cause of joint failure in reinforced concrete frames is the high concentration of shear stresses, resulting in insufficient joint shear strength. Joint failures during earthquakes have been identified as a major cause of damage to existing structures. Properly designed and detailed joints with sufficient strength and ductility are essential for the seismic resistance of structures. Exterior joints are more susceptible to failure due to torsional effects. Many existing building codes do not meet current standards for reinforced concrete structures in seismic-prone areas. Various techniques have been proposed to enhance joint strength, but they can lead to construction complications. Researchers have explored the use of fiber-reinforced cementitious composites and alternative reinforcement detailing options to improve joint performance. Retrofit techniques such as jacketing and FRP wrapping have shown efficacy but also have limitations. Diagonal reinforcement has been suggested to strengthen joints and improve their behavior. However, there is a gap in understanding the underlying failure mechanisms of beam-column joints and the development of effective strengthening strategies. The high congestion in practical applications poses a challenge for implementing strengthening measures. New approaches are needed to address these limitations and provide a deeper understanding of failure mechanisms to develop more effective strengthening strategies for the safety and resilience of reinforced concrete structures. This paper is organized into the following three sections: numerical modelling; main findings and results; and conclusions and recommendations. The overall scheme of the present study is provided in Figure 9: Overall scheme of the present study.

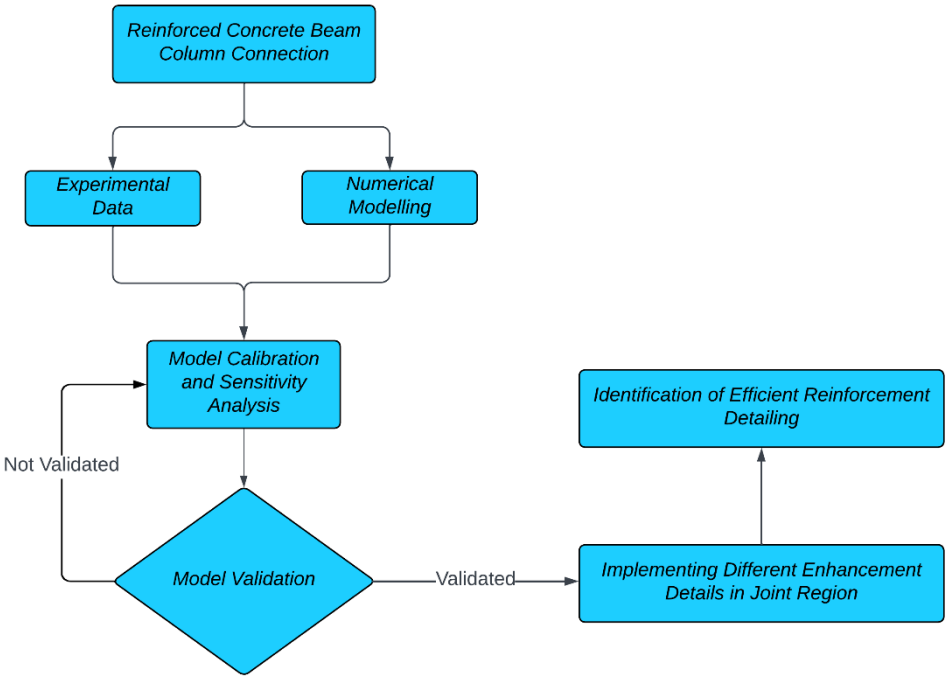

Figure 9: Overall scheme of the present study

2. Materials and Methods

2.1 Model Description

The aim of this investigation was to analyze the performance of a beam-column joint in a reinforced concrete building system, which is a crucial element of constructions designed for moment-resistance. This study utilizes the experimental data from a large-scale BCJ test conducted by Badrashi et al [54] under reversed-cyclic loading. The specimen was designed to meet the design standards set for Special Moment Resistance Frame SMRF buildings. The numerical model of the specimen was constructed using the Abaqus software. The model includes a beam with cross-sectional dimensions of 304 mm by 457 mm and a length of 2438 mm and joined to columns at mid-height. The beams have a total reinforcement percentage of 1.22%, comprising of three #19 bars at the top and bottom. Shear reinforcement in the beams near the beam-column joint is provided by closed ties measuring 10 mm in diameter and spaced at 76 mm center-to-center, extending 812 mm from the support surface. In addition, after that point, the shear reinforcement is provided with a center-to-center spacing of 152 mm. The stirrup ends meet the SMRF detailing requirements by bending at 135 degrees. The column's dimensions are 2743 mm in height, 304 mm in width, and a depth that is equivalent to that of the beams. The column reinforcement consists of eight uniformly distributed #19 bars along the perimeter, resulting in a total reinforcement percentage of 1.83%. Closed ties are placed at 76 mm center-to-center spacing to reinforce shear in the column along its entire length, including the joint section. To comply with the reinforcement detailing specifications for SMRF buildings, the ties terminate with 135-degree seismic bends. The model's reinforcement detailing is depicted in Figure 2.

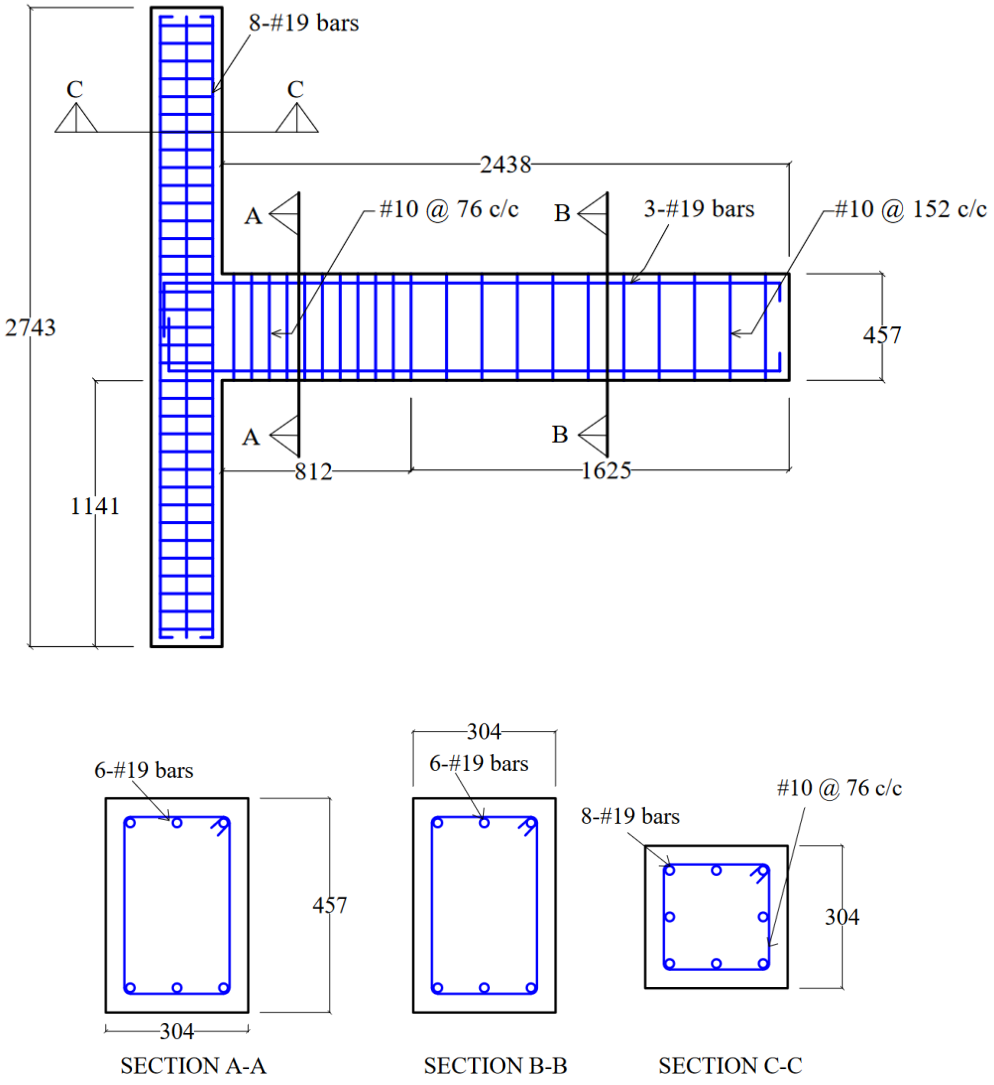

Figure 10: Reinforcement details of specimens (all dimensions in mm)

2.2 Materials

The Concrete Damage Plasticity (CDP) model is utilized as the primary constitutive model for the concrete material. [55]. To simulate the behavior of the steel material, an elastic-plastic model is employed. The CDP model is a commonly used numerical method that can replicate the nonlinear behavior of concrete, such as damage initiation and propagation, plastic deformation, and post-peak softening, under complicated loading scenarios. The model is formulated based on a combination of damage and plasticity mechanics principles. It considers the effects of micro-cracking, tensile and compressive strength, and the material's stress-strain relationship. The initiation of damage in the CDP model is determined through a holistic evaluation of both tensile and compressive stresses, while the advancement of damage is depicted by utilizing a degradation function. The plastic response of concrete is modeled using a plasticity law, which considers the material's stress-strain relationship as follows.

$$\boldsymbol{\varepsilon_c^{pl} = \varepsilon_c^{in} - \frac{d_c}{(1 - d_c)} \frac{\sigma_c}{E_0}} \tag{5}$$

The compression damage parameter is denoted by d_c, while the tension damage parameter is represented by d_t, E_0 is modulus of elasticity of the material ε_c^{pl} is compressive plastic strain and ε_c^{in} is compressive inelastic strain. Similarly, it is defined for tension region.

$$\boldsymbol{\varepsilon_t^{pl} = \varepsilon_t^{in} - \frac{d_t}{(1 - d_t)} \frac{\sigma_t}{E_0}} \quad (6)$$

Where ε_t^{pl} is tensile plastic strain and ε_t^{in} is tensile inelastic strain.

The uniaxial stress-strain response of concrete is usually classified into three distinct phases: linear-elastic, hardening, and post-peak softening. The linear-elastic stage corresponds to the initial loading up to the elastic limit (5.52 MPa), as illustrated in **Error! Reference source not found.**a. During the hardening stage, the stress-strain curve exhibits an upward trend from the elastic point (5.52 MPa) to the peak (13.79 MPa). The post-peak softening phase marks the onset and development of compressive damage in the concrete material until it reaches the ultimate compressive strain. This characterization of the concrete behavior is important for understanding the failure mechanisms and predicting the failure loads of concrete structures.

In the CDP model, the initiation of damage in uniaxial compression is defined during the softening procedure, which begins at the peak compressive strength, typically around 13.79 MPa, and corresponds to a strain level of 0.0014 or zero cracking strain. As the cracking strain increases, the damage increases in a non-linear manner, with damage reaching 10% at 0.003 cracking strain and almost 90% at 0.021 cracking strain, as illustrated in **Error! Reference source not found.**b. Having knowledge about the correlation between cracking strain and damage is critical in comprehending the failure mechanisms of concrete, as well as in designing and analyzing concrete structures.

The uniaxial stress-strain behavior of concrete in tension is modeled using a two-phase approach, as depicted in **Error! Reference source not found.**c. The initial phase of the concrete's behavior is characterized by its linear elastic response until it reaches its tensile strength, which is typically at about 1.134 MPa. The second phase involves the development and spread of cracks in the concrete, leading to a nonlinear descending branch in the uniaxial tensile stress-strain curve. Understanding the non-linear behavior of concrete under tensile loading is essential for enhancing the design and analysis of concrete structures, as it enables more precise prediction of their performance.

The initiation of damage in uniaxial tension within the CDP model is defined at the point of tensile strength, which is typically around 1.134 MPa and corresponds to a strain level of 0.0011, or the onset of cracking as shown in **Error! Reference source not found.**d as the cracking strain increases, the damage to the concrete material also increases in a non-linear manner. At a cracking strain of 0.01, the damage to the concrete material is observed to be almost 94%.

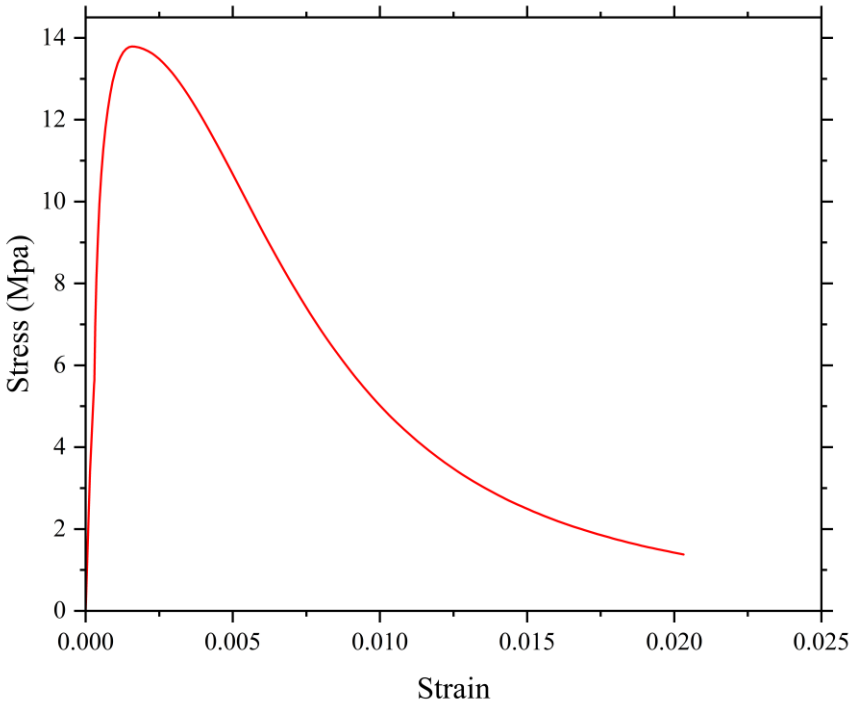
Stress (Mpa)
Strain
0
2
4
6
8
10
12
14
0.000
0.005
0.010
0.015
0.020
0.025

(a)

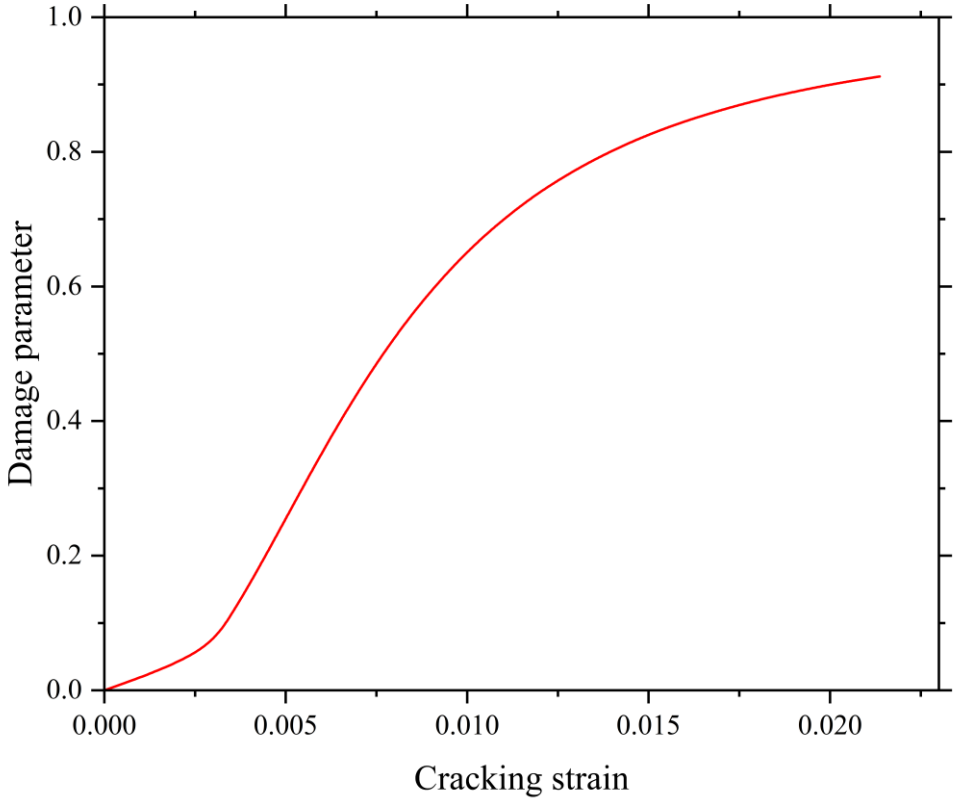
Damage parameter
Cracking strain
0.0
0.2
0.4
0.6
0.8
1.0
0.000
0.005
0.010
0.015
0.020

(b)

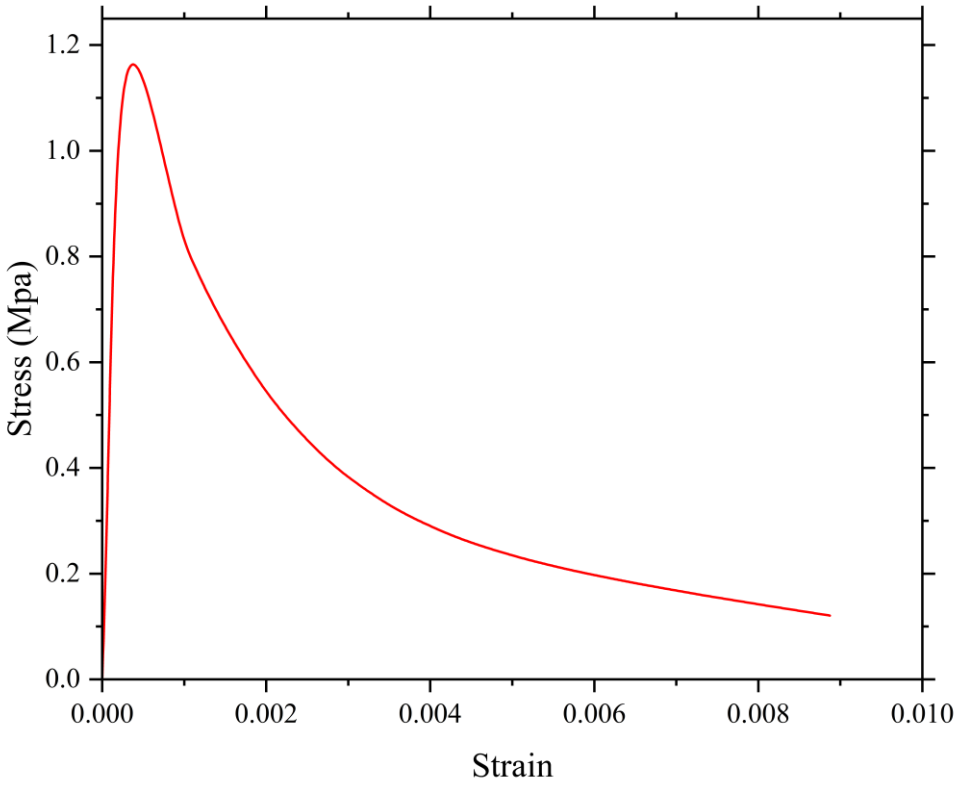

(c)

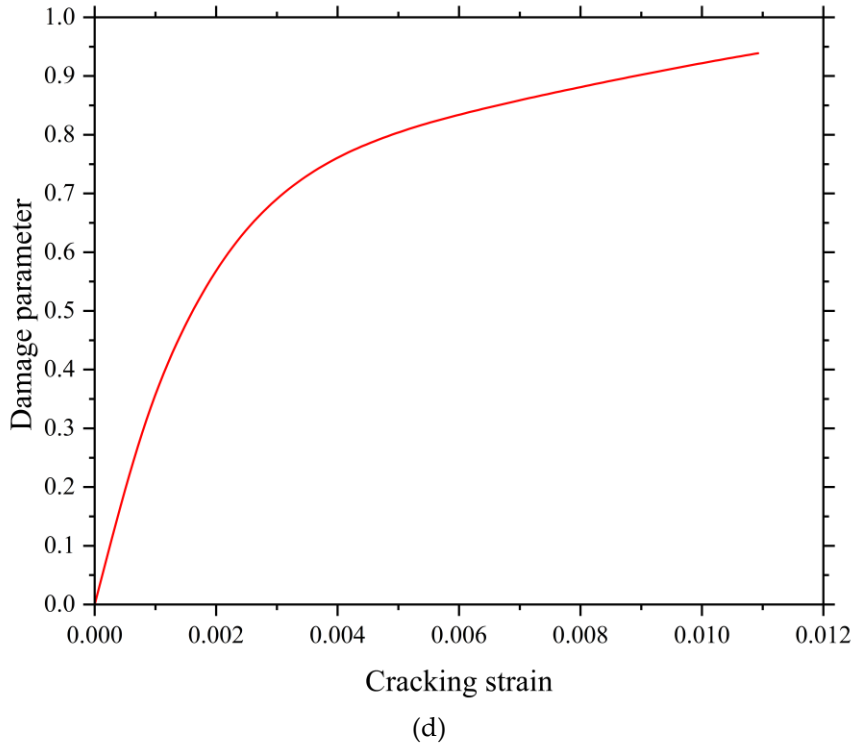

(d)

Figure 11. (a) Concrete Uniaxial Compressive Stress-Strain Curve; (b) Concrete compression damage; (c) Concrete Uniaxial Tensile Stress-Strain Curve; (d) Concrete tension damage.

In the Abaqus software, the model requires four parameters, which include dilation angle, eccentricity, ratio of biaxial stress to yield compressive stress, and K parameter to define the yield surface. The dilation angle (ψ) describes the angle at which the plastic behavior of concrete occurs. It determines the extent of plastic dilation in concrete under different

loading conditions. The value typically falls between 30-40. The eccentricity (ϵ) represents the speed at which the function approaches the asymptote. It characterizes the discrepancy between the major and minor principal stresses in concrete, and it impacts the plastic behavior of concrete, specifically with regard to the arrangement and spread of cracks. The ratio of biaxial stress to yield compressive stress $\left(\frac{\sigma_{b0}}{\sigma_{c0}}\right)$ denotes the connection between biaxial stress and yield compressive stress in concrete. This parameter is used to determine the conditions under which plastic deformation begins to occur in concrete. The K parameter represents the ratio of the second stress invariant on the tensile meridian to the compressive meridian at the point of yield, and it characterizes the rate of plastic hardening in concrete. The K parameter has an impact on the behavior of concrete following the point of peak stress, including the rate at which the stress-strain relationship becomes linear. The viscosity parameter describes the rate of plastic deformation in concrete. It is used to model the viscosity of concrete and to simulate its behavior under different loading conditions.

The values of ψ, ϵ, $\frac{\sigma_{b0}}{\sigma_{c0}}$ and K are determined from complete triaxial tests of concrete, while laboratory tests under biaxial loading conditions are necessary to ascertain the value of $\frac{\sigma_{b0}}{\sigma_{c0}}$. In this study, however, the values are accepted from the previous research [56]. Table 5: Material information of the study [56] shows the properties of steel and concrete materials, and Table 6: Plasticity flow parameters for CDP model Table 6 shows the flow parameters of the CDP model. The model validation and calibration section discuss calibration for various plastic flow parameters.

Table 5: Material information of the study [56]

Details	Concrete	Steel
Mass Density (Kg/m^3)	2400	7850
Compressive Strength (MPa)	13.79	414
Yield Strength (MPa)	-	276
Tensile Strength (MPa)	1.134	414
Poisson's ratio	0.2	0.3
Elastic Modulus (MPa)	19546	200000
Post Yield Modulus of Elasticity (MPa)	-	20000

Table 6: Plasticity flow parameters for CDP model

Plasticity Parameters	Notation	Values
Dilation angle	ψ	30 (Calibrated)
Eccentricity	ϵ	0.1 (Default)
Stress Ratio	$\frac{\sigma_{b0}}{\sigma_{c0}}$	1.16 (Default)
Shape Factor	K	0.66 (Default)
Viscosity	μ	0.0045 (Calibrated)

The material behavior of steel reinforcement is characterized by both elastic and plastic behavior, with the elastic behavior described by Young's modulus and the plastic behavior defined by the post-yielding Young's modulus. The properties of the plastic phase are modeled using bilinear behavior. This approach is crucial for understanding the failure mechanisms and predicting the failure loads of reinforced concrete (RC) structures as it enables the simulation of the complex behavior of reinforcement under tensile loading.

2.3 Boundary conditions and interactions

In the analysis of the exterior BCJ, the boundary conditions were established to replicate the work of Badrashi et al [54]. At the lower end, the column was secured by a pin joint, while at the upper end, it was supported by a roller joint, with the out-of-plane degree of freedom constrained. These boundary conditions are shown in the Figure 12.

The embedded region method was utilized to account for the bond between steel and concrete. This method enables the evaluation of reinforcement elements stiffness independently from concrete elements. By employing this technique, the concrete and steel elements are perfectly joined, and the concrete component in the surrounding can be displaced compatibly with steel bars.

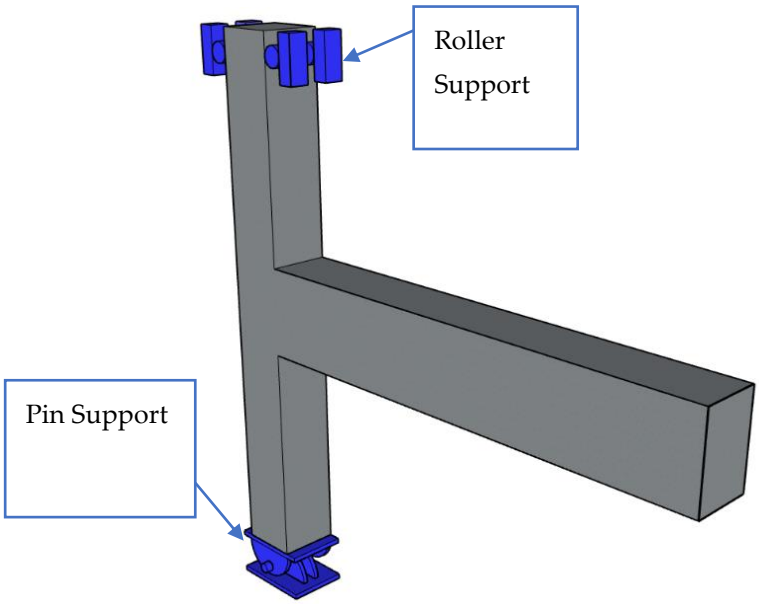

Figure 12: Boundary conditions of test specimen

2.4 Loading

The upper end of the column was subjected to a vertical axial load of 191.229 kN, which was distributed uniformly across the cross-sectional area of the column according to the test setup. The cantilever end of the beam was subjected to a displacement-controlled loading, which imposed a monotonic load of 124 mm as shown in Figure 13. The laboratory experiment applied a two-step loading procedure to the specimen to simulate the actual loading conditions [54].

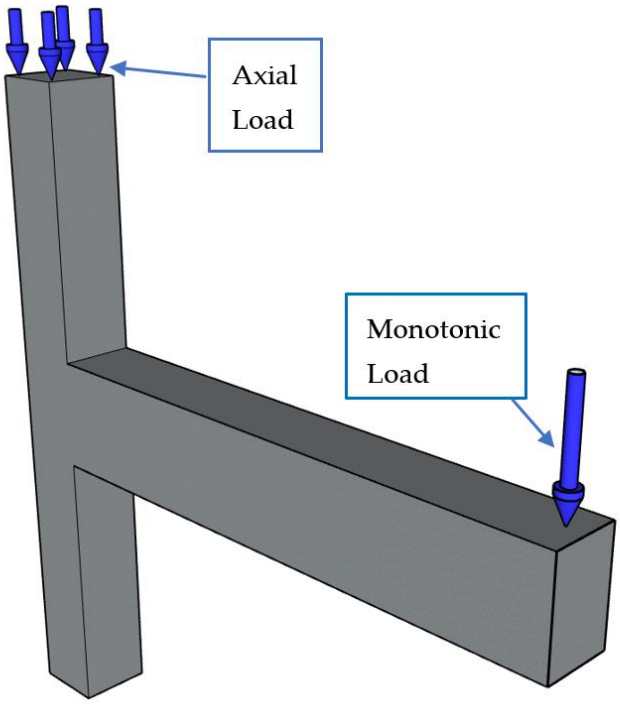

Figure 13: Monotonic load at the beam end and column axial load at top of column

2.5 Meshing

To perform FEM analysis, the steel and concrete elements were discretized into distinct sections. The reinforcing elements were represented by three-dimensional wire elements, while the concrete components were modeled using 3D solid elements. The reinforcement components were represented by 3D Truss, 2 node (T3D2) elements, withstand axial loads and were not intended to consider moments or forces that act perpendicular to the central axis which only withstand axial loads and do not intend to consider moments or forces that act perpendicular to the centerline. The concrete components in the analysis were divided into smaller segments using C3D8R elements, which are 3D, 8 node continuum elements with reduced integration. These elements are commonly used for stress analysis and have a lower number of integration points compared to other types of elements. The mesh convergence analysis was conducted to determine the appropriate mesh size for the simulation. The size of mesh was varied to achieve mesh convergence, with coarser meshes yielding faster solution convergence and finer meshes providing more accurate results at the cost of additional computational expense. The meshed geometry of model is shown in Figure 14 and results of mesh sensitivity analysis are discussed in the next section.

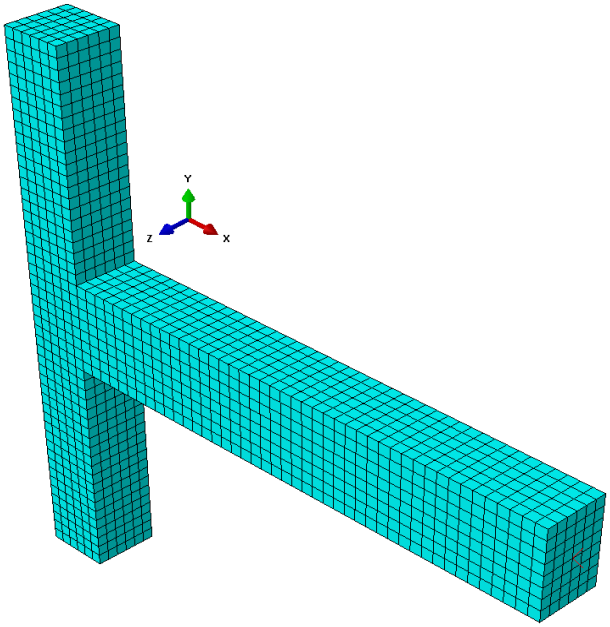

Figure 14: Meshed geometry of structure

3. Model Validation

A thorough analysis was carried out to investigate the impact of parameters on the constitutive equations of the CDP model and to precisely calibrate the model. The investigation includes evaluating the impact of varying the viscosity parameter and dilation angle on the model's behavior. Additionally, a mesh sensitivity analysis has been performed to ensure the reliability of the results. The concept of dilatancy in concrete pertains to the occurrence of inelastic strain due to the expansion of the material's volume when subjected to a triaxial stress state. In the case of connection joint specimens under simulated lateral loads, high shear stress in the joint core creates a compound stress state that is highly sensitive to dilatancy in the analytical model.

A sensitivity analysis was carried out on the dilation angle to examine the impact of dilatancy on the lateral load-displacement response. Figure 15a displays the results, indicating that an increase in the dilation angle leads to a subsequent increase in the ultimate failure load and displacement capacity of the connection.

Previous studies [57]–[59] have suggested that a dilation angle parameter ranging between 30° to 42° is appropriate for modeling concrete materials. The results depicted in Figure 15a indicate that a dilation angle value of 30° is capable of accurately reproducing the load-deformation curve.

The impact of visco-plastic regularization on the CDP constitutive equations was assessed in this study by introducing a viscosity parameter, which was also incorporated in the calibration process of the FEM. The results demonstrated that selecting a relatively small value of 0.0045 for the viscosity parameter, while maintaining a constant element mesh size, led to accurate numerical results that closely matched the experimental data. Figure 15b demonstrates a comparison between the experimental and calculated outcomes, demonstrating the effectiveness of the viscosity parameter in achieving accurate calibration of the FEM model.

To assess the impact of mesh size on the behavior and predicted results of an FEM analysis of an RC exterior beam-column joint, a mesh sensitivity analysis was performed. Four distinct mesh sizes were employed for the concrete, longitudinal rebars, and stirrups, as depicted in the Figure 15c and outlined in the Table 7. The model featured identical geometry, support conditions, loading, mechanical properties, and material models. Through this analysis, it was determined that further refinement of the mesh size beyond 55 mm for concrete, 55 mm for longitudinal rebars, and 20 mm for stirrups had a minimal impact on the predicted results and did not significantly alter the behavior of the model. This suggests that these mesh sizes provide an appropriate level of resolution for the analysis.

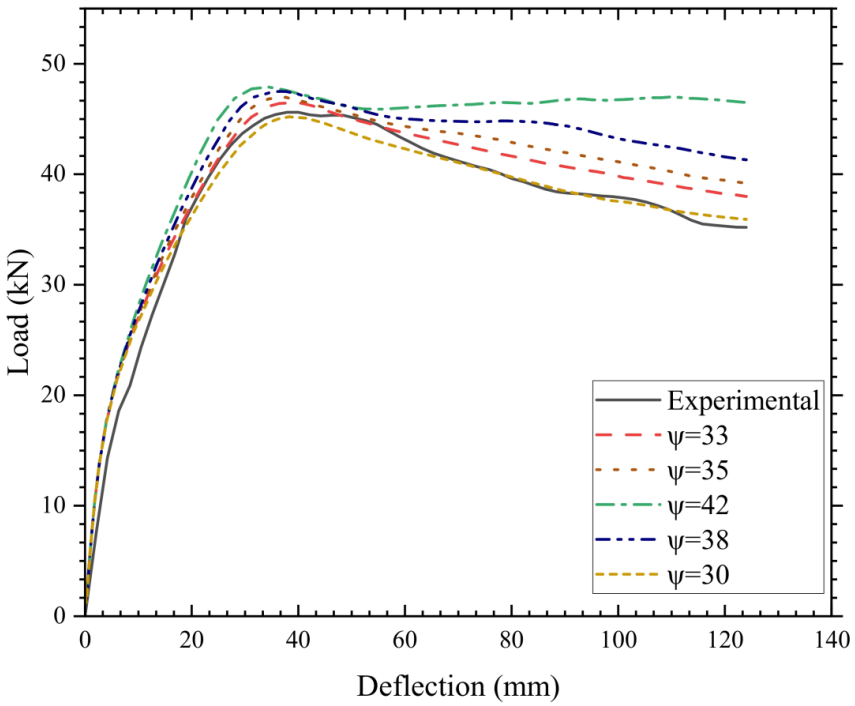
Load (kN)
Deflection (mm)
Experimental
ψ=33
ψ=35
ψ=42
ψ=38
ψ=30

(a)

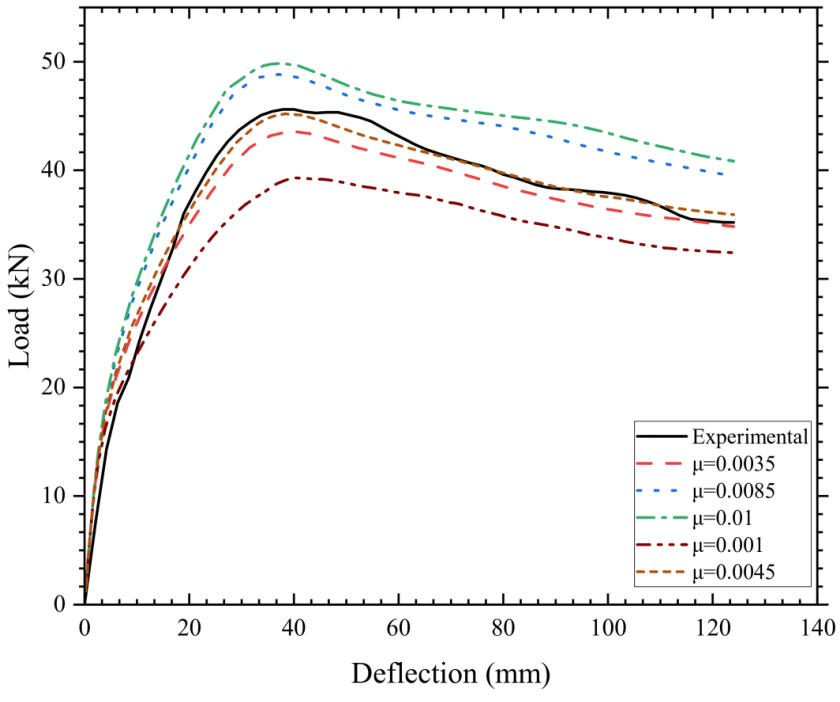
Load (kN)
Deflection (mm)
Experimental
μ=0.0035
μ=0.0085
μ=0.01
μ=0.001
μ=0.0045

(b)

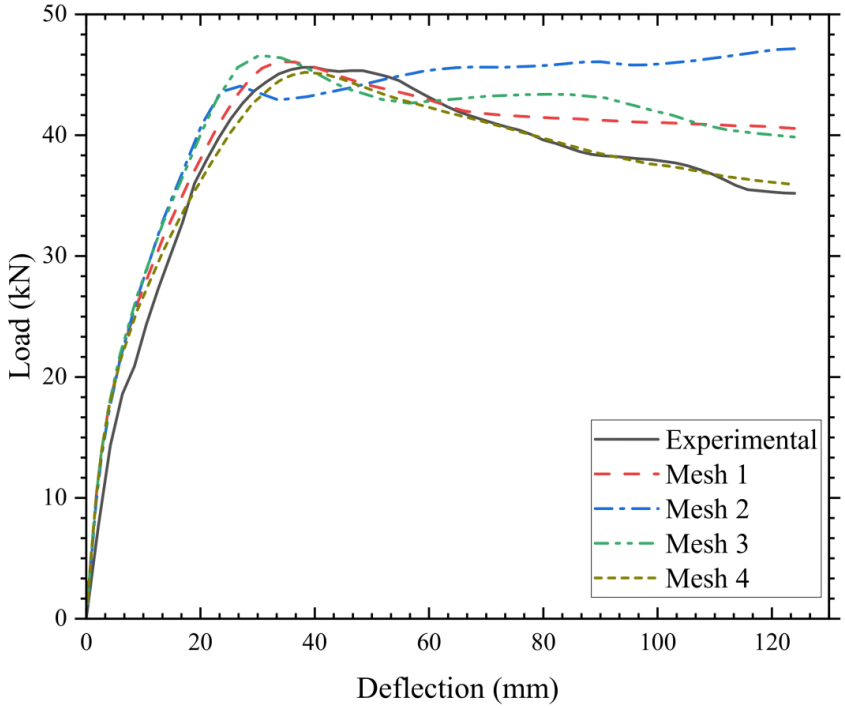

(c)

Figure 15. (a) Force deflection curve of FEM for different values of dilation angle; (b) Force deflection curve of FEM for different values of viscosity parameter; b) Mesh sensitivity analysis for the numerical model depicting the influence of mesh size on the accuracy of the simulation results.

Table 7: Results of mesh sensitivity analysis

Mesh Name	**Mesh Size(mm)**		
	Concrete	**Longitudinal Rebar**	**Stirrups**
Mesh-1	150	150	50
Mesh-2	100	100	40
Mesh-3	70	70	30
Mesh-4	55	55	20

To evaluate the performance of a reinforced concrete BCJ using FEM, it is essential to validate the numerical model against experimental findings. To validate the numerical model, an exterior beam-column joint specimen was utilized as a reference experiment in this study. The experimental data from a large-scale experimental test by Badrashi et al [54] was utilized for validation. The load-displacement response of the numerical model was compared to experimental findings, which were in close agreement with those reported by Badrashi et al as shown in Figure 16. The agreement between FEM and experimental results is good in terms of ultimate and failure load, and deformation as shown in **Error! Reference source not found.**.

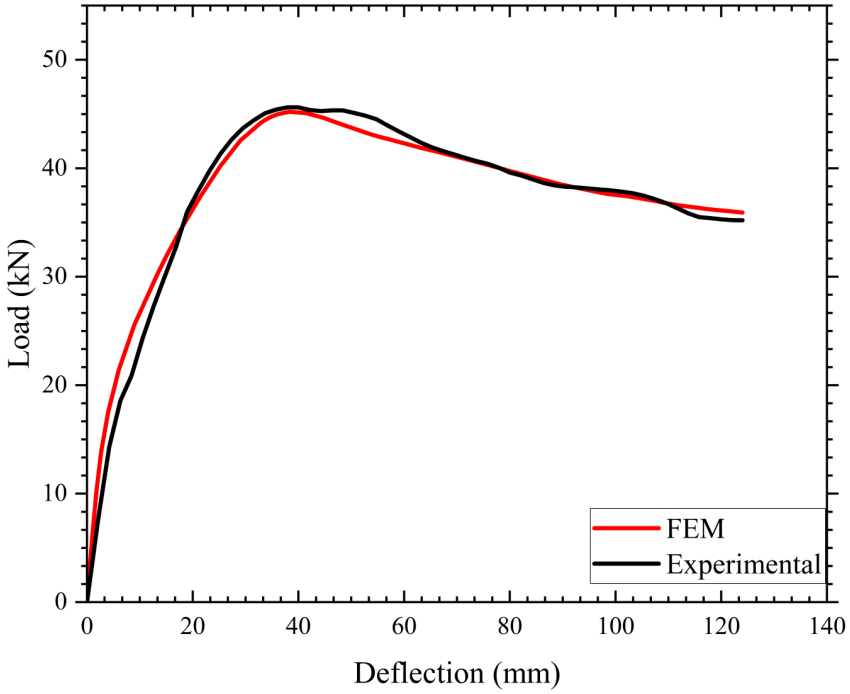

Figure 16: Comparison of experimental and numerical results

Table 8. Comparison of peak and failure loads obtained from FEM and experimental results.

Loads	Experimental	FEM	Percentage Difference
Peak	45.6	45.2	0.88
Failure	35.2	35.9	1.97

4. Results and Discussions

In this investigation, the validated reference numerical model was reinforced with additional diagonal crossbar reinforcement, applied to different faces of the column in BCJs with different configurations, to assess its effectiveness. The impact of the additional reinforcement on performance indicator and damage of the BCJs was investigated by comparing the results with the reference model without the additional reinforcement and joint stirrups.

For clear identification and comparison of the effectiveness of different strengthening configurations, the numerical models were designated with two letter component designation system. The first letter represents the location of the diagonal cross-bracing reinforcement on the beam-column joint, with "F" indicating the front face, "B" indicating the back face, "R" indicating the right face, "L" indicating the left face, "FB" indicating both the front and back faces, "RL" indicating both the right and left faces, and "FBRL" indicating all four faces of the beam-column connection. The second component of the letter designation system indicates the number of diagonal cross-bracing reinforcements applied to the joint, with configuration "A" indicating one diagonal crossbar and "B" indicating two diagonal crossbars. The detail of each model is provided in Table 9.

Table 9: Details of model with different reinforcement configurations

Models	**Description**
Reference Model	No additional reinforcement
Model-F-A	Front face and one crossbar

Model-F-B	Front face and two cross bars
Model-FB-A	Front and back faces and one crossbar on each face
Model-B-A	Back face and one crossbar
Model-B-B	Back face and two crossbars
Model-R-A	Right face and one crossbar
Model-RL-A	Right and left faces and one crossbar on each face
Model-FBRL-A	One crossbar on all faces
Model-FB-B	Front and back faces and two crossbar on each face
Model-FB-XA	Front and Back face and one X-shaped reinforcement
Model-FB-XB	Front and back faces and two X-shaped reinforcement

4.1 Comparing the effectiveness of in-plane and out-of-plane diagonal bars in reinforced concrete beam-column joints under in-plane monotonic loading

In order to determine the most optimal configuration of additional diagonal bars in beam-column joints that would replace joint stirrups and minimize reinforcement congestion, both in-plane and out-of-plane diagonal bars in the joint region were investigated under applied in-plane monotonic loading. Six models, including a reference model, were analyzed, and designated as Model-RL-A, Model-R-A, Model-FB-A, Model-F-A, and Model-FBRL-A. The first two models featured diagonal bars parallel to the applied loading, representing an in-plane diagonal bar configuration, while the next two models had diagonal bars perpendicular to the applied loading, representing an out-of-plane diagonal bar configuration.

Figure 17 provides visual representations of the models used in the study, depicting the details of their reinforcement configurations and their effects on damage distribution. The images in Figure 17 enable a comprehensive analysis of the damage distribution in each model, thereby aiding in the evaluation of the effectiveness of different reinforcement configurations.

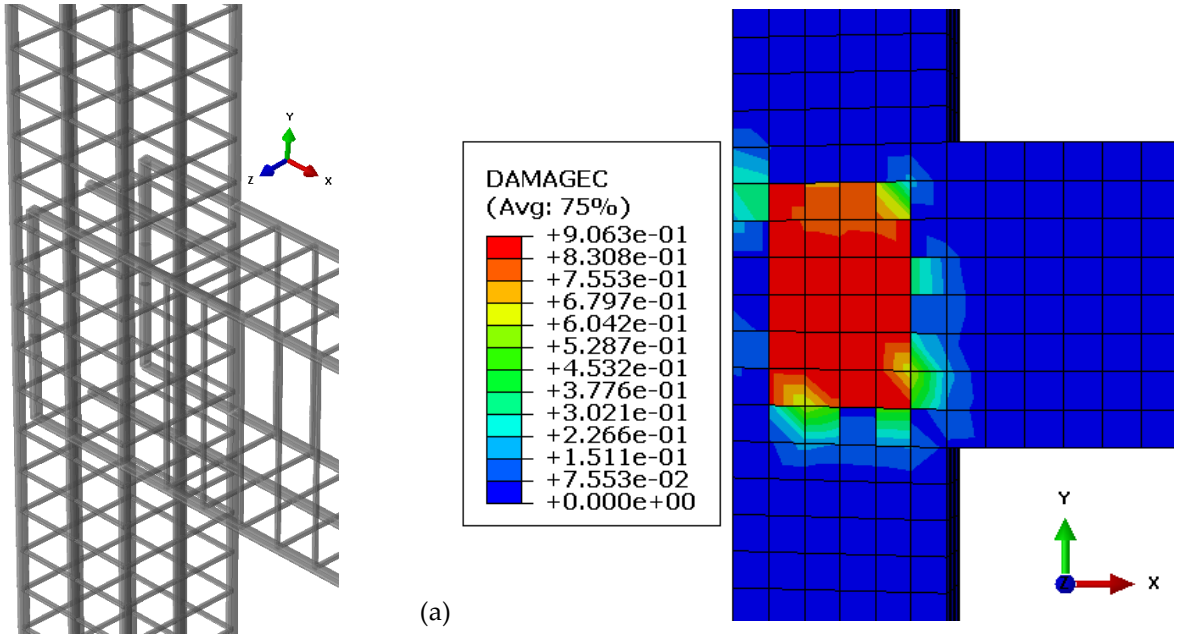

(a)

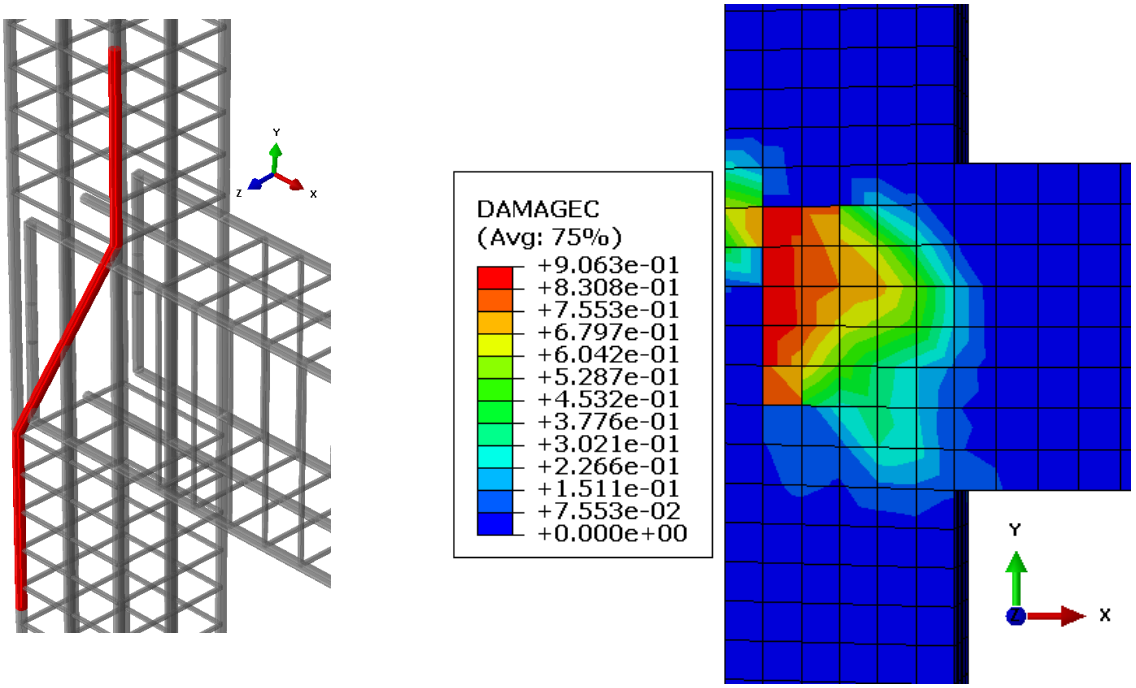
DAMAGEC
(Avg: 75%)
+9.063e-01
+8.308e-01
+7.553e-01
+6.797e-01
+6.042e-01
+5.287e-01
+4.532e-01
+3.776e-01
+3.021e-01
+2.266e-01
+1.511e-01
+7.553e-02
+0.000e+00
Y
X

(b)

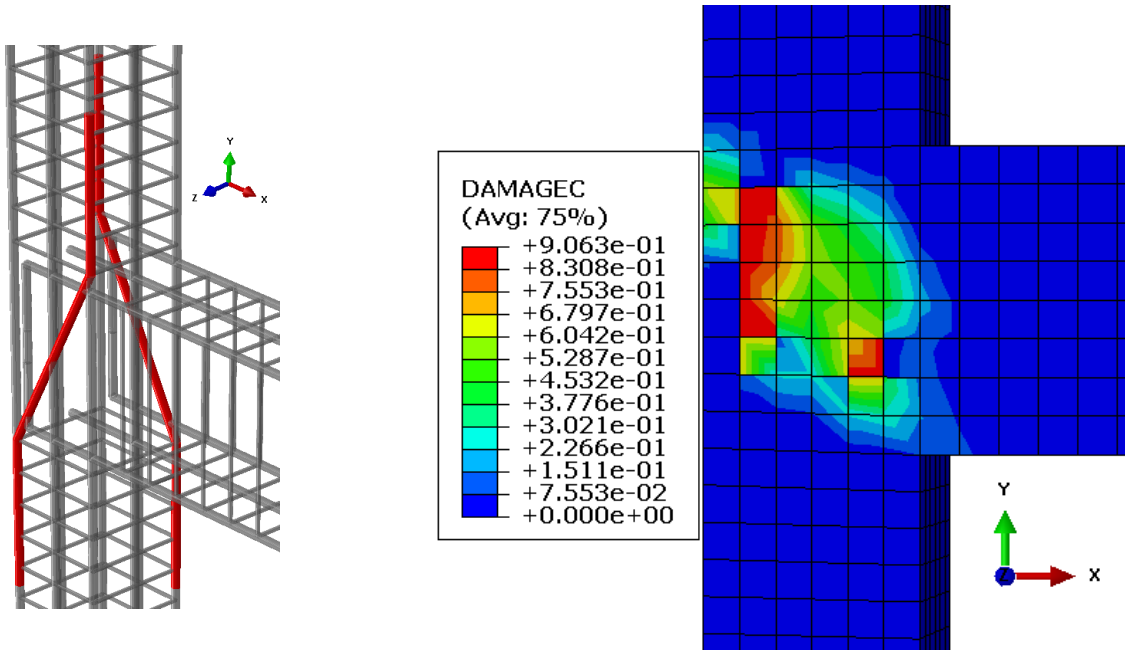
DAMAGEC
(Avg: 75%)
+9.063e-01
+8.308e-01
+7.553e-01
+6.797e-01
+6.042e-01
+5.287e-01
+4.532e-01
+3.776e-01
+3.021e-01
+2.266e-01
+1.511e-01
+7.553e-02
+0.000e+00
Y
X

(c)

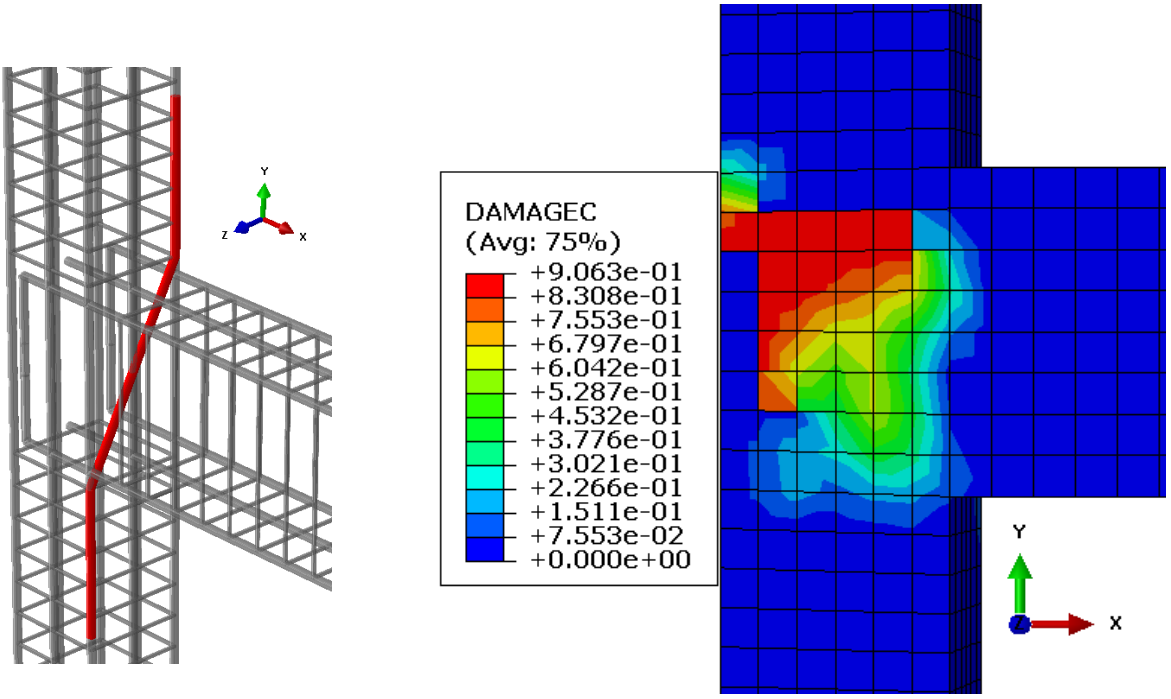
DAMAGEC
(Avg: 75%)
+9.063e-01
+8.308e-01
+7.553e-01
+6.797e-01
+6.042e-01
+5.287e-01
+4.532e-01
+3.776e-01
+3.021e-01
+2.266e-01
+1.511e-01
+7.553e-02
+0.000e+00
Y
X

(d)

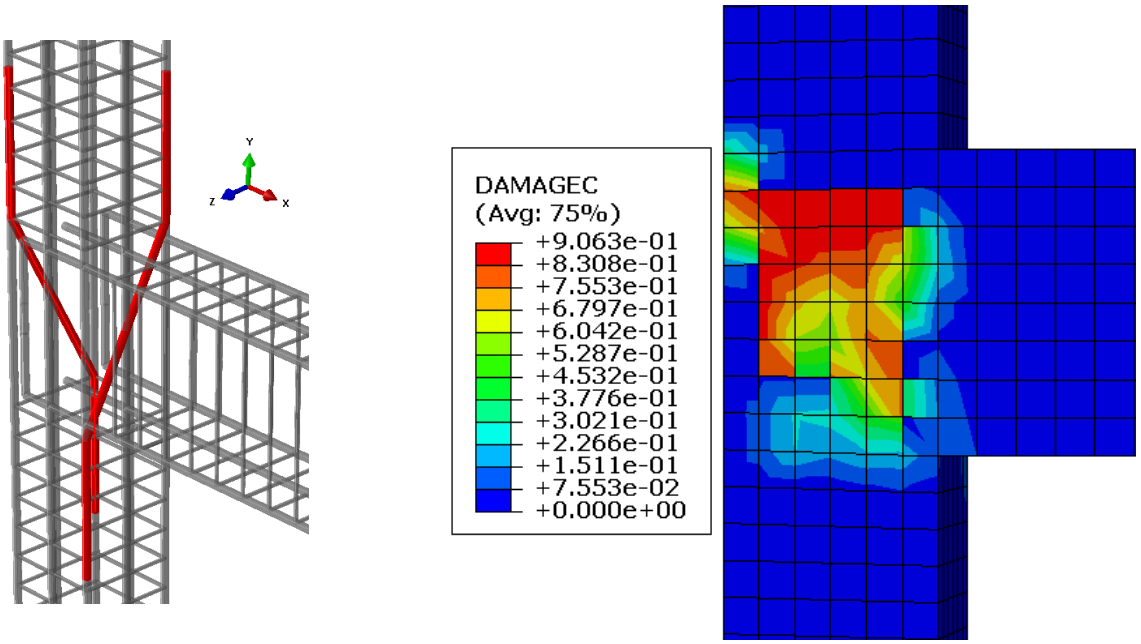
DAMAGEC
(Avg: 75%)
+9.063e-01
+8.308e-01
+7.553e-01
+6.797e-01
+6.042e-01
+5.287e-01
+4.532e-01
+3.776e-01
+3.021e-01
+2.266e-01
+1.511e-01
+7.553e-02
+0.000e+00

(e)

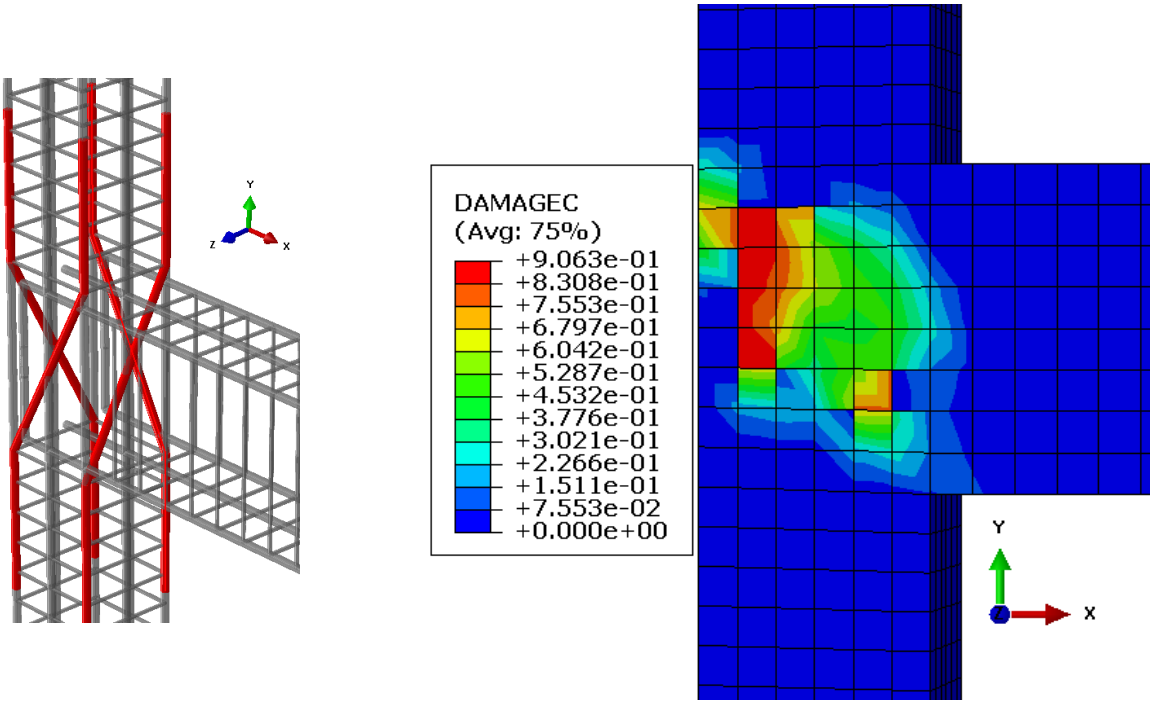

(f)

Figure 17: Shows the details of these models with different reinforcement configurations and their effects on damage distribution. (a) Reference Model without additional reinforcement (b) Model-F-A: Front face, One crossbar (c) Model-FB-A: Front and back faces, One crossbar on each face. (d) Model-R-A: Right face, One crossbar (e) Model-RL-A: Right and left faces, One crossbar on each face (f) Model-FBRL-A: one crossbar on All faces

Damage and rotation were compared among these models to identify the most suitable configuration of additional diagonal bars in beam-column joints. Figure 18 (a) presents the damage versus rotation graphs of the models, where it is observed that the reference model exhibits the highest core damage percentage of around 52%. Model-RL-A shows the second-highest core damage percentage of approximately 48%, followed by Model-R-A with a percentage of 47%. Model-F-A, which has in-plane diagonal bars, shows a comparatively lower core damage percentage of around 41% than Model-R-A, which has out-of-plane diagonal bars. Model-FB-A and Model-FBRL-A have similar core damage percentages, approximately 31% and 32%, respectively. However, Model-FB-A demonstrates comparatively less joint damage than Model-RL-A. Based on these findings, in-plane diagonal bars are concluded to be more effective than out-of-plane diagonal bars in reducing core damage.

Figure 18 (b) displays the percentage reduction in core damage for each model. It is observed that the in-plane diagonal bars of Model-R-A and Model-RL-A exhibit a higher percentage reduction, around 11.74% and 10.36%, respectively, than Model-F-A and Model-FB-A, which exhibit reductions of approximately 22% and 37%, respectively. This result further confirms the effectiveness of in-plane diagonal bars in reducing core damage compared to out-of-plane diagonal bars.

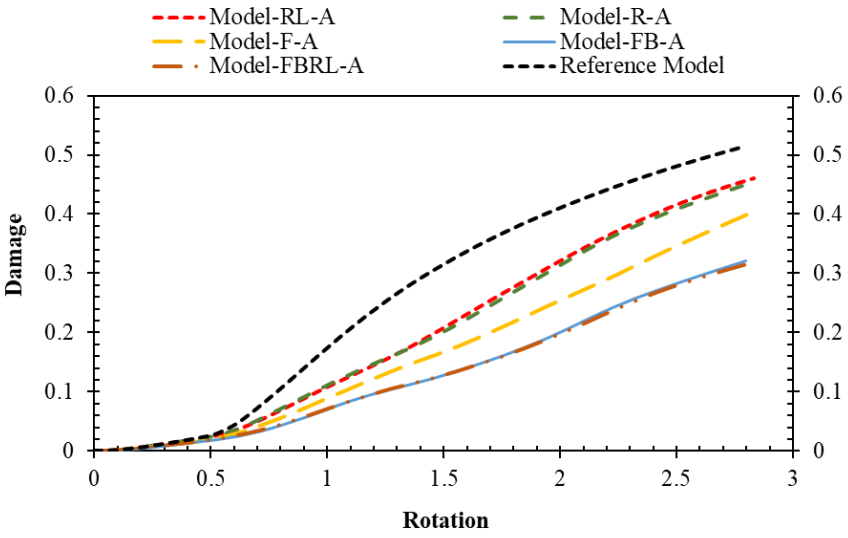

(a)

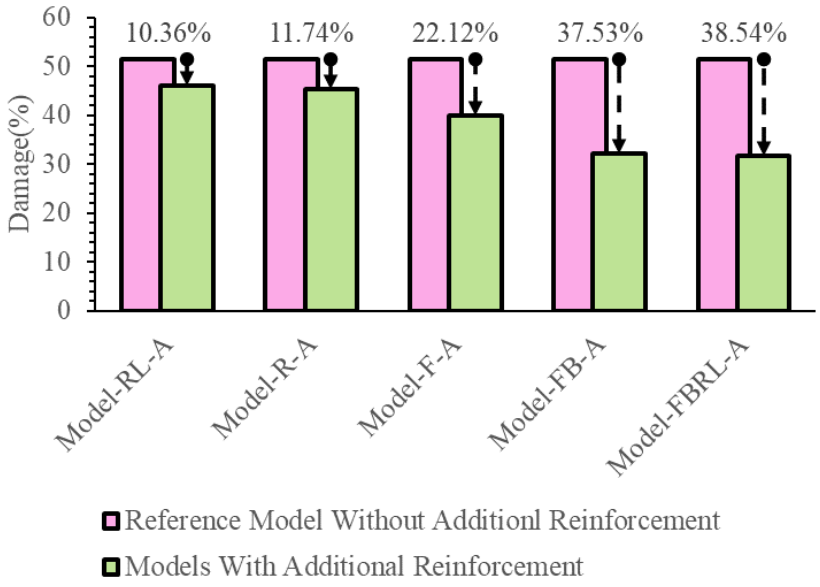

(b)

Figure 18: (a) Damage and rotation comparison of different models for single diagonal crossbar (b)Damage comparison of reference model and model with additional reinforcement for single diagonal crossbar

In conclusion, the study shows that in-plane diagonal bars are more effective than out-of-plane diagonal bars in reducing core damage. Therefore, they can be considered as a better alternative to joint stirrups, as they lead to less reinforcement congestion in the joint.

4.2 Comparison of in-plane diagonal bar configurations for enhanced joint performance under monotonic loading

The objective of this study is to analyze the impact of in-plane diagonal bar configurations on the damage and rotation of reinforced concrete joints under monotonic loading, as it has been established that in-plane diagonal bars are more effective in improving joint performance. The objective is to identify the most efficient and effective configuration that offers relatively less damage to the joint region and a high stiffness towards the applied loading.

Figure 19 illustrates the models used in the study and presents the reinforcement configurations employed in each model, enabling a detailed visual analysis of the effects of these configurations on damage distribution. This allows for

a comprehensive evaluation of the effectiveness of different reinforcement configurations. The images in Figure 19 provide a valuable tool for analyzing the damage distribution in each model and assessing the impact of different reinforcement strategies.

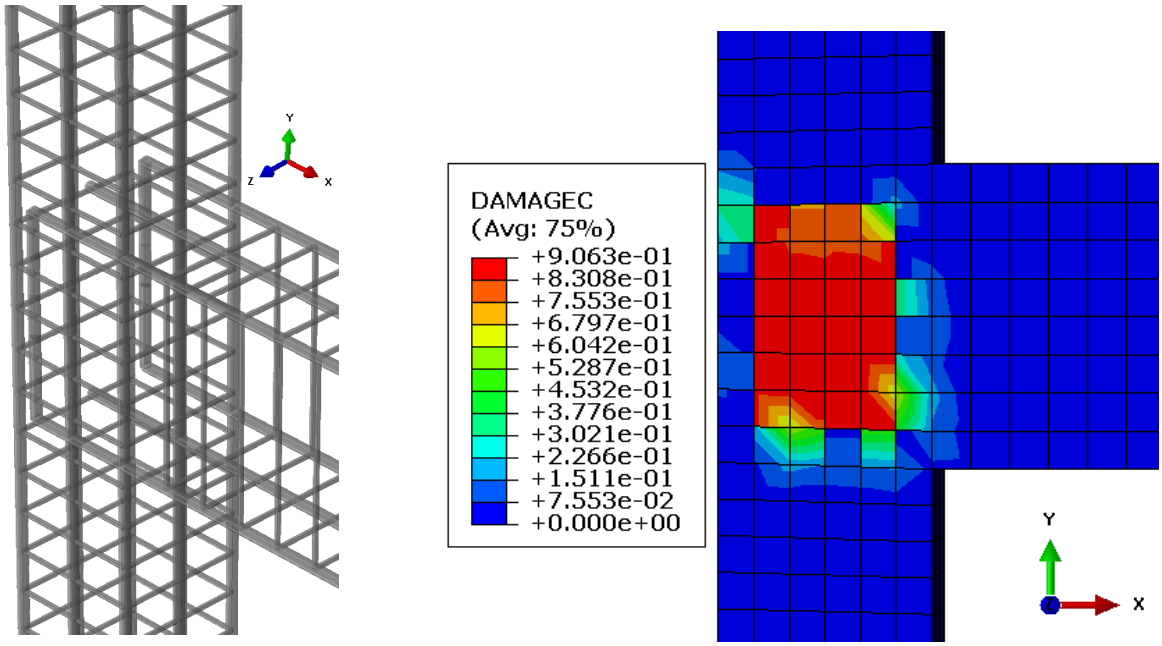

(a)

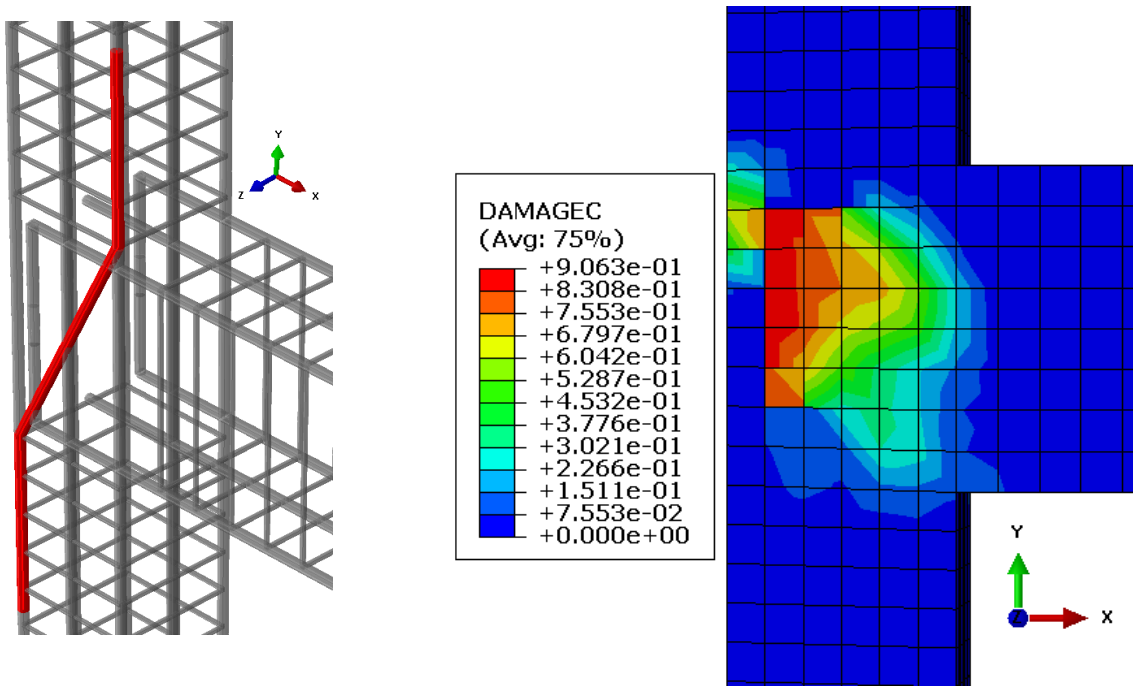

(b)

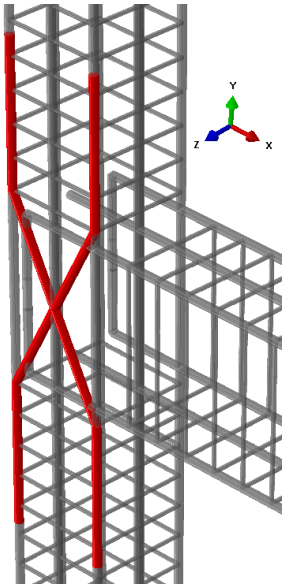

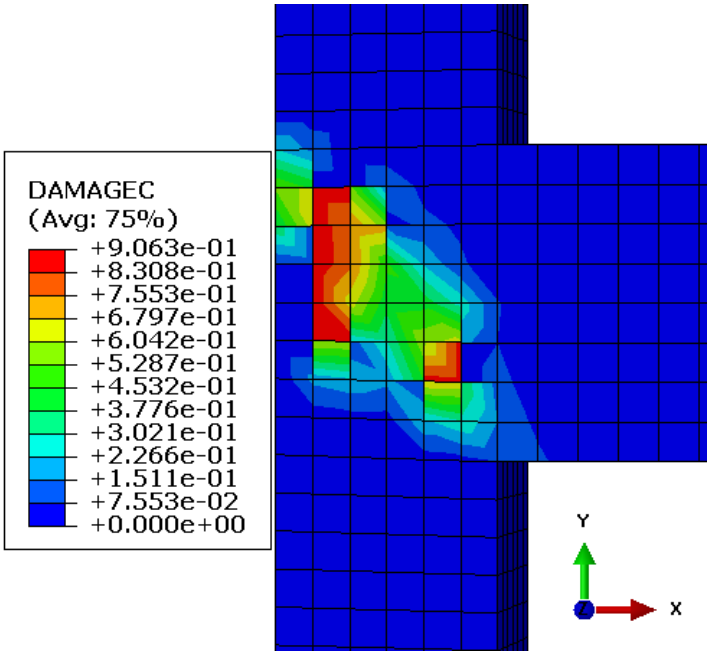
DAMAGEC
(Avg: 75%)
+9.063e-01
+8.308e-01
+7.553e-01
+6.797e-01
+6.042e-01
+5.287e-01
+4.532e-01
+3.776e-01
+3.021e-01
+2.266e-01
+1.511e-01
+7.553e-02
+0.000e+00
Y
X

(c)

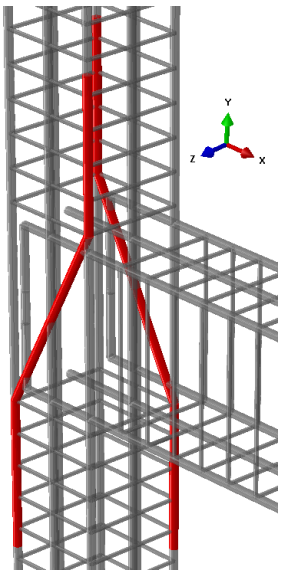

(d)

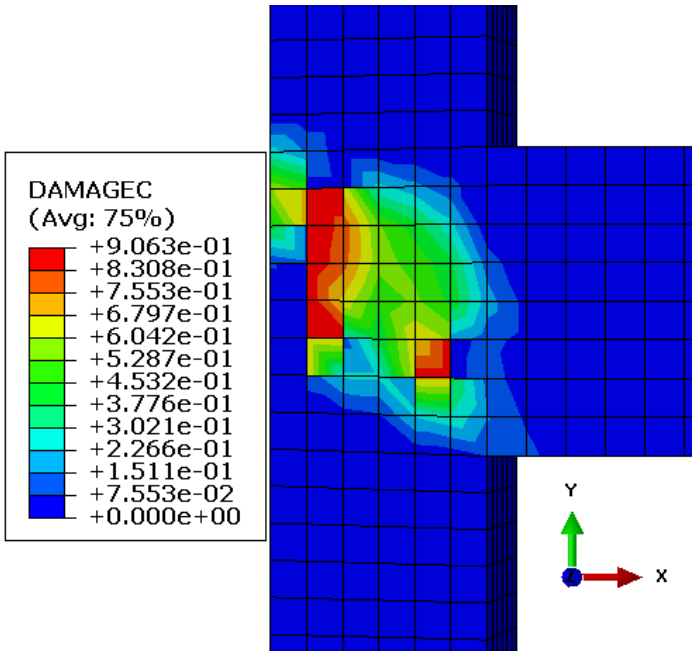
DAMAGEC
(Avg: 75%)
+9.063e-01
+8.308e-01
+7.553e-01
+6.797e-01
+6.042e-01
+5.287e-01
+4.532e-01
+3.776e-01
+3.021e-01
+2.266e-01
+1.511e-01
+7.553e-02
+0.000e+00
Y
X

(d)

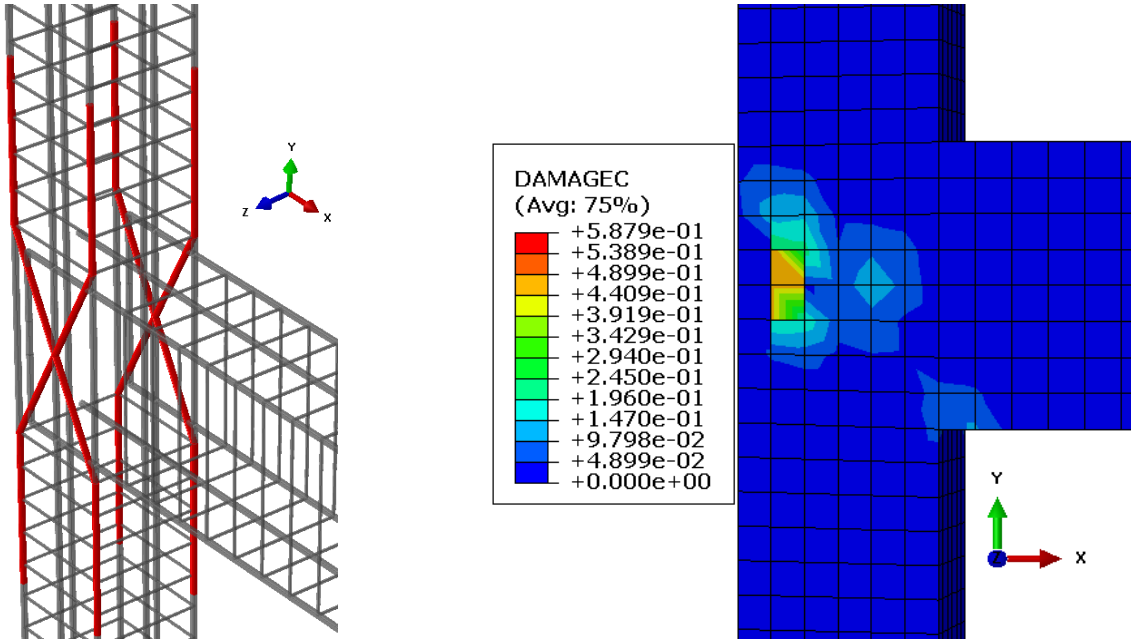
Y
Z
X
DAMAGEC
(Avg: 75%)
+5.879e-01
+5.389e-01
+4.899e-01
+4.409e-01
+3.919e-01
+3.429e-01
+2.940e-01
+2.450e-01
+1.960e-01
+1.470e-01
+9.798e-02
+4.899e-02
+0.000e+00
Y
X

(e)

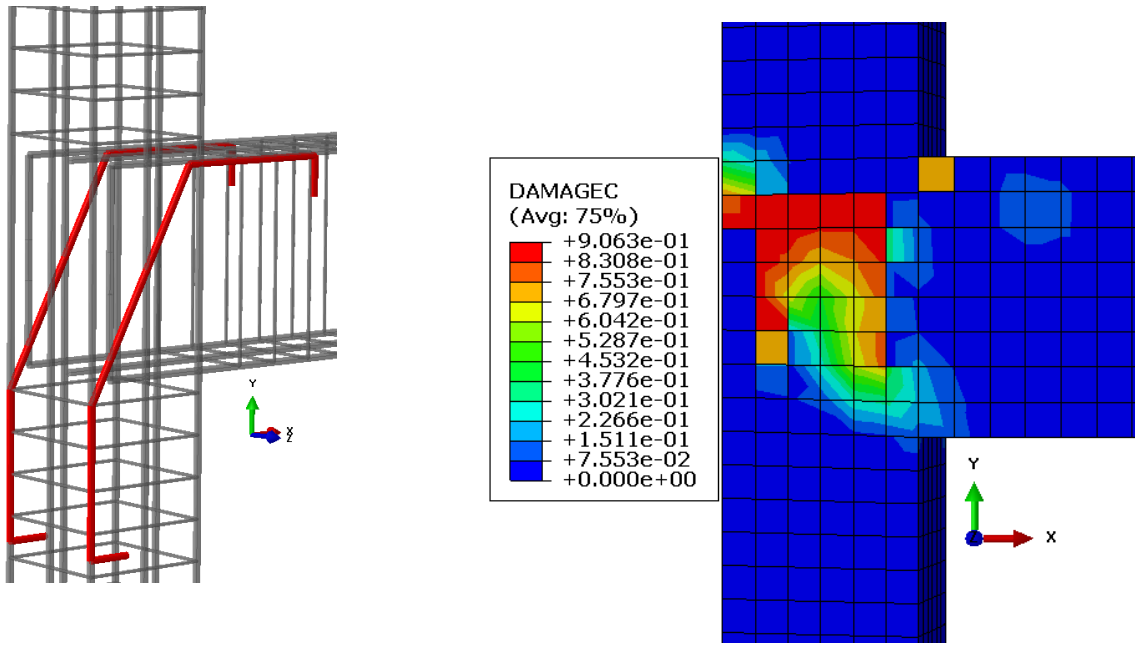
Y
X
Z
DAMAGEC
(Avg: 75%)
+9.063e-01
+8.308e-01
+7.553e-01
+6.797e-01
+6.042e-01
+5.287e-01
+4.532e-01
+3.776e-01
+3.021e-01
+2.266e-01
+1.511e-01
+7.553e-02
+0.000e+00
Y
X

(f)

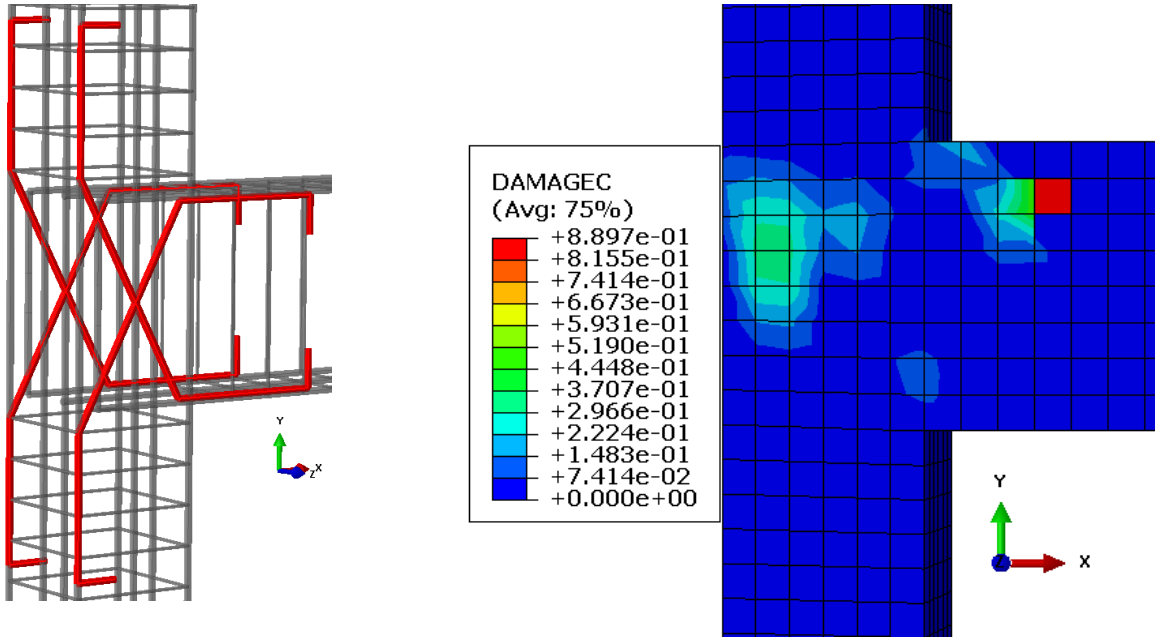

(g)

Figure 19: Shows the details of these models with different reinforcement configurations and their effects on damage distribution. (a) Reference Model without additional reinforcement (b) Model-F-A: Front face, One crossbar (c) Model-F-B: Front face, two cross-bars (d) Model-FB-A: Front and back faces, One crossbar on each face (e) Model-FB-B: Front and back faces, two cross bars on each face (f) Model-FB-XA: Front and Back face, one X-shaped reinforcement (g) Model-FB-XB: Front and back faces, two X-shaped reinforcement.

Seven models were investigated and compared based on their damage vs rotation graphs, as shown in Figure 20 (a). It was found that Model-F-A showed the highest damage of about 40%, but when the diagonal bars at the front face were doubled (Model-F-B), the damage was reduced to 34%. Further, when a single cross diagonal bar was inserted at the front and back face (Model-FB-A), the damage was almost the same at about 33%. However, Model FB-B showed relatively the lowest core damage and rotation value, indicating that this model is stiffer and provides more additional stiffness to the applied loading, preventing core damage and enhancing the load carrying capacity of the joint.

A bar chart was also created in Figure 20 (b) to observe the percentage reduction in damage between various models. It was found that Model-FB-B exhibited the highest percentage reduction in damage of nearly 83% as compared to the reference model without diagonal bars. This bar chart also represents the percentage reduction of damage for all the other models.

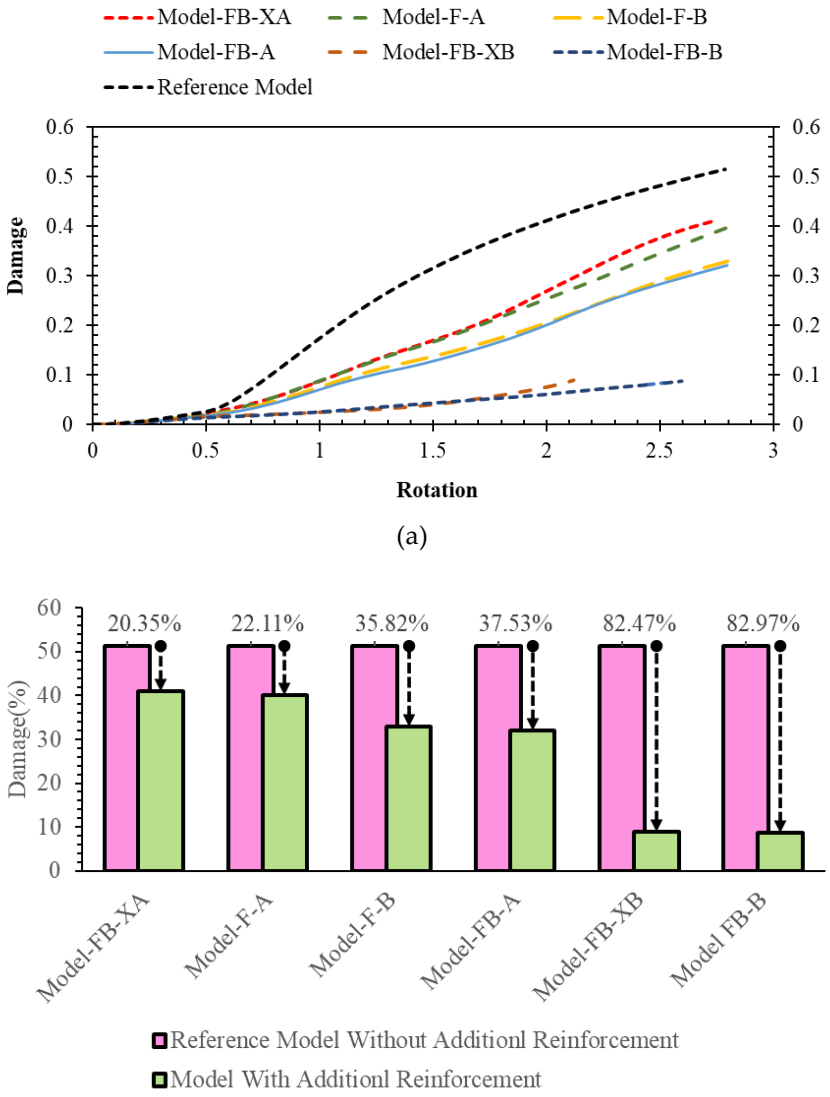

Figure 20: (a) Damage and rotation comparison of different models for double diagonal crossbar. (b)Damage comparison of reference model and model with additional reinforcement for double diagonal crossbar.

The comparison of the different in-plane diagonal bar configurations showed that doubling the diagonal bars at the front face or inserting a single cross diagonal bar at the front and back face could significantly reduce the damage of the joint region. However, the Model FB-B with the optimal configuration of diagonal bars showed the lowest core damage and rotation values, indicating enhanced joint performance under monotonic loading. Thus, the in-plane diagonal bars can be used as an effective reinforcement strategy for reinforced concrete joints, and the Model FB-B can be considered as an optimum configuration for improved joint performance under monotonic loading.

4.3 Study of in-plane cross diagonal bars inserted into the beam instead of column

After mitigating the compression damage in the joint region, the tension damage was analyzed for the most effective model discussed above, i.e., Model-FB-B. It was observed that the top of the beam near the joint face experienced significant tension damage, as shown in Figure 21. This can lead to the formation of plastic hinges near the joint, indicating an unfavorable condition for the beam-column joint. To address this issue, two additional numerical models, namely Model-FB-XA and Model-FB-XB, were developed and investigated. As the applied monotonic load acted in the downward direction, tension was generated at the top of the beam near the joint. Since concrete is weaker in tension than in compression, all the concrete cracks at the top of the beam near the joint and fails before the yielding of steel, which is stronger in tension. To prevent such tension failures, steel bars must be provided in the tension-dominant region. Hence,

in Model-FB-XA and Model-FB-XB, the diagonal cross bars were inserted into the beam instead of the column, as studied previously.

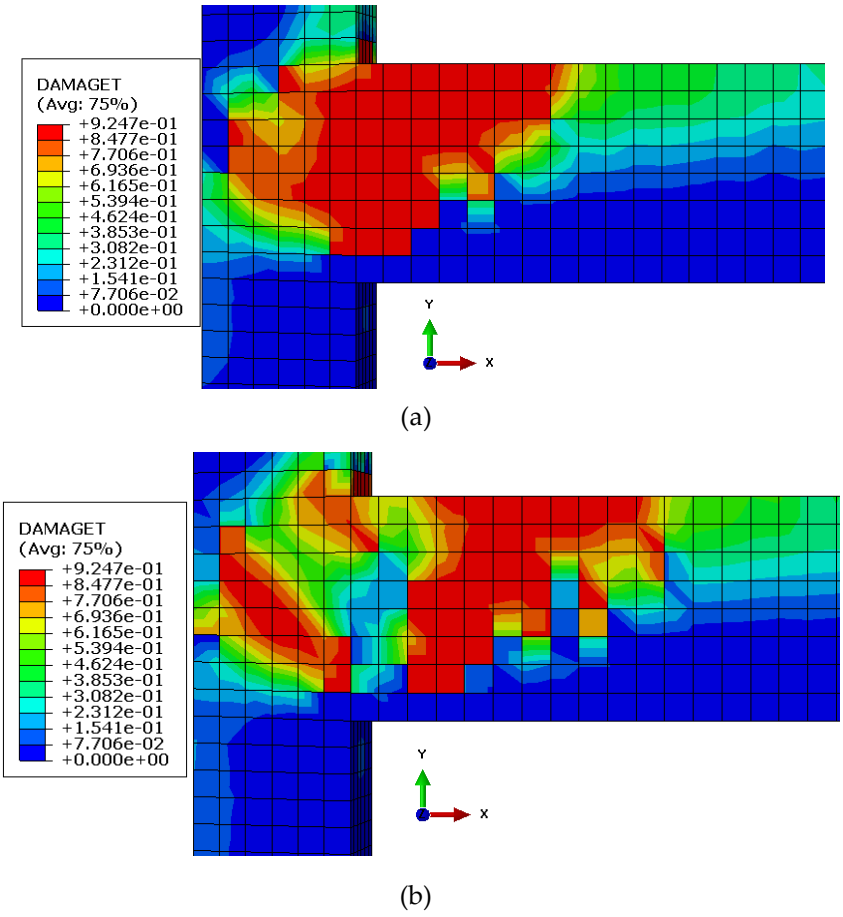

Figure 21: Tension damage distribution (a) Model-FB-B (b) Model-FB-XB

The results showed that Model FB-XA had a core damage percentage of approximately 41%, which was higher than the other models, making it unsuitable. On the other hand, Model-FB-XB was found to reduce both tension and compression damage effectively, with a damage percentage of about 11% as shown in Figure 20 (a). Additionally, the percentage reduction of damage was almost similar to Model-FB-B, at approximately 82.5% (almost 85%), as shown in Figure 20 (b). Figure 21 also indicated a significant reduction in tension damage due to the use of diagonal bars inserted into the beam rather than into the column.

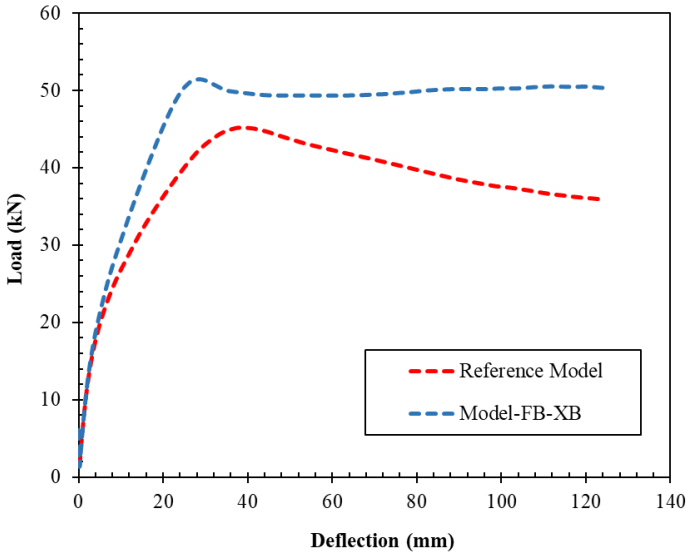

Figure 22: Comparison of force deflection curve of reference model and model FB-XB

Furthermore, Model-FB-XB provided the highest additional rotational stiffness to the joint with minimum damage in both tension and compression, which significantly enhanced the load-carrying capacity by about 20% that is the load carrying capacity increase from 43 KN to 52 KN as shown in Figure 22. Therefore, it can be concluded that inserting diagonal bars into the beam, as in Model-FB-XB, is a highly effective solution to prevent tension and compression damage and improve the performance of beam-column joints.

Therefore, this study concludes that the Model-FB-XB configuration is recommended for the future design of beam column joints due to its superior performance in reducing both tension and compression damage while providing additional rotational stiffness to the joint. This configuration also reduces the congestion of reinforcement at the joint, allowing for full compaction of concrete at the joint region. As a result, it improves the stiffness and load carrying capacity of the joint, which ultimately leads to less core damage and prevents the building from collapsing due to joint failure.

5. Conclusion

This study utilized the finite element modeling technique to evaluate the performance of various reinforcement configurations in the joint area of RC BCJs. Twelve numerical models with different reinforcement configurations in the joint area were prepared to investigate the effectiveness of in-plane and out-of-plane diagonal bars in minimizing core damage and improving the load-carrying capacity of RC BCJs. The study evaluated two specific models, FB-XA and FB-XB, for their ability to reduce tension and compression damage while providing additional rotational stiffness to the joint. The main conclusions of this study are summarized below.

- The study found that the in-plane diagonal bars, represented by Model-F-A and Model-FB-A, were more effective in reducing core damage than the out-of-plane diagonal bars, represented by Model-R-A and Model-RL-A. The reference model had the highest core damage percentage of around 52%. Model-RL-A and Model-R-A followed with percentages of 48% and 47%, respectively. Model-F-A had a lower core damage percentage of around 41%, while Model-FB-A and Model-FBRL-A had similar percentages of around 31% and 32%, respectively. Model-FB-A demonstrated less joint damage than Model-RL-A.

- The in-plane diagonal bars of Model-F-A and Model-FB-A also exhibited a higher percentage reduction in core damage, which is about 22% and 37%, respectively, compared to the out-of-plane diagonal bars. These findings suggest that in-plane diagonal bars can be a better alternative to joint stirrups in reducing core damage and minimizing reinforcement congestion problem in beam-column joints.

- The study identified Model FB-XA as ineffective due to its core damage percentage of approximately 41%, whereas Model-FB-XB was effective in reducing both tension and compression damage, with a damage percentage of around 11%. Model-FB-XB's reduction in damage percentage was comparable to Model-FB-B, which was approximately 82.5%.

- Finally, this study found that the Model-FB-XB configuration was highly effective in reducing tension and compression damage while providing the highest additional rotational stiffness to the joint. This model was able to increase the load-carrying capacity of the joint by almost 20% and demonstrated minimum damage in both tension and compression. As a result, it is recommended for future design of beam-column joints.

The results of this research are important for the design of beam-column joints in reinforced concrete structures. The use of Model-FB-XB configuration can be considered a feasible alternative to conventional joint stirrups, as it effectively reduces reinforcement congestion and enhances the stiffness and load-carrying capacity of beam column joints in reinforced concrete structures. These findings can be valuable for the future design and optimization of such structures. Incorporating diagonal bars within the beam instead of the column can effectively decrease tension damage close to the joint and guarantee a more ductile failure mode. This would reduce the likelihood of sudden or brittle failure, leading to a significant reduction in the risk of catastrophic building collapse.

Furthermore, this improved design offers the added benefit of providing occupants with warning signs before a failure occurs, allowing them ample time to evacuate the building and seek shelter from potential danger. This not only provides additional safety measures for occupants but also allows building owners to retrofit the joint region before severe damage occurs.

Overall, the findings of this study highlight the importance of continually exploring and innovating new techniques and configurations to improve the design of reinforced concrete structures. This Model-FB-XB configuration offers a promising solution to reduce joint failure and improve overall safety, making it a valuable addition to the field of structural engineering.

References

[1] S. M. Allam, H. M. F. Elbakry, and I. S. E. Arab, "Exterior reinforced concrete beam column joint subjected to monotonic loading," *Alexandria Engineering Journal*, vol. 57, no. 4, pp. 4133–4144, 2018, doi: 10.1016/j.aej.2018.10.015.

[2] G. Calvi, G. Magenes, and S. Pampanin, "RELEVANCE OF BEAM-COLUMN JOINT DAMAGE AND COLLAPSE IN RC FRAME ASSESSMENT," *http://dx.doi.org/10.1080/13632460209350433*, vol. 6, pp. 75–100, 2009, doi: 10.1080/13632460209350433.

[3] R. Park, "A SUMMARY OF RESULTS OF SIMULATED SEISMIC LOAD TESTS ON REINFORCED CONCRETE BEAM-COLUMN JOINTS, BEAMS AND COLUMNS WITH SUBSTANDARD REINFORCING DETAILS," *http://dx.doi.org/10.1080/13632460209350413*, vol. 6, no. 2, pp. 147–174, 2008, doi: 10.1080/13632460209350413.

[4] S. H. Alsayed, Y. A. Al-Salloum, T. H. Almusallam, and N. A. Siddiqui, "Seismic Response of FRP-Upgraded Exterior RC Beam-Column Joints," *Journal of Composites for Construction*, vol. 14, no. 2, pp. 195–208, Mar. 2010, doi: 10.1061/(ASCE)CC.1943-5614.0000067.

[5] D. Todd *et al.*, *1994 Northridge earthquake*, vol. 8, no. 1. 1999. doi: 10.1108/dpm.1999.07308aag.053.

[6] V. V. Mehta. Murty, C. V. R., Rupen, Goswami., A. R. Vijayanarayanan., "E a r t h q u a k e B e h a v i o u r o f B u i l d i n g s," *Gujarat State Disaster Management Authority Government of Gujarat*, p. 268, 2012.

[7] K. Le-Trung, K. Lee, J. Lee, D. H. Lee, and S. Woo, "Experimental study of RC beam-column joints strengthened using CFRP composites," *Compos B Eng*, vol. 41, no. 1, pp. 76–85, 2010, doi: 10.1016/j.compositesb.2009.06.005.

[8] L. N. Lowes, N. Mitra, and A. Altoontash, "A Beam-Column Joint Model for Simulating the Earthquake Response of Reinforced Concrete Frames," Feb. 2003. [Online]. Available: https://peer.berkeley.edu/publications/2003-10

[9] W. M. Hassan, S. Park, R. R. Lopez, K. M. Mosalam, and J. P. Moehle, "SEISMIC RESPONSE OF OLDER-TYPE REINFORCED CONCRETE CORNER JOINTS," Lisbon, Portugal: 15th World Conference on Earthquake Engineering, Sep. 2012. [Online]. Available: https://www.researchgate.net/publication/314042936_Experimental_Assessment_of_Seismic_Vulnerability_of_Corner_Beam-Column_Joints_in_Older_Concrete_Buildings/references#fullTextFileContent

[10] R. Chitra and S. J. Mohan, "Reinforced concrete beam-column joint's ductility behavior," *Mater Today Proc*, vol. 51, pp. 1069–1073, Jan. 2022, doi: 10.1016/J.MATPR.2021.07.096.

[11] O. Bedair, "A Simplified Procedure for Prediction of Ultimate Strength of Beam-Column Channel Sections," *Engineering*, vol. 03, no. 10, pp. 973–977, 2011, doi: 10.4236/ENG.2011.310120.

[12] M. T. Ramírez-Herrera, D. Romero, N. Corona, H. Nava, H. Torija, and F. H. Maguey, "The 23 June 2020 Mw 7.4 La Crucecita, Oaxaca, Mexico Earthquake and Tsunami: A Rapid Response Field Survey during COVID-19 Crisis," *Seismological Research Letters*, vol. 92, no. 1, pp. 26–37, Jan. 2021, doi: 10.1785/0220200263.

[13] K. O. Cetin, G. Mylonakis, A. Sextos, and J. P. Stewart, "Reconnaissance of 2020 M 7.0 Samos Island (Aegean Sea) earthquake," *Bulletin of Earthquake Engineering*, vol. 20, no. 14, pp. 7707–7712, Nov. 2022, doi: 10.1007/S10518-021-01212-Y/FIGURES/1.

[14] M. Stepinac *et al.*, "Damage classification of residential buildings in historical downtown after the ML5.5 earthquake in Zagreb, Croatia in 2020," *International Journal of Disaster Risk Reduction*, vol. 56, p. 102140, Apr. 2021, doi: 10.1016/J.IJDRR.2021.102140.

[15] T. H. Almusallam and Y. A. Al-Salloum, "Seismic Response of Interior RC Beam-Column Joints Upgraded with FRP Sheets. II: Analysis and Parametric Study," *Journal of Composites for Construction*, vol. 11, no. 6, pp. 590–600, Dec. 2007, doi: 10.1061/(ASCE)1090-0268(2007)11:6(590).

[16] M. S. Alhaddad, N. A. Siddiqui, A. A. Abadel, S. H. Alsayed, and Y. A. Al-Salloum, "Numerical Investigations on the Seismic Behavior of FRP and TRM Upgraded RC Exterior Beam-Column Joints," *Journal of Composites for Construction*, vol. 16, no. 3, pp. 308–321, Jun. 2012, doi: 10.1061/(ASCE)CC.1943-5614.0000265.

[17] F. Yuan, J. Pan, Z. Xu, and C. K. Y. Leung, "A comparison of engineered cementitious composites versus normal concrete in beam-column joints under reversed cyclic loading," *Materials and Structures/Materiaux et Constructions*, vol. 46, no. 1–2, pp. 145–159, Jan. 2013, doi: 10.1617/S11527-012-9890-6/FIGURES/17.

[18] T. Paulay, R. Park, and M. J. N. Priestley, "Reinforced Concrete Beam-Column Joints Under Seismic Actions," *Journal Proceedings*, vol. 75, no. 11, pp. 585–593, Nov. 1978, doi: 10.14359/10971.

[19] T. Paulay and A. Scarpas, "The behaviour of exterior beam-column joints," *Bulletin of the New Zealand Society for Earthquake Engineering*, vol. 14, no. 3, pp. 131–144, Sep. 1981, doi: 10.5459/bnzsee.14.3.131-144.

[20] "Recommendations for Design of Beam-Column Connections in Monolithic Reinforced Concrete Structures," 2002.

[21] A. J. Durrani and J. K. Wight, "Behavior of Interior Beam-to-Column Connections Under Earthquake-Type Loading," *Journal Proceedings*, vol. 82, no. 3, pp. 343–349, May 1985, doi: 10.14359/10341.

[22] M. Azimi, A. Bin Adnan, A. R. Bin Mohd Sam, M. M. Tahir, I. Faridmehr, and R. Hodjati, "Seismic performance of RC beam-column connections with continuous rectangular spiral transverse reinforcements for low ductility classes," *Scientific World Journal*, vol. 2014, 2014, doi: 10.1155/2014/802605.

[23] A. Ebanesar, H. Gladston, E. Noroozinejad Farsangi, and S. V. Sharma, "Strengthening of RC beam-column joints using steel plate with shear connectors: Experimental investigation," *Structures*, vol. 35, pp. 1138–1150, Jan. 2022, doi: 10.1016/J.ISTRUC.2021.08.042.

[24] H. Dabiri, A. Kaviani, and A. Kheyroddin, "Influence of reinforcement on the performance of non-seismically detailed RC beam-column joints," *Journal of Building Engineering*, vol. 31, p. 101333, Sep. 2020, doi: 10.1016/J.JOBE.2020.101333.

[25] H. Dabiri, A. Kheyroddin, and A. Kaviani, "A Numerical Study on the Seismic Response of RC Wide Column–Beam Joints," *International Journal of Civil Engineering*, vol. 17, no. 3, pp. 377–395, Mar. 2019, doi: 10.1007/S40999-018-0364-2/FIGURES/14.

[26] A. D. Tsonos, G. Kalogeropoulos, P. Iakovidis, M. Z. Bezas, and M. Koumtzis, "Seismic Performance of RC Beam–Column Joints Designed According to Older and Modern Codes: An Attempt to Reduce Conventional Reinforcement Using Steel Fiber Reinforced Concrete," *Fibers 2021, Vol. 9, Page 45*, vol. 9, no. 7, p. 45, Jul. 2021, doi: 10.3390/FIB9070045.

[27] A. Bossio, F. Fabbrocino, G. P. Lignola, A. Prota, and G. Manfredi, "Simplified Model for Strengthening Design of Beam–Column Internal Joints in Reinforced Concrete Frames," *Polymers 2015, Vol. 7, Pages 1732-1754*, vol. 7, no. 9, pp. 1732–1754, Sep. 2015, doi: 10.3390/POLYM7091479.

[28] P. W. Karya and T. Kanakubo, "Shear Performance of Fiber-Reinforced Cementitious Composites Beam-Column Joint Using Various Fibers," *Journal of the Civil Engineering Forum*, vol. 3, no. 2, pp. 113–124, Sep. 2017, doi: 10.22146/JCEF.26571.

[29] X. Li *et al.*, "Cyclic behavior of joints assembled using prefabricated beams and columns with Engineered Cementitious Composite (ECC)," *Eng Struct*, vol. 247, p. 113115, Nov. 2021, doi: 10.1016/J.ENGSTRUCT.2021.113115.

[30] A. Annadurai and A. Ravichandran, "Seismic Behavior of Beam–Column Joint Using Hybrid Fiber Reinforced High-Strength Concrete," *Iranian Journal of Science and Technology - Transactions of Civil Engineering*, vol. 42, no. 3, pp. 275–286, Sep. 2018, doi: 10.1007/S40996-018-0100-9/FIGURES/13.

[31] B. of Indian Standards, "IS 13920 (1993): Ductile detailing of reinforced concrete structures subjected to seismic forces - Code of practice."

[32] ACI Committee 318., American Concrete Institute., and International Organization for Standardization., *Building code requirements for structural concrete (ACI 318-08) and commentary*. American Concrete Institute, 2008.

[33] "10_vol9_5235".

[34] G. I. Kalogeropoulos, A. D. G. Tsonos, D. Konstandinidis, and S. Tsetines, "Pre-earthquake and post-earthquake retrofitting of poorly detailed exterior RC beam-to-column joints," *Eng Struct*, vol. 109, pp. 1–15, Feb. 2016, doi: 10.1016/J.ENGSTRUCT.2015.11.009.

[35] A. Pimanmas and P. Chaimahawan, "Shear strength of beam–column joint with enlarged joint area," *Eng Struct*, vol. 32, no. 9, pp. 2529–2545, Sep. 2010, doi: 10.1016/J.ENGSTRUCT.2010.04.021.

[36] R. Realfonzo, A. Napoli, and J. G. R. Pinilla, "Cyclic behavior of RC beam-column joints strengthened with FRP systems," *Constr Build Mater*, vol. 54, pp. 282–297, Mar. 2014, doi: 10.1016/J.CONBUILDMAT.2013.12.043.

[37] M. S. M. Ali, D. J. Oehlers, and M. A. Bradford, "Shear Peeling of Steel Plates Bonded to Tension Faces of RC Beams," *Journal of Structural Engineering*, vol. 127, no. 12, pp. 1453–1459, Dec. 2001, doi: 10.1061/(ASCE)0733-9445(2001)127:12(1453).

[38] S. S. Mahini and H. R. Ronagh, "Web-bonded FRPs for relocation of plastic hinges away from the column face in exterior RC joints," *Compos Struct*, vol. 93, no. 10, pp. 2460–2472, Sep. 2011, doi: 10.1016/J.COMPSTRUCT.2011.04.002.

[39] C. G. Karayannis and G. M. Sirkelis, "Strengthening and rehabilitation of RC beam–column joints using carbon-FRP jacketing and epoxy resin injection," *Earthq Eng Struct Dyn*, vol. 37, no. 5, pp. 769–790, Apr. 2008, doi: 10.1002/EQE.785.

[40] "(PDF) Selective upgrade of underdesigned reinforced beam-column joints using carbon fiber-reinforced concrete."

https://www.researchgate.net/publication/280016258_Selective_upgrade_of_underdesigned_reinforced_beam-column_joints_using_carbon_fiber-reinforced_concrete (accessed May 29, 2023).

[41] R. M. Oinam, P. C. A. Kumar, and D. R. Sahoo, "Cyclic performance of steel fiber-reinforced concrete exterior beam-column joints," *Earthquakes and Structures*, vol. 16, no. 5, pp. 533–546, May 2019, doi: 10.12989/EAS.2019.16.5.533.

[42] T.-S. Eom, H.-G. Park, H.-J. Hwang, and S.-M. Kang, "Plastic Hinge Relocation Methods for Emulative PC Beam–Column Connections," *Journal of Structural Engineering*, vol. 142, no. 2, p. 04015111, Jul. 2015, doi: 10.1061/(ASCE)ST.1943-541X.0001378.

[43] "(PDF) Strength and behaviour of exterior beam column joints with diagonal cross bracing bars." https://www.researchgate.net/publication/268060700_Strength_and_behaviour_of_exterior_beam_column_joints_with_diagonal_cross_bracing_bars (accessed May 29, 2023).

[44] S. Rajagopal and S. Prabavathy, "Investigation on the seismic behavior of exterior beam–column joint using T-type mechanical anchorage with hair-clip bar," *Journal of King Saud University - Engineering Sciences*, vol. 27, no. 2, pp. 142–152, Jul. 2015, doi: 10.1016/J.JKSUES.2013.09.002.

[45] A. G. Tsonos, I. A. Tegos, and G. G. Penelis, "Seismic Resistance of Type 2 Exterior Beam-Column Joints Reinforced With Inclined Bars," *Structural Journal*, vol. 89, no. 1, pp. 3–12, Jan. 1993, doi: 10.14359/1278.

[46] F. T. K. Au, K. Huang, and H. J. Pam, "Diagonally-reinforced beam?column joints reinforced under cyclic loading," *Structures <html_ent glyph="@amp;" ascii="&"/> Buildings*, vol. 158, no. 1, pp. 21–40, Feb. 2005, doi: 10.1680/STBU.158.1.21.58530.

[47] C. E. Chalioris, M. J. Favvata, and C. G. Karayannis, "Reinforced concrete beam-column joints with crossed inclined bars under cyclic deformations," *Earthq Eng Struct Dyn*, vol. 37, no. 6, pp. 881–897, 2008, doi: 10.1002/EQE.793.

[48] P. G. Bakir, "Seismic resistance and mechanical behaviour of exterior beam-column joints with crossed inclined bars," *Structural Engineering and Mechanics*, vol. 16, no. 4, pp. 493–517, 2003, doi: 10.12989/SEM.2003.16.4.493.

[49] C. E. Chalioris, M. J. Favvata, and C. G. Karayannis, "Reinforced concrete beam–column joints with crossed inclined bars under cyclic deformations," *Earthq Eng Struct Dyn*, vol. 37, no. 6, pp. 881–897, May 2008, doi: 10.1002/EQE.793.

[50] N. Attari, Y. S. Youcef, and S. Amziane, "Seismic performance of reinforced concrete beam–column joint strengthening by frp sheets," *Structures*, vol. 20, pp. 353–364, Aug. 2019, doi: 10.1016/J.ISTRUC.2019.04.007.

[51] R. Suhail, G. Amato, B. Broderick, M. Grimes, and D. McCrum, "Efficacy of prestressed SMA diagonal loops in seismic retrofitting of non-seismically detailed RC beam-column joints," *Eng Struct*, vol. 245, p. 112937, Oct. 2021, doi: 10.1016/J.ENGSTRUCT.2021.112937.

[52] J. G. Ruiz-Pinilla, A. Cladera, F. J. Pallarés, P. A. Calderón, and J. M. Adam, "Joint strengthening by external bars on RC beam-column joints," *Journal of Building Engineering*, vol. 45, p. 103445, Jan. 2022, doi: 10.1016/J.JOBE.2021.103445.

[53] X. Shen, B. Li, Y. T. Chen, and W. Tizani, "Experimental and numerical study on reinforced concrete beam-column joints with diagonal bars: Effects of bonding condition and diameter," *Structures*, vol. 37, pp. 905–918, Mar. 2022, doi: 10.1016/J.ISTRUC.2022.01.050.

[54] Y. I. Badrashi, "RESPONSE MODIFICATION FACTORS FOR REINFORCED CONCRETE BUILDINGS IN PAKISTAN," 2016.

[55] M. Hafezolghorani, F. Hejazi, R. Vaghei, M. S. Bin Jaafar, and K. Karimzade, "Simplified damage plasticity model for concrete," in *Structural Engineering International*, Int. Assoc. for Bridge and Structural Eng. Eth-Honggerberg, Feb. 2017, pp. 68–78. doi: 10.2749/101686616X1081.

[56] Y. Xiao, Z. Chen, J. Zhou, Y. Leng, and R. Xia, "Concrete plastic-damage factor for finite element analysis: Concept, simulation, and experiment," *Special Issue Article Advances in Mechanical Engineering*, vol. 9, no. 9, pp. 1–10, 2017, doi: 10.1177/1687814017719642.

[57] J. Y. Wu, J. Li, and R. Faria, "An energy release rate-based plastic-damage model for concrete," *Int J Solids Struct*, vol. 43, no. 3–4, 2006, doi: 10.1016/j.ijsolstr.2005.05.038.

[58] J. Lee and G. L. Fenves, "Plastic-Damage Model for Cyclic Loading of Concrete Structures," *J Eng Mech*, vol. 124, no. 8, 1998, doi: 10.1061/(asce)0733-9399(1998)124:8(892).

[59] A. Wosatko, A. Winnicki, M. A. Polak, and J. Pamin, "Role of dilatancy angle in plasticity-based models of concrete," *Archives of Civil and Mechanical Engineering*, vol. 19, no. 4, 2019, doi: 10.1016/j.acme.2019.07.003.

Chapter 4: Predicting the Response of Beam-Column Connections using Gene Expression Programming.

Abstract: Accurately predicting the capacity of exterior beam-column joints subjected to cyclic loading is a complex issue. The development of reliable prediction models is crucial for cost-effective and safe design of reinforced concrete (RC) structures. In this study, an empirical model is proposed for predicting the joint capacity of exterior RC joints exposed to cyclic loading. The model is developed using gene expression programming (GEP), a nonlinear regression analysis (NLR) technique. A database of 128 joint capacity results of exterior beam-column joints, obtained from a validated finite element (FE) model, is used to develop the proposed model. The model incorporates the effects of material and geometric factors that are often overlooked in existing models. These factors include beam and column geometries, concrete material properties, longitudinal beam and column reinforcements, and column axial loads. The results of the proposed model were compared to the experimental data and demonstrated good accuracy and reliability. The proposed model has the potential to improve the accuracy and reliability of joint capacity predictions, and thus aid in the design of safe and cost-effective RC structures.

Keywords: gene expression programming (GEP), reinforce concrete, exterior joint, joint capacity.

1. Introduction:

Joint shear failure represents the predominant mode of failure observed in existing buildings that were not designed in accordance with modern seismic codes and the recommended capacity design method. This brittle form of failure can lead to the complete collapse of structures even under relatively low deformation conditions. To address this vulnerability, contemporary seismic codes have adopted the capacity design method, which allows for controlled beam hinging failure. This design approach enables localized failure with substantial deformation and enhanced energy dissipation, effectively mitigating the risk of catastrophic collapse [1]. Multiple factors, including the aspect ratio of the joint, the compressive strength of the concrete, and the presence of transverse reinforcement, have been identified by researchers as influential parameters affecting the shear strength of beam-column joints. These studies have demonstrated that augmenting the compressive strength of concrete can lead to a proportional enhancement in the shear strength of reinforced concrete (RC) joints [2]–[5]. Studies conducted on confined joints have revealed a significant relationship between joint transverse reinforcement and shear strength. Specifically, researchers have demonstrated that increasing the level of transverse reinforcement within the joint leads to a corresponding increase in shear strength [1]. In contrast, researchers also have observed that the shear strength of confined joints decreases as the joint aspect ratio is increased [5]. The influence of column axial load on the shear strength of RC joints remains incompletely understood, as the existing literature offers differing perspectives. While some researchers have argued that the effect of column axial load on shear strength is insignificant, comprehensive explanations are lacking. Further investigation is required to gain a more comprehensive understanding of the relationship between column axial load and the shear strength of RC joints [5]. A number of analytical and empirical models have been developed by researchers to forecast the response of RC beam-to-column joints subjected to cyclic loading. Lima et al. [6] conducted a comprehensive analysis, summarizing the existing models documented in the literature that aim to predict the shear strength of RC exterior beam-to-column joints. In his research, Murad [7] employed gene expression programming (GEP) as a computational tool to anticipate the shear strength of exterior beam-to-column joints under both biaxial and uniaxial cyclic loading conditions. This innovative approach demonstrates the application of GEP in predicting the joint shear strength of such joints, adding valuable insights to the field. Recent investigations have substantiated the effectiveness of gene expression programming (GEP) and artificial neural networks (ANN) in the domain of civil engineering. These computational methods have demonstrated their potential in developing explicit models for forecasting the behavior of reinforced concrete (RC)

members. These findings contribute to the growing body of knowledge in the application of GEP and ANN in civil engineering research, showcasing their utility in enhancing predictive capabilities in this field. In situations where code formulations are absent, the utilization of GEP and ANN proves valuable in formulating predictive models. By leveraging experimental findings documented in the literature, GEP and ANN can be employed to develop robust formulations [8,9]. GEP exhibits superiority over ANN due to its distinct characteristic of not relying on predefined functions. Unlike ANN, GEP possesses the capability to develop formulations by dynamically adjusting the inclusion or exclusion of various parameters to achieve the best fit with experimental results [8], [9].

The field of computer engineering has witnessed a notable surge in the prominence of artificial intelligence (AI) over the past years, permeating various industries. This advancement in AI technology, specifically in machine learning (ML), has brought about a paradigm shift in approach, enabling the utilization of ML techniques to predict the shear strength of beam-column connections. This innovative application of ML methods represents a significant departure from conventional methodologies and contributes to the evolving landscape of research in this domain. ML, as a subset of (AI), encompasses a diverse range of tasks including regression, classification, prediction, and clustering. Leveraging the available database, ML algorithms possess the capability to learn inherent properties within specific datasets, subsequently facilitating tasks such as classification, summarization, and forecasting of relevant elements. In the context of predicting shear strength in reinforced concrete (RC) joints, ML techniques have been employed to develop predictive models [8]. This utilization of ML in the field of RC joint shear strength prediction exemplifies the application of advanced computational methods to enhance forecasting capabilities. The realm of engineering structures has witnessed the emergence of numerous efficient ML-based prediction techniques. These techniques encompass a range of applications, including the evaluation of cement strength utilizing fuzzy logic, ANN, and GEP [10-12]. Prior research has predominantly relied on individual-type learning algorithms, such as ANN-PSO [13], support vector machines (SVM), XGBoost [14], and decision tree (DT) families [15], as the principal ML algorithms. This array of ML algorithms has been employed effectively in previous studies, underscoring their potential in enhancing prediction capabilities within the domain of engineering structure.

In a recent study, a data-driven approach was employed to analyze the shear capacity and failure mode of beam-column joints, utilizing a collection of test data. Through rigorous statistical analysis, a calculated model for the shear capacity of beam-column joints was derived. This data-driven methodology presents a novel avenue for investigating the shear behavior of these joints, providing valuable insights into their structural performance and failure characteristics [16]. In their research, Jeon et al. [17] introduced shear capacity models for beam-column joints utilizing various regression techniques, including linear regression, multivariate adaptive regression splines, and symbolic regression. These models were developed as part of their investigation into enhancing the understanding of shear capacity in joints. The utilization of diverse regression methods contributes to the comprehensive analysis and formulation of accurate predictive models for shear capacity in beam-column joints. Mitra et al. [18] presented a binomial logit model for predicting non-ductile and ductile failure in beam-column joints based on the sequence of joint shear failure and beam yielding. Their proposed model aims to enhance the ability to anticipate and differentiate between non-ductile and ductile failure modes in these joints. By conducting comprehensive evaluations of different machine learning techniques, researchers proposed an expression using the lasso regression algorithm to effectively determine the failure mode of beam-column joints [19]. This approach, which involves comparing the efficiency and accuracy of various methods, offers valuable insights into accurately identifying the failure mode of joints. Alwanas et al [20] employed the extreme learning machine method to predict joint failure modes, while utilizing a multivariate adaptive regression spline model to estimate shear capacity. On the other hand, Naderpour and Mirrashid [21] introduced two distinct failure mode classifiers, based on decision tree algorithms, for both interior and exterior beam-column joints. These contributions offer valuable insights

into the prediction of failure modes and shear capacity in beam-column joints, utilizing advanced machine learning and decision tree techniques.

It is worth noting that the previous research studies were limited in terms of the size of the training dataset. As the availability of experimental data increases, there exists the potential to further enhance the accuracy of the failure mode recognition models. With larger and more diverse datasets, these models can be refined and calibrated, leading to improved performance and increased precision in identifying failure modes in beam-column joints. This emphasizes the importance of continued data collection and expansion to advance the accuracy and reliability of these models in practical applications. The failure mode of beam-column joints is influenced by several parameters, including the dimensions of the beam and column, concrete strength, stirrup ratios of the beams, columns, and joint cores, as well as the reinforcement ratios of beams and columns. Furthermore, these factors exhibit interdependencies, forming a coupling relationship. Consequently, leveraging big data analysis emerges as a viable solution for predicting the failure mode of beam-column joints. By harnessing the power of extensive datasets, comprehensive insights can be gained, allowing for accurate and reliable predictions of failure modes in beam-column joints.

For the purposes of this investigation, a dataset consisting of 120 interior beam-column joints was meticulously collected. Leveraging a gene expression tool, an equation was derived to predict the load capacity of these joints. The accuracy and validity of the obtained equation were confirmed through a comprehensive validation process, involving a comparison of gene expression and numerical results. The findings of this analysis revealed a significant level of agreement between the two approaches, as evidenced by a high coefficient of determination (r^2) value of approximately 98%. This demonstrates the robustness and reliability of the developed equation in accurately predicting the load capacity of interior beam-column joints.

2. Materials and Methods

2.1 Model Description

The aim of this investigation was to analyze the performance of a beam-column joint in a reinforced concrete building system, which is a crucial element of constructions designed for moment-resistance. This study utilizes the experimental data from a large-scale BCJ test conducted by Badrashi et al [22] under reversed-cyclic loading. The specimen was designed to meet the design standards set for Special Moment Resistance Frame (SMRF) buildings. A special moment resisting frame in concrete structures is a system designed to resist lateral forces, like earthquakes, using reinforced concrete beams and columns with strong connections to handle large bending moments. The numerical model of the specimen was constructed using the Abaqus software [23]. The model includes a beam with cross-sectional dimensions of 304 mm by 457 mm and a length of 2438 mm and joined to columns at mid-height. The beams have a total reinforcement percentage of 1.22%, comprising of three #19 bars at the top and bottom. Shear reinforcement in the beams near the beam-column joint is provided by closed ties measuring 10 mm in diameter and spaced at 76 mm center-to-center, extending 812 mm from the support surface. In addition, after that point, the shear reinforcement is provided with a center-to-center spacing of 152 mm. The stirrup ends meet the SMRF detailing requirements by bending at 135 degrees. The column's dimensions are 2743 mm in height, 304 mm in width, and a depth that is equivalent to that of the beams. The column reinforcement consists of eight uniformly distributed #19 bars along the perimeter, resulting in a total reinforcement percentage of 1.83%. Closed ties are placed at 76 mm center-to-center spacing to reinforce shear in the column along its entire length, including the joint section. To comply with the reinforcement detailing specifications for SMRF buildings, the ties terminate with 135-degree seismic bends. The dimensions and details of the exterior beam-column connection is depicted in figure 1.

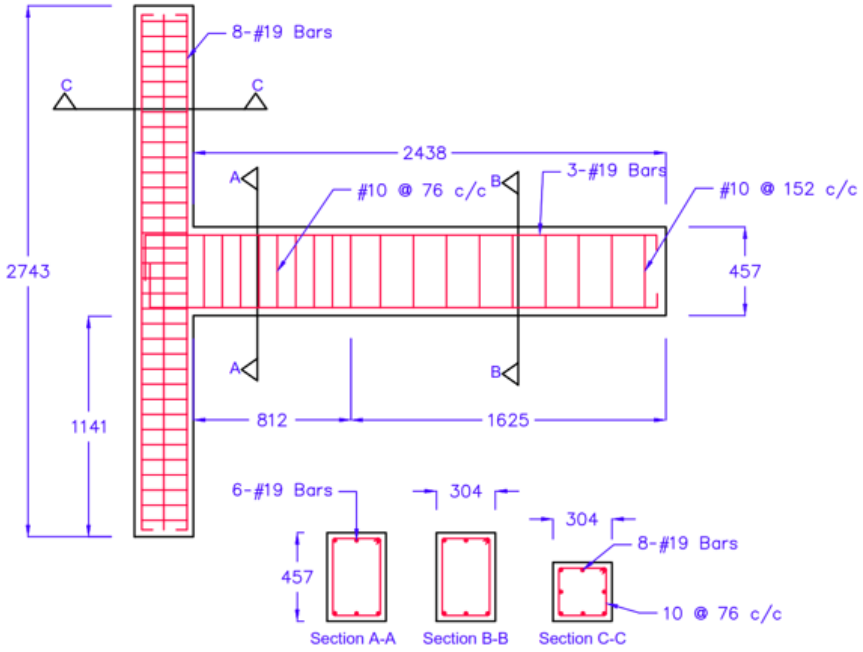

Figure 1: Dimensions and details of the exterior beam-column connection, all units are in mm.

2.2 Model Validation

A mesh sensitivity analysis has been performed to ensure the reliability of the results. To assess the impact of mesh size on the behavior and predicted results of an FEM analysis of an RC exterior beam-column joint, a mesh sensitivity analysis was performed. Four distinct mesh sizes were employed for the concrete, longitudinal rebars, and stirrups, as depicted in figure 2 and outlined in the Table 1. The model featured identical geometry, support conditions, loading, mechanical properties, and material models. Through this analysis, it was determined that further refinement of the mesh size beyond 55 mm for concrete, 55 mm for longitudinal rebars, and 20 mm for stirrups had a minimal impact on the predicted results and did not significantly alter the behavior of the model. This suggests that these mesh sizes provide an appropriate level of resolution for the analysis.

Table 10: Results of mesh sensitivity analysis

Mesh Name	Mesh Size(mm)		
	Concrete	Longitudinal Rebar	Stirrups
Mesh-1	150	150	50
Mesh-2	100	100	40
Mesh-3	70	70	30
Mesh-4	55	55	20

To evaluate the performance of a reinforced concrete BCJ using FEM, it is essential to validate the numerical model against experimental findings. To validate the numerical model, an exterior beam-column joint specimen was utilized as a reference experiment in this study. The experimental data from a large-scale experimental test by Badrashi et al was utilized for validation. The load-displacement response of the numerical model was compared to experimental findings, which were in close agreement with those reported by Badrashi et al as shown in Figure 3. The agreement between FEM and experimental results is good in terms of ultimate and failure load, and deformation as shown in Table 2.

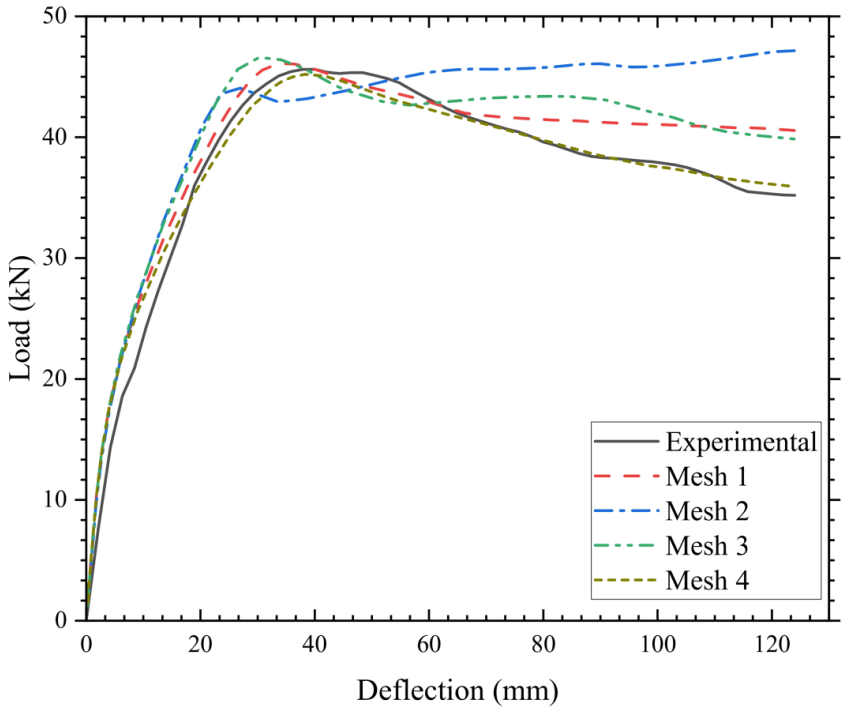

Figure 2: Mesh sensitivity analysis for the numerical model depicting the influence of mesh size on the accuracy of the simulation results.

Table 11: Comparison of peak and failure loads obtained from FEM and experimental results.

Loads	Experimental	FEM	Percentage Difference
Peak	45.6	45.2	0.88
Failure	35.2	35.9	1.97

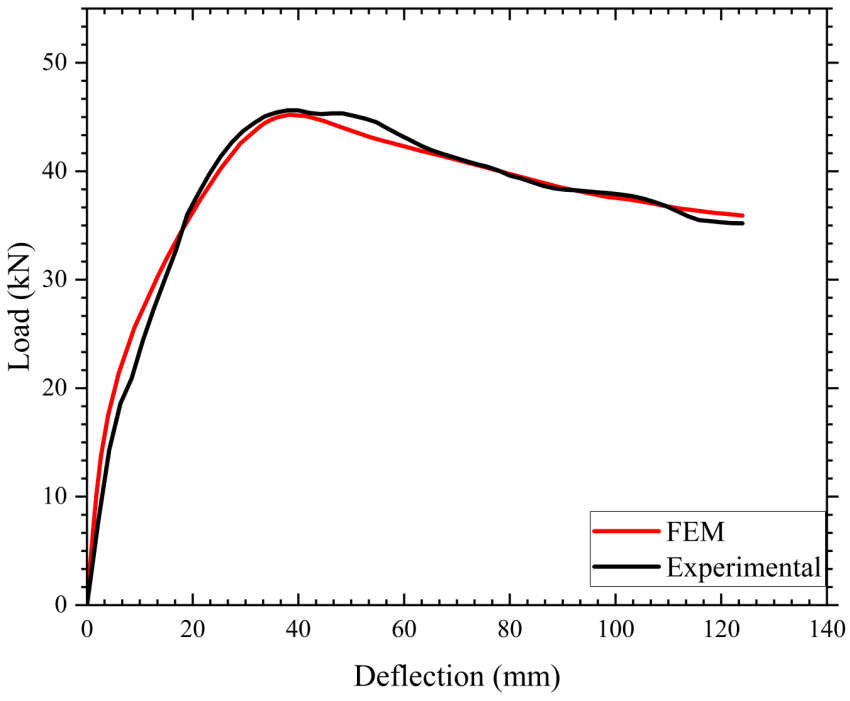

Figure 3: Comparison of experimental and numerical results

2.3 Parametric study:

Beam-column joints are critical components in reinforced concrete (RC) structures, and understanding their behavior is crucial for ensuring structural integrity. In recent years, gene expression programming (GEP) has emerged as a powerful tool for developing artificial intelligence (AI) equations that accurately model complex systems. This research aims to leverage GEP to establish AI equations that capture the relationships between six key parameters governing the behavior of beam-column joints. By employing GEP, this study seeks to uncover the optimal values of these parameters to achieve efficient and reliable structural designs. The parameters under investigation include axial load, column bar area, column width, longitudinal beam bar area, beam width, and concrete compressive strength. The resulting AI equations will contribute to the advancement of structural engineering practices, facilitating the optimization of beam-column joint performance while considering trade-offs between structural strength, cost-effectiveness, and other design considerations.

The study investigates the relationship between the axial load applied to a structure (measured in tons) and the corresponding ultimate force it can withstand. The graph presents a comprehensive analysis of this relationship, revealing a gradual increase in the ultimate force as the axial load increases. Initially, there is a steep incline, indicating a higher efficiency in load-bearing capacity. However, as the axial load approaches 30 tons, the rate of increase starts to decelerate, suggesting a decrease in the structure's efficiency. This finding underscores the significance of considering the diminishing returns associated with increasing axial load beyond a certain point to optimize the structural design of beam-column joints as shown in Figure 4.

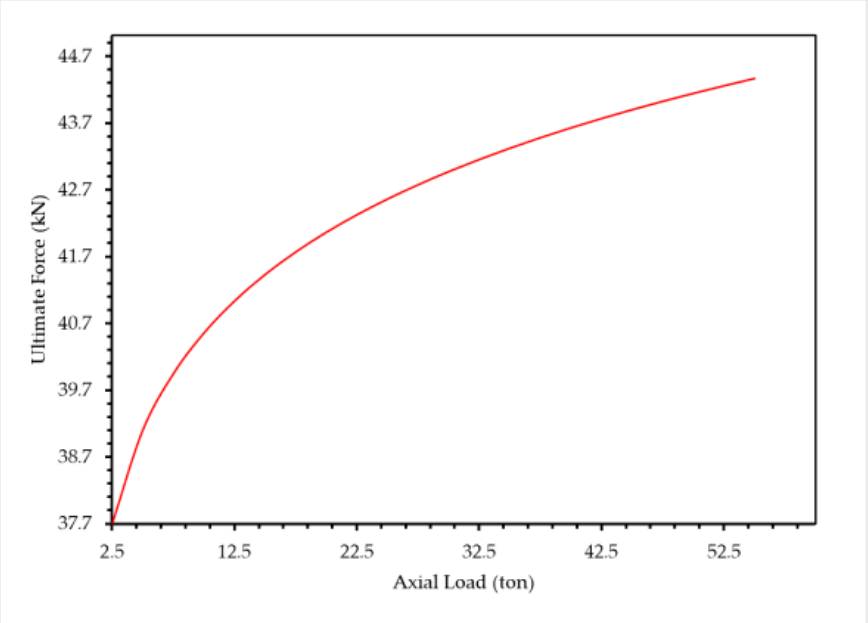

Figure 4: Effect of concentrated Axial load on Ultimate load carrying capacity.

The second graph illustrates the relationship between the column bar area (mm^2) and the corresponding ultimate force (kN) it can withstand. The graph effectively portrays this relationship, showcasing that as the column bar area increases, there is a marginal enhancement in the ultimate force capacity as shown in Figure 5. However, it is noteworthy that the rate of increase progressively diminishes, indicating the presence of diminishing returns beyond a specific threshold. This suggests that surpassing a certain column bar area may not yield substantial improvements in structural strength.

Consequently, the graph emphasizes the necessity of meticulously considering the optimal column bar area to achieve an efficient and cost-effective structural design.

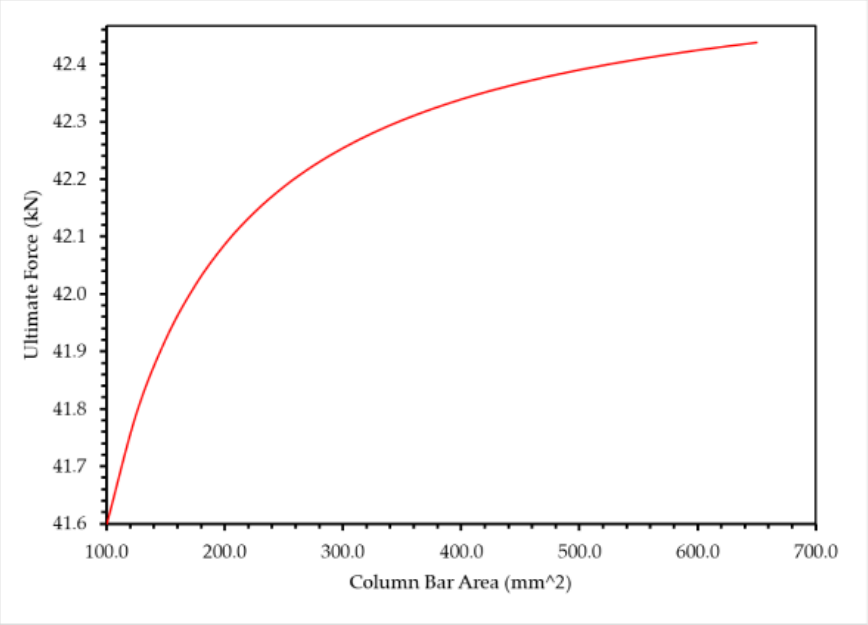

Figure 5: Effect of Column bar area on Ultimate load carrying capacity.

The analysis focused on the relationship between the column width (mm) and the corresponding ultimate force (kN) the beam-column joint can withstand. Increasing the column width resulted in a noticeable increase in the ultimate force capacity. However, beyond a certain point, the rate of increase diminished, indicating diminishing returns as shown in Figure 6. This observation highlights the significance of careful consideration of the column width to ensure efficient and reliable structural design by striking a balance between structural strength and cost-effectiveness.

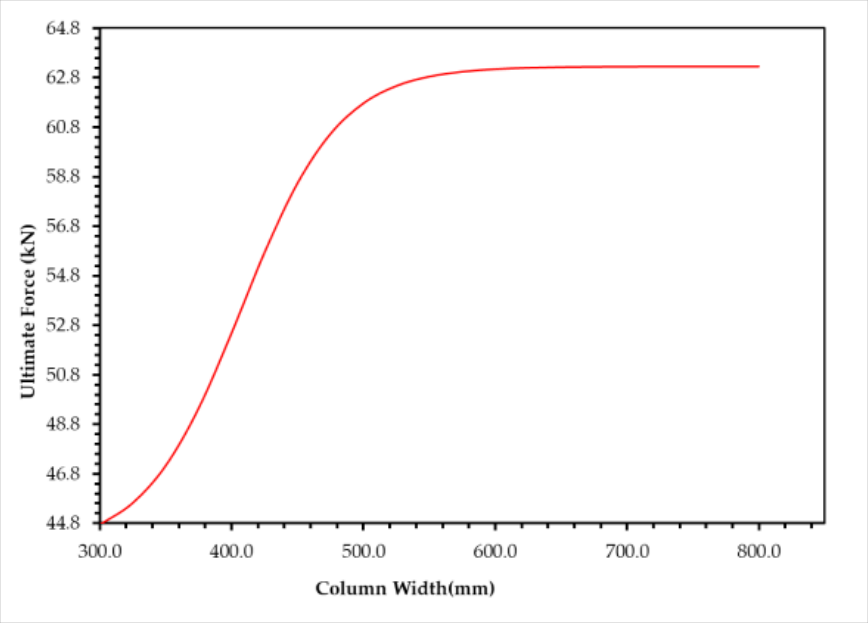

Figure 6: Effect of column width on Ultimate load carrying capacity.

The graph explored the relationship between the longitudinal beam bar area and the corresponding ultimate force the beam-column joint can withstand. Increasing the beam bar area led to a gradual improvement in the ultimate force

capacity. However, beyond a certain point, the rate of increase became negligible, indicating diminishing returns as shown in Figure 7. This finding underscores the importance of carefully selecting the longitudinal beam bar area within an optimal range to achieve an efficient and reliable structural design.

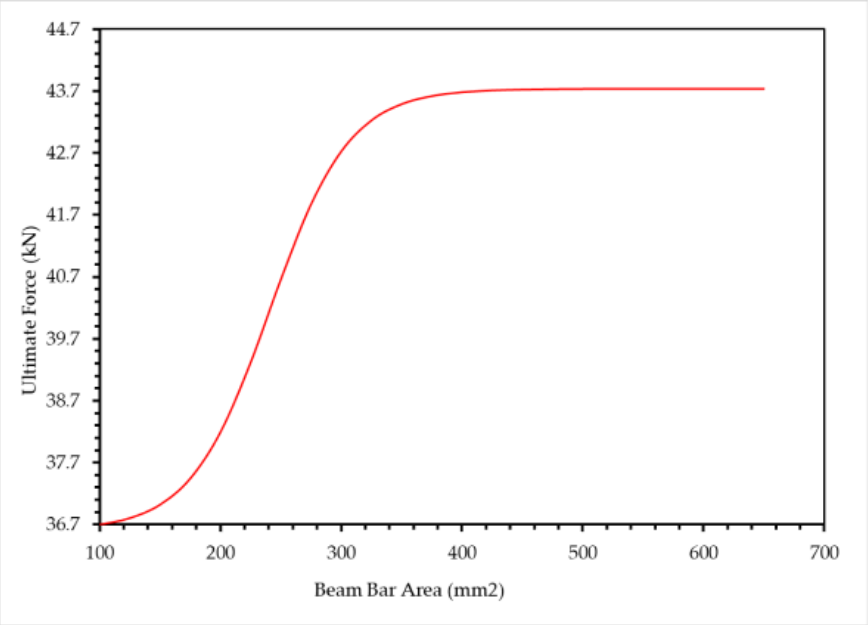

Figure 7: Effect of Beam longitudinal bar area on Ultimate load carrying capacity.

Figure 7 shows relationship between the beam width and the corresponding ultimate force the beam-column joint can withstand. Increasing the beam width resulted in a significant increase in the ultimate force capacity. The rate of increase remained relatively steady up to a certain point, beyond which it started to diminish, indicating diminishing returns as shown in Figure 8. This observation emphasizes the need to select an appropriate beam width within the optimal range to achieve optimal structural performance.

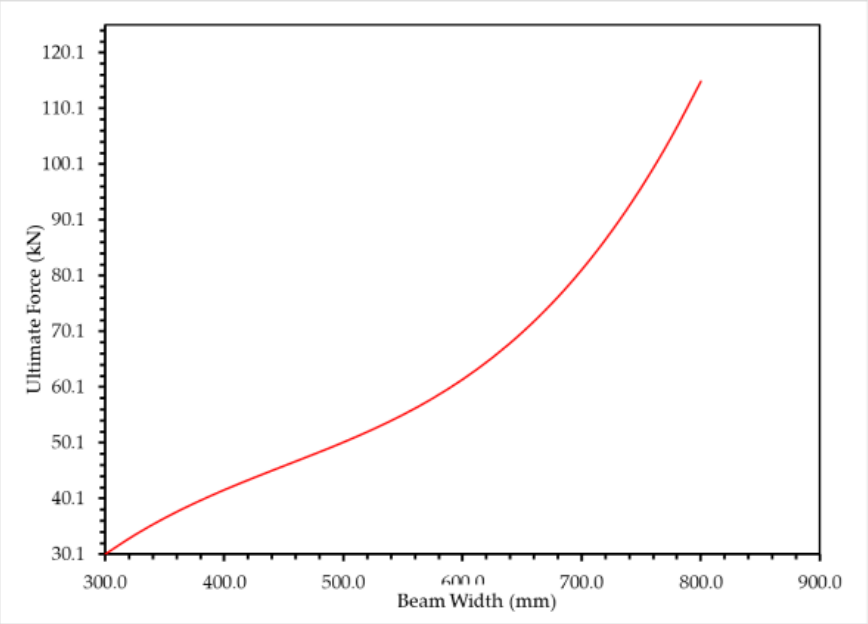

Figure 8: Effect of Beam width on Ultimate load carrying capacity.

Finally, the study investigates the relationship between the concrete compressive strength and the corresponding ultimate force that a structure can withstand. The graph presented in the research provides a comprehensive analysis of this relationship. It demonstrates that as the concrete compressive strength increases, there is a gradual improvement in the ultimate force capacity as shown in Figure 9. The rate of increase remains relatively steady up to a certain point; however, beyond this threshold, the rate of increase starts to diminish, indicating the presence of diminishing returns. This finding suggests the existence of an optimal range for concrete compressive strength, which effectively balances structural strength with other design considerations. The graph underlines the significance of selecting an appropriate concrete strength to ensure the desired structural performance.

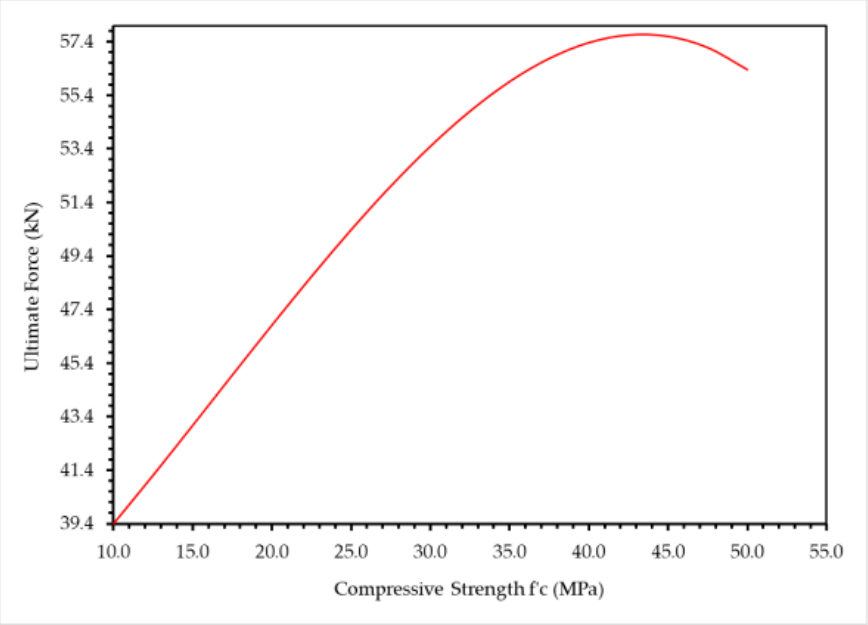

Figure 9: Effect of concreate compressive strength on Ultimate load carrying capacity.

3. GEP Algorithms:

Gene Expression Programming (GEP) is a type of evolutionary algorithm used for optimization and modeling tasks. It uses a chromosome-like structure to represent a computer program, where each gene represents a mathematical function or an operation. These genes are then combined to form a program that can be evaluated to produce an output, which is compared to a target value. The program is then modified through a process of mutation and recombination to improve its fitness. GEP is unique in that it uses both a fixed-length linear string and a ramified structure of varying sizes and shapes for chromosome representation.

One of the key advantages of GEP is its ability to use multiple data types, such as real numbers, integers, and Boolean values. This makes it versatile and applicable to a wide range of problems, including data mining, pattern recognition, and optimization. In addition, GEP can handle nonlinear relationships between variables, making it well-suited for modeling complex systems. To optimize the performance of the GEP algorithm, several parameters can be adjusted, such as the number of chromosomes, the number of genes, the size of the head, and the linking functions. Increasing the number of genes and chromosomes can lead to more complex functions that fit the data more precisely, but there is a trade-off between achieving a simplified mathematical model and achieving the desired level of accuracy.

One of the challenges of GEP is achieving convergence to the global optimal solution. The algorithm may fail to select an optimal solution from among several competing candidate solutions, leading to an indefinite sequence of steps or a

non-terminating program. To solve this problem, the algorithm can adjust the linking function or change the number of genes and chromosomes.

GEP is a powerful algorithm for modeling complex systems and finding optimal solutions to a wide range of problems. Its ability to use multiple data types and handle nonlinear relationships makes it a popular choice in the field of evolutionary computing. GEP has found many applications in structural engineering, where it has been used to develop models for estimating the capacity of various structural components.

Figure 10 show various stages of GEP optimization. The optimization procedure in GEP starts by selecting the control parameters, which include the function set, terminal set, fitness function, control parameters, and stop condition. The fitness function is defined beforehand, and an initial population of random strings, or chromosomes, is created using genetic programming. The chromosomes are then translated into expression trees, and the results are evaluated based on their fitness score. If the fitness criterion is not met, a roulette-wheel sampling method is used to select some chromosomes, which are then mutated to produce new generations. This iterative process continues until the variables are optimally tuned to the fitness function and the chromosomes are optimized. The success of the optimization process depends on the appropriate selection of control parameters and the ability of the algorithm to converge to the global optimal solution.

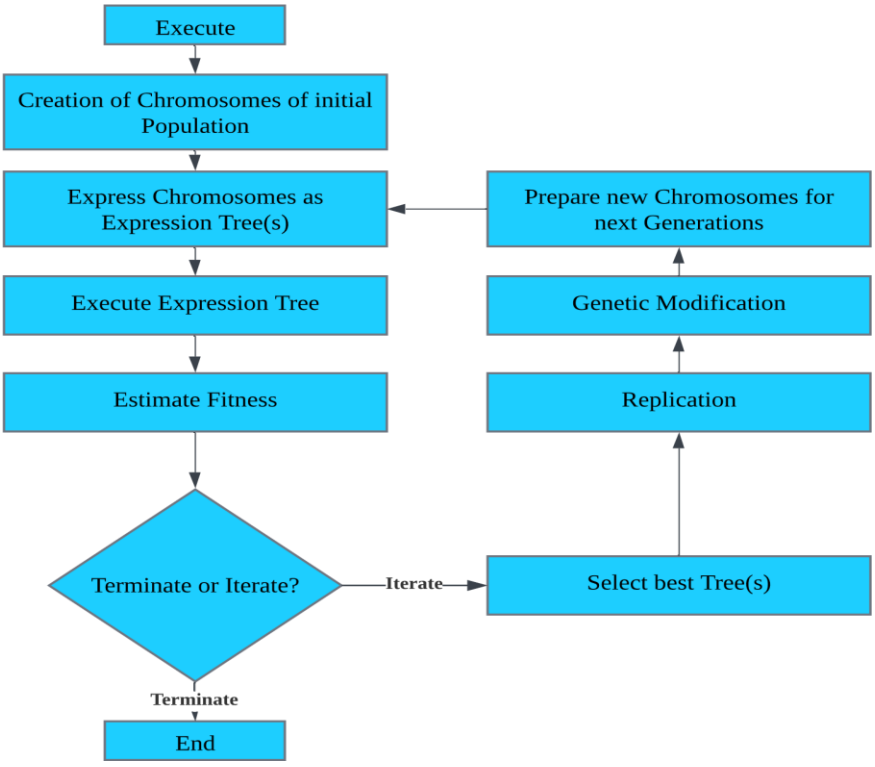

Figure 10: Flowchart for GEP model constuct

3.1 Proposed GEP Model for Estimating Ultimate Load Capacity:

A regression model was generated using the GeneXpro tool software. The model was trained using 127 records, and its performance was evaluated using an independent validation set consisting of 25 records. The fitness function used for model training was the root mean square error (RMSE). The training fitness was 146.62, and the training R-square was 0.908, indicating a good fit of the model to the training data. The validation fitness was 175.57, and the validation R-square was 0.906, indicating the model's ability to generalize to new data.

The resulting regression model takes in an array of input variables, denoted as "x" in the code, and returns a single output value. The model is expressed as a mathematical equation, which is represented in the code as a function named "gepModel". The function contains three constants, G2C2, G2C3 and G2C1, and three mathematical operations: logarithm, exponentiation, and multiplication. The input variables are used to calculate the value of the output variable using these operations.

The equation generated by the model is complex and nonlinear, involving multiple logarithmic and exponential terms. However, its functional form can be interpreted as a combination of the input variables, weighted by the constants, and modified by the logarithmic and exponential operations. The equation can be used to predict the output variable for new sets of input variables, and its accuracy can be evaluated using the RMSE metric.

$$y = \left(x3 - \left(\log\left(\frac{x2}{x6}\right) + \left(\frac{x5}{x1}\right) \right)^3 \right) \left(\frac{log(log(G2C2)^2)}{(G2C3 - G2C1)^2} \right) \left(log\left(\sqrt{4x6 + x4}\right)^2 \right)$$

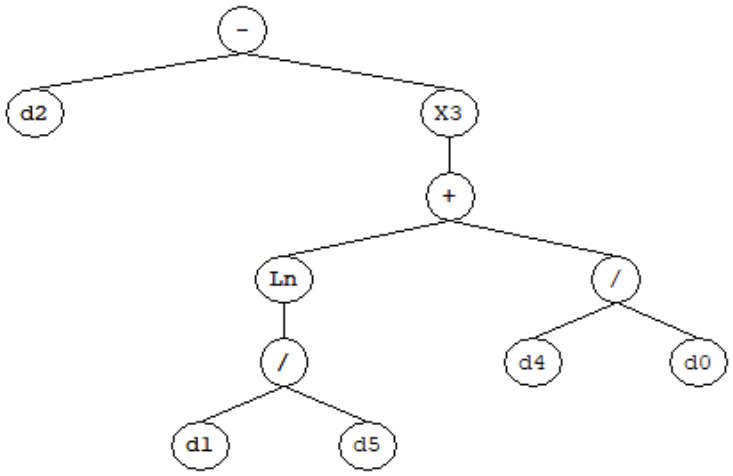

(a)

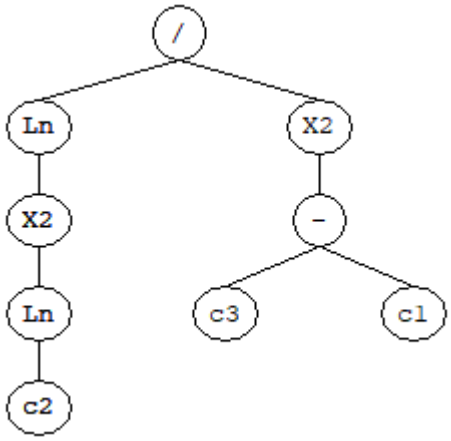

(b)

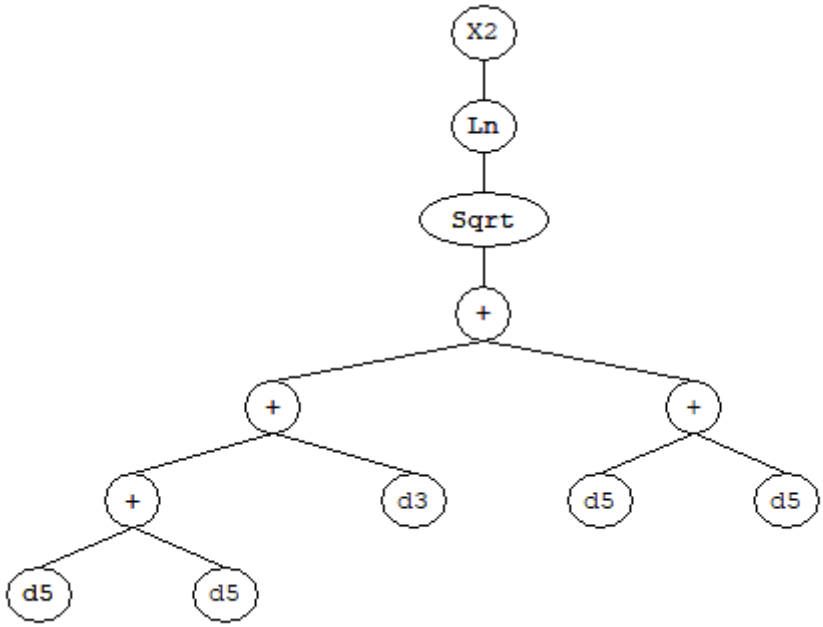

(c)

Figure 11: Gene Expression for load carrying capacity (a) Sub ET-1 (b) Sub ET-2 (c) Sub ET-3

Table 3: Model construction parameters**Error! Not a valid link.**

3.2 Accuracy of the proposed Model:

The fitness of the proposed model is 251.45, which indicates that the model has performed well in optimizing the fitness function to minimize the error between the predicted values and actual values. The mean square error (MSE) is 33.87, which shows the average of the squared differences between the predicted and actual values. The root mean square error (RMSE) is 5.819, indicating that the model has an average error of 5.8 units in predicting the output values. The mean absolute error (MAE) of the model is 4.27, which is the average absolute difference between the predicted and actual values.

The relative squared error (RSE) is 19.7%, indicating that the model has a good fit for the given data. The relative root squared error (RRSE) is 44.36% which is a normalized version of RMSE that considers the scale of the output variable. The relative absolute error (RAE) is 44.82% which is the average absolute difference between the predicted and actual values normalized by the means of the actual values.

The correlation coefficient between the predicted and actual values is 0.908, which indicates a strong positive correlation between the two variables. The R-square value of the model is 0.908, which means that 90% of the variation in the output variable can be explained by the input variables.

In addition, the calculation errors of the proposed model are zero, indicating that the model has successfully converged to the optimal solution without any errors in the calculations. These results demonstrate that the proposed model is accurate and reliable in predicting the output values based on the given input variables.

Errors	Formulas
MSE =	$E_i = \frac{1}{n}\sum_{j=1}^{n}\left(P_{(ij)} - T_j\right)^2$
RMSE =	$E_i = \sqrt{\frac{1}{n}\sum_{j=1}^{n}\left(P_{(ij)} - T_j\right)^2}$
MAE =	$E_i = \sqrt{\frac{1}{n}\sum_{j=1}^{n}\left(P_{(ij)} - T_j\right)^2}$
RSE =	$E_i = \frac{\sum_{j=1}^{n}\left(P_{(ij)} - T_j\right)^2}{\sum_{j=1}^{n}\left(T_j - \overline{T}\right)^2}$
RRSE =	$E_i = \sqrt{\frac{\sum_{j=1}^{n}\left(P_{(ij)} - T_j\right)^2}{\sum_{j=1}^{n}\left(T_j - \overline{T}\right)^2}}$
RAE=	$E_i = \frac{\sum_{j=1}^{n}\left\lvert P_{(ij)} - T_j\right\rvert}{\sum_{j=1}^{n}\left\lvert T_j - \overline{T}\right\rvert}$

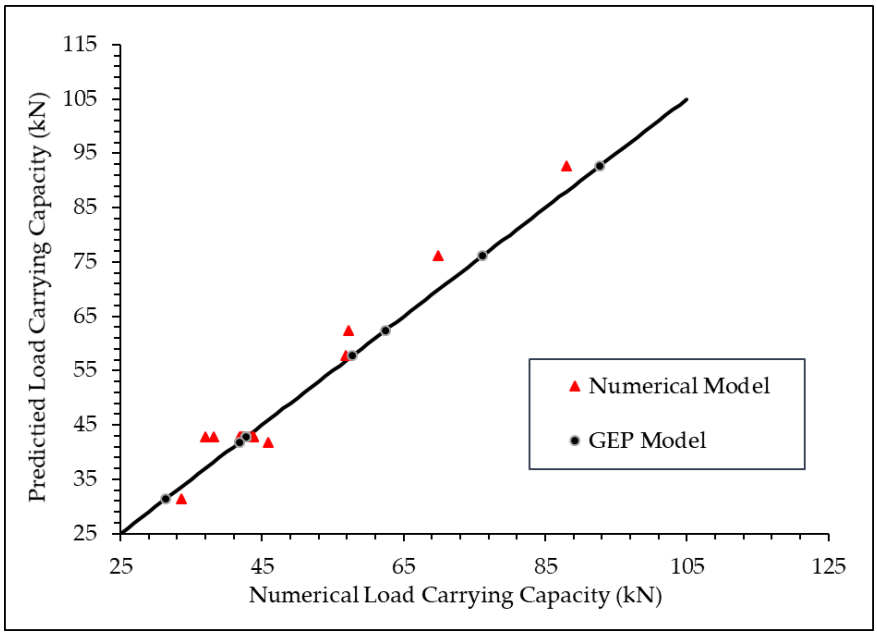

Figure 11: Comparasion of predicted and numerical results of load caryying capacity

4. Conclusion:

The proposed equation can predict the load-carrying capacity of the beam-column joint with R-Square value of 0.97. The equation has been validated through a numerical scheme. In the future, it is recommended to explore various techniques, such as using steel haunches and engineered cementitious composite (ECC) materials, to enhance the performance of RC beam-column connections under cyclic and blast loading.

References:

[1] T. Paulay and M. J. N. Priestley, "Seismic design of reinforced concrete and masonry buildings," p. 744, 1992, Accessed: May 29, 2023. [Online]. Available: https://www.wiley.com/en-us/Seismic+Design+of+Reinforced+Concrete+and+Masonry+Buildings-p-9780471549154

[2] Y. Z. Murad, "Analytical and numerical assessment of seismically vulnerable corner connections under bidirectional loading in RC framed structures," 2016, doi: 10.25560/44493.

[3] Y. Murad, Y. Abu-Haniyi, A. Alkaraki, and Z. Hamadeh, "An experimental study on cyclic behaviour of reinforced concrete connections using waste materials as cement partial replacement," *Can. J. Civ. Eng.*, vol. 46, no. 6, pp. 522–533, 2019, doi: 10.1139/CJCE-2018-0555.

[4] "(11) (PDF) Strut and tie models for analysis/design of external beam-column joints." https://www.researchgate.net/publication/250072589_Strut_and_tie_models_for_analysisdesign_of_external_beam-column_joints (accessed May 29, 2023).

[5] R. L. Vollum and J. B. Newman, "Strut and tie models for analysis/design of external beam-column joints," *Mag. Concr. Res.*, vol. 53, no. 1, pp. 63–66, Feb. 2001, doi: 10.1680/MACR.53.1.63.39499.

[6] Y. Murad, W. Al Bodour, and A. Ashteyat, "Seismic retrofitting of severely damaged RC connections made with recycled concrete using CFRP sheets," *Front. Struct. Civ. Eng.*, vol. 14, no. 2, pp. 554–568, Apr. 2020, doi: 10.1007/S11709-020-0613-8.

[7] Y. Murad, "Joint shear strength models for exterior RC beam-column connections exposed to biaxial and uniaxial cyclic loading," *J. Build. Eng.*, vol. 30, p. 101225, Jul. 2020, doi: 10.1016/J.JOBE.2020.101225.

[8] M. Sonebi and A. Cevik, "Genetic programming based formulation for fresh and hardened properties of self-compacting concrete containing pulverised fuel ash Genetic programming based formulation for fresh and hardened properties of self-compacting concrete containing pulverised fuel ash," *Constr. Build. Mater.*, vol. 23, no. 7, pp. 2614–2622, Jul. 2009, doi: 10.1016/J.CONBUILDMAT.2009.02.012.

[9] A. Cevik and M. Sonebi, "Modelling the performance of self-compacting SIFCON of cement slurries using genetic programming technique," *Comput. Concr.*, vol. 5, no. 5, pp. 475–490, 2008, doi: 10.12989/CAC.2008.5.5.475.

[10] J. Amani and R. Moeini, "Prediction of shear strength of reinforced concrete beams using adaptive neuro-fuzzy inference system and artificial neural network," *Sci. Iran.*, vol. 19, no. 2, pp. 242–248, Apr. 2012, doi: 10.1016/J.SCIENT.2012.02.009.

[11] D. J. Armaghani, G. D. Hatzigeorgiou, C. Karamani, A. Skentou, I. Zoumpoulaki, and P. G. Asteris, "Soft computing-based techniques for concrete beams shear strength," *Procedia Struct. Integr.*, vol. 17, pp. 924–933, 2019, doi: 10.1016/J.PROSTR.2019.08.123.

[12] Y. Z. Murad, R. Hunifat, and W. AL-Bodour, "Interior Reinforced Concrete Beam-to-Column Joints Subjected to Cyclic Loading: Shear Strength Prediction using Gene Expression Programming," *Case Stud. Constr. Mater.*, vol. 13, p. e00432, Dec. 2020, doi: 10.1016/J.CSCM.2020.E00432.

[13] X. L. Chen, J. P. Fu, J. L. Yao, and J. F. Gan, "Prediction of shear strength for squat RC walls using a hybrid ANN–PSO model," *Eng. Comput.*, vol. 34, no. 2, pp. 367–383, Apr. 2018, doi: 10.1007/S00366-017-0547-5/TABLES/10.
[14] H. R. M. Mohammed and S. Ismail, "Proposition of new computer artificial intelligence models for shear strength prediction of reinforced concrete beams," *Eng. Comput.*, vol. 38, no. 4, pp. 3739–3757, Aug. 2022, doi: 10.1007/S00366-021-01400-Z.
[15] D. C. Feng and B. Fu, "Shear strength of internal reinforced concrete beam-column joints: Intelligent modeling approach and sensitivity analysis," *Adv. Civ. Eng.*, vol. 2020, 2020, doi: 10.1155/2020/8850417.
[16] J. Kim and J. M. LaFave, "A Simplified Approach to Joint Shear Behavior Prediction of RC Beam-Column Connections," *https://doi.org/10.1193/1.4000064*, vol. 28, no. 3, pp. 1071–1096, Aug. 2012, doi: 10.1193/1.4000064.
[17] J. S. Jeon, A. Shafieezadeh, and R. Desroches, "Statistical models for shear strength of RC beam-column joints using machine-learning techniques," *Earthq. Eng. Struct. Dyn.*, vol. 43, no. 14, pp. 2075–2095, Nov. 2014, doi: 10.1002/EQE.2437.
[18] N. Mitra, S. Mitra, and L. N. Lowes, "Probabilistic model for failure initiation of reinforced concrete interior beam–column connections subjected to seismic loading," *Eng. Struct.*, vol. 33, no. 1, pp. 154–162, Jan. 2011, doi: 10.1016/J.ENGSTRUCT.2010.09.029.
[19] S. Mangalathu and J. S. Jeon, "Classification of failure mode and prediction of shear strength for reinforced concrete beam-column joints using machine learning techniques," *Eng. Struct.*, vol. 160, pp. 85–94, Apr. 2018, doi: 10.1016/J.ENGSTRUCT.2018.01.008.
[20] A. A. H. Alwanas, A. A. Al-Musawi, S. Q. Salih, H. Tao, M. Ali, and Z. M. Yaseen, "Load-carrying capacity and mode failure simulation of beam-column joint connection: Application of self-tuning machine learning model," *Eng. Struct.*, vol. 194, pp. 220–229, Sep. 2019, doi: 10.1016/J.ENGSTRUCT.2019.05.048.
[21] H. Naderpour and M. Mirrashid, "Classification of failure modes in ductile and non-ductile concrete joints," *Eng. Fail. Anal.*, vol. 103, pp. 361–375, Sep. 2019, doi: 10.1016/J.ENGFAILANAL.2019.04.047.

Chapter 5: Conclusions, and Recommendations for Future Research

Conclusions:

The following conclusions were drawn from the research reported in the preceding chapters:

1. Rotation of the joint is an Efficient response parameter compared to response parameters such as deflection and strain of reinforcement.
2. In-plane diagonal bars are more effective in reducing core damage compared to out-of-plane diagonal bars in beam-column joints.
3. Model-FB-XB configuration is highly effective in reducing tension and compression damage while providing the highest additional rotational stiffness to the joint, thereby increasing the load-carrying capacity of the joint by almost 20%.
4. Incorporating diagonal bars within the beam instead of the column can decrease tension damage near the joint and ensure a more ductile failure mode, reducing the risk of catastrophic building collapse.
5. The Model-FB-XB configuration offers a promising solution to reduce joint failure and improve overall safety, making it a valuable addition to the field of structural engineering.

Recommendations for Future Research:

1. Optimize design by considering rotation as the primary response parameter for joint damage in beam-column connections.
2. Further investigate the effectiveness of in-plane diagonal bars and their potential as an alternative to joint stirrups in reducing core damage and minimizing reinforcement congestion.
3. Explore the use of the Model-FB-XB configuration for the future design of beam-column joints and evaluate its performance in various structural scenarios.
4. Study the effects of steel haunches and perforation amounts on the load-carrying capacity and damage characteristics of beam-column joints under different loading conditions.
5. Investigate the performance of beam-column connections retrofitted with engineered cementitious composite (ECC) materials under cyclic and blast loading conditions.
6. Conduct research on the seismic performance of different haunch shapes and perforation percentages in beam-column connections to enhance their resilience in seismically active regions.
7. Validate the proposed equation for predicting the load-carrying capacity of beam-column joints using various numerical schemes and explore its applicability in different scenarios.
8. Continue exploring and innovating new techniques and configurations to improve the design and performance of reinforced concrete structures.